VOLUME XL

GEMS & GEMOLOGY

WINTER 2004

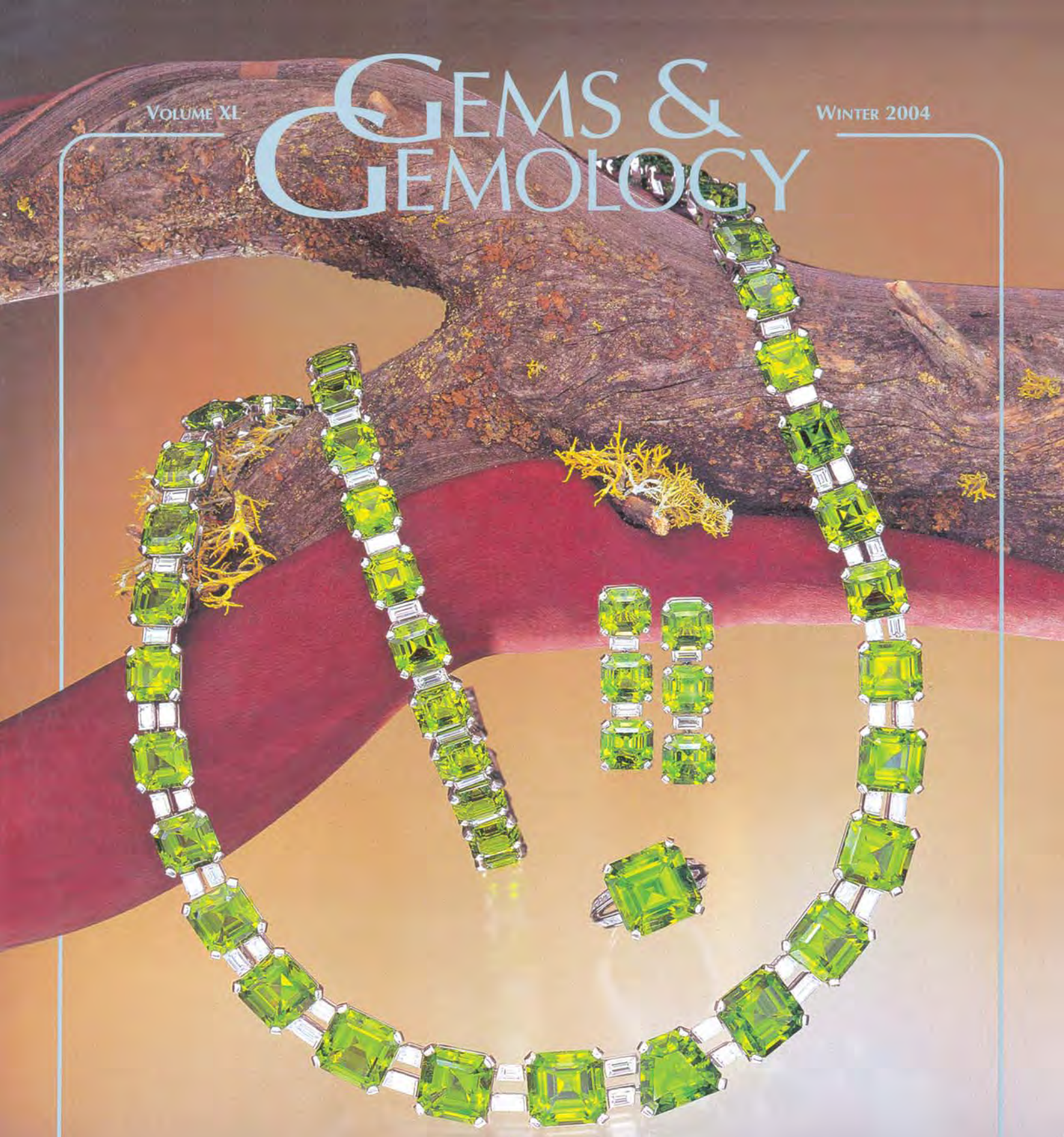

Creating a Peridot Jewelry Suite
New Synthetic Diamonds Chart
LIBS to Detect Be-Diffused Sapphire

THE QUARTERLY JOURNAL OF THE GEMOLOGICAL INSTITUTE OF AMERICA

GEMS & GEMOLOGY

Winter 2004 VOLUME 40, NO. 4

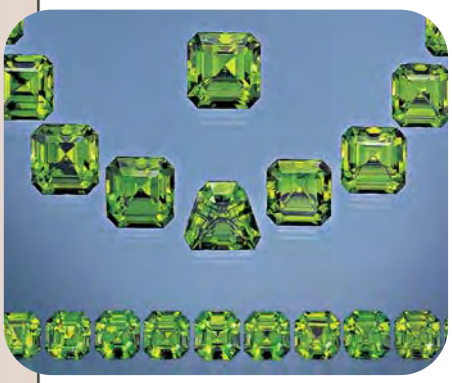

pg. 297

pg. 307

EDITORIAL

LETTERS

FEATURE ARTICLES

NOTES AND NEW TECHNIQUES

REGULAR FEATURES

pg. 331

pg. 338

First GIA Gemological Research Conference

Will Kick Off 2006 International Gemological Symposium

As readers of this journal know, modern gemology is expanding in many exciting directions. Although traditionally rooted in mineralogy and geology, gemology now extends into fields such as physics, chemistry, and materials science. This evolution has come in response to increasingly sophisticated synthetic gem materials and treatments, as well as the availability of natural gems from an ever greater number of sources. Much of contemporary research is focused on the nondestructive characterization of gem materials to document their gemological properties and determine means of identification—of the gem material itself, whether it is natural or synthetic, and the cause (natural or treated) of its color and other features. At the same time, advanced geologic fieldwork at known gem localities, and the documentation of new deposits, continues to yield important insights into the origins of gems.

To explore the latest breakthroughs in gemology and related sciences, GIA will host its first-ever Gemological Research Conference August 26–27, 2006, in San Diego, California, at the Manchester Grand Hyatt Hotel. This event, held in conjunction with the 4th International Gemological Symposium (August 27–29), is being co-chaired by two prominent *G&G* authors and editors, Dr. James Shigley and Brendan Laurs. The Conference will not only provide an international forum for gemologists to share the results of their latest studies, but it will also give scientists and specialists from other disciplines an opportunity to contribute to modern gemological research. GIA hopes to hold subsequent research conferences on a regular basis.

The following six general themes (scheduled in two parallel sessions) will be addressed at the 2006 conference:

- Gem Characterization Techniques
- Diamond and Corundum Treatments
- Laboratory Growth of Gem Materials
- Geology of Gem Deposits
- New Gem Occurrences
- General Gemology (including Pearls)

Each session will feature invited lectures and submitted presentations by prominent gemologists and other researchers from around the world, plus opportunities for interactive discussions with audience members. In addition, a poster session will take place on August 27, for which participants can submit innovative research on any topic of gemological interest. Poster session presenters will be encouraged to show samples, with gemological microscopes available for use. Poster presenters may also leave their exhibits up for viewing during the International Gemological Symposium, which will follow immediately.

Potential presenters are asked to submit an abstract in electronic format by March 1, 2006. Abstracts for oral presentations should be submitted to the organizing committee at gemconference@gia.edu. Abstracts for poster presentations, and requests for information on poster guidelines, should be submitted to Dona Dirlam at ddirlam@gia.edu. Abstracts for both oral and poster presentations given at the research conference will be published by *Gems & Gemology* in a special Proceedings volume.

The science of gemology is the key to preserving the integrity of the gem industry. As new treatments and synthetics are introduced, and new gem materials appear in the marketplace, we must develop the intellectual resources to address them. The GIA Gemological Research Conference will help shape the future of our science.

I urge you to join us in San Diego in 2006 for both the Gemological Research Conference and the International Gemological Symposium. For more information on participating as a presenter or attendee at the Conference, visit *G&G* online at www.gia.edu/gemsandgemology and click on the Gemological Research Conference link, or send an e-mail to gemconference@gia.edu. Regular updates on this Conference and the 4th International Gemological Symposium will appear on GIA's Web site at www.gia.edu.

You, too, can help shape the future of gemology.

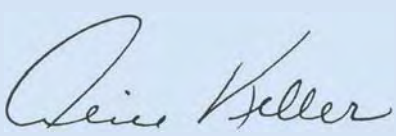

Alice S. Keller
Editor-in-Chief

LETTERS

Photoluminescence Peak in Synthetic Diamonds Due to Ruby Inclusions?

In the Summer 2004 *G&G* (pp. 128–145), Shigley et al. reported on a comprehensive study of colored synthetic diamonds distributed by Chatham Created Gems. In this article, the authors ascribe a photoluminescence feature at 693 nm seen in the pink synthetic diamond samples to a nickel-related defect. I assume this is because, in their references, A.M. Zaitsev (*Optical Properties of Diamond: A Data Handbook*, Springer Verlag, Berlin, 2001) quoted a center at 693.7 nm that was ascribed to nickel by V.A. Nadolinny.

I would like to suggest that there is ample evidence that what the authors have probably seen is, in fact, the Cr^{3+} ruby doublet, such as that seen in near-colorless synthetic diamond and documented on my Web site at www.gis.net/~adamas/raman.html.

The authors state that the synthetic pinks they examined were type IIa (Ib's with low nitrogen) and contained metallic inclusions. This is consistent with the characteristics of near-colorless synthetic diamonds, which use aluminum as a nitrogen getter. The getter seems to result in precipitation of the flux into the crystal as well as eliminating the nitrogen, and where you have aluminum, you typically create oxides, trapping oxygen. The use of low-purity iron and nickel for a catalyst is a source of trace chromium, all the necessary ingredients for the formation of $Al_2O_3 + Cr^{3+}$, i.e., ruby.

At room temperature, the ruby doublet exists at 692.9 nm (1.789 eV) and 694.3 nm (1.785 eV), with the primary luminescence peak shifting with decreasing temperature to 693.4 nm (1.788 eV; see M. J. Weber, *Handbook of Laser Wavelengths,* CRC Press, Boca Raton, Florida, 1999).

K. Iakoubovskii and G. J. Adriaenssens's high-resolution photoluminescence data on a Co-grown synthetic diamond ("Comment on 'Evidence for a Fe-related defect centre in diamond,'" *Journal of Physics: Condensed Matter*, Vol. 14, No. 21, 2002, pp. 5459–5460) and Adamas Gemological Laboratory's lower-resolution (0.35 nm quantization/pixel) SAS2000 photoluminescence data on multiple samples and multiple-sourced Ni-Fe catalyst near-colorless synthetic diamonds, clearly show the presence of this "ruby" doublet.

Possibly because of the very, very strong laser-induced broad-band fluorescence in the two samples of Chatham pink synthetic diamonds I have, I have not been able to personally resolve the 693 nm feature using either 488, 514, or 532 nm excitations. This may also be due to the requisite low integration times, although the authors noted that the feature was "rare," occurring in less than one-third of the samples tested, somewhat consistent with our statistics (see web page above) on the feature in near-colorless synthetic diamond. It would be interesting to know whether, in the authors' samples tested, there was a correlation between fluorescence strength and observability of the 693 nm feature.

Martin D. Haske
Brookline, Massachusetts

Reply

We appreciate the opportunity to respond to Mr. Haske's comments, but we disagree with his suggestions. Upon closer inspection (see figure 1), the luminescence feature

Figure 1. These photoluminescence spectra (taken under identical conditions at 77 K) show the classic "ruby doublet" in corundum at 692.0 and 693.4 nm (top) and a different peak at 694.2 nm in a pink synthetic diamond (bottom). The ruby doublet is due to chromium fluorescence, while it is likely the synthetic diamond peak is due to nickel impurities.

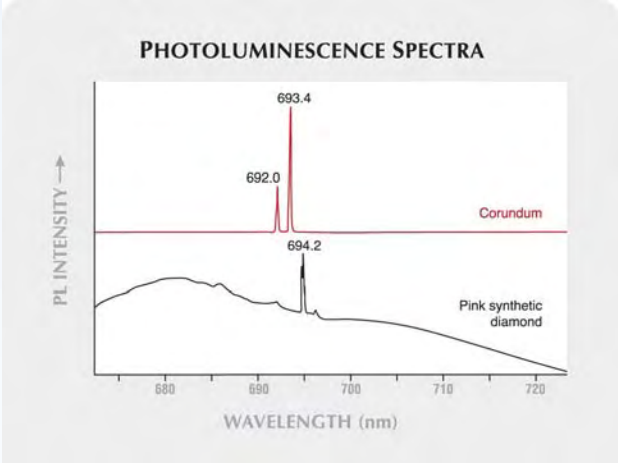

in the pink synthetic diamond spectrum is centered at 694.2 nm, and it lacks a doublet peak at shorter wavelengths. For comparison, a corundum sample was analyzed under identical conditions (i.e., the same instrument and collection parameters and at 77 K; most corundum—from near-colorless varieties to ruby—contains at least small amounts of chromium and thus can exhibit Cr fluorescence peaks at the same positions, depending on the temperature). The position and structure of the chromium fluorescence peaks are very different from the 694.2 nm peak in the pink synthetic diamonds reported in our article. Given the currently available information, the closest, most reasonable correlation for this feature is the 693.7 nm peak attributed to nickel in Zaitsev (2001). Admittedly, the general understanding of photoluminescence features in diamond is evolving, and future research may provide additional information on specific peak positions and causes. Also, we know of no confirmation by other analytical techniques of the occurrence of ruby within submicroscopic inclusions in synthetic diamonds.

While not stated directly in his letter, Mr. Haske suggests on his Web site that this same luminescence feature may be useful as an identification criterion for low-nitrogen synthetic diamonds. We believe this suggestion to also be problematic. This luminescence feature, if interpreted correctly as being due to ruby, is completely inclusion and flux-metal dependent. Unlike other more practical identification features that are based on properties intrinsic to the synthetic diamond or the HPHT growth process (such as color and fluorescence zoning), the occurrence of this so-called "Cr^{3+} fluorescence" depends solely on the quantity of inclusions present and the composition of the flux metals used. These two factors vary widely between manufacturers, and even between growth runs at a single manufacturer, making this feature unreliable and inappropriate as a means of identification. Furthermore, as indicated by Iakoubovskii and Adriaenssens, the analysis spot location (i.e., its proximity to inclusions) dictates whether or not "chromium fluorescence" is observed in a diamond.

Perhaps even more problematic is the fact that inclusions of corundum in natural diamond have been reported on occasion (see, e.g., H. O. A. Meyer and E. J. Gübelin, "Ruby in diamond," Fall 1981 *Gems & Gemology*, pp. 153–156; E. J. Gübelin and J. I. Koivula, *Photoatlas of Inclusions in Gemstones*, ABC Edition, Zurich, 1986, p. 97). GIA is currently working with a natural colorless diamond that contains several blue sapphire inclusions. Figure 2 shows a photoluminescence spectrum collected near one of the corundum inclusions in this diamond using the same operating conditions as used for the spectra in figure 1. In addition to the common diamond peaks, a distinct chromium fluorescence doublet at 692.0 and 693.4 nm is present. The fact that these spectral features can be detected in natural diamonds sheds additional doubt on their reliability for synthetic diamond identification.

James E. Shigley
Christopher M. Breeding
Andy Hsi-tien Shen

Figure 2. The photoluminescence spectrum of a natural colorless diamond with corundum inclusions shows a distinct chromium fluorescence doublet at 692.0 and 693.4 nm. Thus, while this feature has also been observed in some synthetic diamonds, it should not be considered diagnostic.

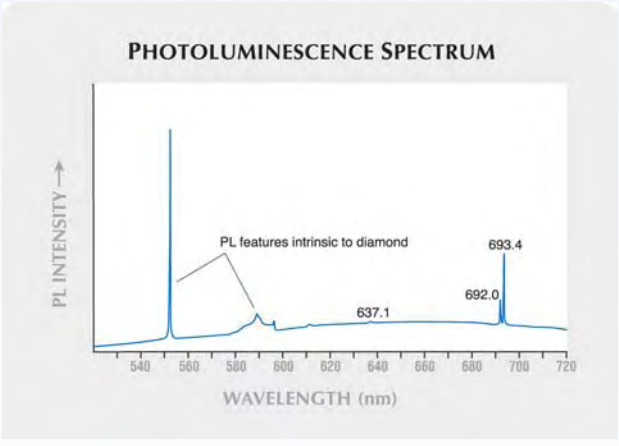

Patents on Treatment Processes for Certain Colored Synthetic Diamonds

The colored synthetic diamonds described by J. E. Shigley and co-authors (Summer 2004, pp. 128–145) include both as-grown samples (especially yellow, blue, and green of type Ib, type IIb, and a mixed Ib + IIb type) and those that were treated after crystal growth (especially green and pink type Ib). Unfortunately, no details of the irradiation or irradiation-plus-heat treatment procedures were given.

Thus, it is worth mentioning that the processes of creating various colors in type Ib synthetic diamonds by irradiation and subsequent heat treatment are described in detail in a series of Japanese (JP), European (EP), German (DE), and United States (US) patent documents, all with priority dates in the late 1980s–early 1990s and all assigned to Sumitomo Electric Industries, Osaka, Japan.

Detailed production information for the following colors is described in these patents:

- Purple: JP 01-131014A, EP 0 316 856 A1, DE 38 78 532 T2, US 4,950,463, priority date November 17, 1987
- Bluish green: JP 01-138112 A, November 25, 1987
- Green: JP 01-183409 A, EP 0 324 179 A1, DE 38 75 604

T2, US 4,959,201, January 13, 1988

- Red and pink: JP 06-263418 A, EP 0 615 954 A1, March 15, 1993.

In a first step, irradiation of type Ib synthetic diamonds is performed by electrons in the 2–4 MeV energy range (to obtain a purple, bluish green, or green color) or in the 1–10 MeV energy range (to obtain red or pink). Subsequently, the synthetic diamonds are annealed in a vacuum at temperatures of 550–600°C (bluish green), 800–1100°C (purple), 1500–1800°C (green), 600–800°C (red), and 800–1100°C (pink). The production of various defect centers (e.g., H2, H3, H4, GR1, and N-V), which are responsible for the different colorations, is also described in detail.

These patent documents may be helpful in understanding the mechanism of color formation and the properties of these treated type Ib synthetic diamonds, and in completing the knowledge necessary for a separation of natural and synthetic samples. For further details, the reader is referred to the documents cited, which are available via the Internet from the respective patent offices.

Karl Schmetzer
Petershausen, Germany

Cut Article Recognizes Contributions of "Outside" Efforts

I very much enjoyed the article, "A Foundation for Grading the Overall Cut Quality of Round Brilliant Cut Diamonds" in the Fall 2004 *G&G* (pp. 202–228). I especially appreciated the references to contributions from amateurs Bob Long, Norm Steele, and Bob Strickland. The article is top notch.

Reading this article called to mind a visit I made to the Henry Ford Museum in Detroit, Michigan. One aim of their exhibits is to show how technology evolves with time. There are wheat harvesting machines in a line ranging from the earliest models to the most current. The same can be said for several other exhibits, such as milk purification machines, artificial lights for cameras, and locomotives. The one lesson that is apparent from these exhibits is that steady improvements usually come from people inside their field. It is the dramatic jumps in technology that come from the fringe players outside of the mainstream. So the world is a result of both types of contributions. *Gems & Gemology* recognizes both, and I couldn't be happier.

Thanks once again for such a great journal as *G&G*.

Bob Ayres
Birmingham, Michigan

THE CREATION OF A MAGNIFICENT SUITE OF PERIDOT JEWELRY: FROM THE HIMALAYAS TO FIFTH AVENUE

Robert E. Kane

The ultimate value of a gemstone suite lies not only in the cost and quality of the materials themselves, but also in the selection of the rough, the quality of the faceting, and the intricacy of the setting in a well-designed and well-manufactured suite of jewelry. This article chronicles the creation of a fine suite of peridot jewelry from the mine in the Himalayas to the manufacture of the necklace, bracelet, ring, and earrings. Eight kilograms (40,000 carats) of peridot rough from the Sapat Valley region of Pakistan was purchased in early 2004. Following the assessment of the rough, careful preforming and faceting produced a precisely matched suite of Asscher-cut peridots. The suite comprises 54 gems ranging from 3.57 to 18.30 ct, for a total weight of 350.40 ct. Van Cleef & Arpels in Paris designed the jewelry, and the New York atelier of Van Cleef & Arpels manufactured the five pieces.

Assembling even one matched pair of gems for earrings can be a difficult process. Assembling an elaborate matched suite—for a necklace, bracelet, ring, and earrings—is the ultimate challenge. Typically, a matched suite is compiled by selecting gems that have essentially the same color, clarity, dimensions, and cutting proportions from a large group of faceted gems. The greater the number of gems to choose from (e.g., hundreds to thousands), the faster a large or intricate matched suite can be assembled. Elaborate suites may take years to complete if they are not intentionally cut from the rough. As gems of the appropriate size, shape, color, and clarity are purchased or come from the cutting factory, they are added one at a time to the suite. Re-cutting of gems that are close in appearance is often necessary. Only rarely does a gem dealer–cutter have the opportunity, take the time, or incur the cost to intentionally fashion a large set of precisely matched gemstones for a jewelry ensemble from a large parcel of rough.

This article describes and chronicles the making of just such an ensemble, the magnificent peridot, diamond, and platinum jewelry suite shown on the cover and in figure 1. The availability of a continued supply of large, fine peridots from a relatively new locality in Pakistan provided the material needed to compile the stones for this suite, which were expertly preformed and faceted by two master craftsmen. Although many excellent books and articles explain the details of jewelry manufacture (see, e.g., Untracht, 1982; Revere, 2001), few also explore the intricacies of creating a suite of haute couture jewelry, as is provided here by a unique visit to the workshops at Van Cleef & Arpels. This article takes the reader from the mines high in the Himalaya Mountains of Pakistan, through the assessment of the rough and the cutting of the faceted gems, to the design and creation of the final jewelry suite.

THE SAPAT VALLEY PERIDOT DEPOSIT IN PAKISTAN

In the early 1990s, the famous Arizona peridot mines supplied 80–95% of the world's peridots;

See end of article for About the Authors and Acknowledgments.
GEMS & GEMOLOGY, Vol. 40, No. 4, pp. 288–302.

Figure 1. This unique suite of peridots and diamonds set in platinum was designed and manufactured by Van Cleef & Arpels. The necklace contains 31 faceted peridots ranging from 3.78 to 13.78 ct, with a total weight of 228.22 ct; the ring stone weighs 18.30 ct; the peridots in the earrings range from 3.57 to 4.55 ct, with a total weight of 24.31 ct, and the bracelet contains 16 matching peridots weighing a total of 79.57 ct. The custom-cut Pakistani peridots were provided by Fine Gems International, Helena, Montana. The diamonds (D-E color, VVS clarity) were supplied by Van Cleef & Arpels. Photo by Harold & Erica Van Pelt.

most of these weighed less than 1 ct, and only rarely did they reach 3 ct (Federman, 1992). Although Burma/Myanmar has long been known to produce some beautiful large faceted peridots (as, historically, has Egypt), such stones have never been consistently available in large quantities.

In 1994, however, extraordinary amounts of fine, large gem peridot entered the international gem and mineral markets (Koivula et al., 1994a; Federman, 1995; Milisenda et al., 1995; Frazier and Frazier, 1997). This new source of peridot was in Pakistan: near Sapat Nala, in the Sapat Valley, Mansehra district, North West Frontier Province (Kausar and Khan, 1996; Hammer, 2004—see figure 2). According to Jan and Khan (1996, p. 17), "the peridot occurs in pockets and veins located in shear zones in partially serpentinized dunitic host rocks." The mine is situated in the western Himalaya Mountains at an elevation of 4,500 m (15,000 feet) above sea level. Koivula et al. (1994a) reported that the mine could be reached by a seven-hour horseback ride and a two-day hike from the closest populated area, Basham Village. The typical route through the Jalkot Valley to the mine is potentially very dangerous and not recommended for nonlocals.

This discovery—along with current production of smaller stones from China, Vietnam, Ethiopia, Tanzania, and Myanmar, as well as Arizona—has transformed peridot into even more of a "mainstream" gemstone for jewelry manufacture around the world. The Pakistani peridot is far cleaner and larger than the Arizona material and typically is more uniform in color than the Burmese material. One of the author's international manufacturing suppliers reported faceting nearly half a million carats of Arizona peridot during the last 15 years, with no more than a handful of clean (nearly flawless) stones over 10 ct produced; the average size of relatively clean faceted stones was about 2 ct. However, over the last three years, his operation has faceted more than 30,000 carats of Pakistani peridot; 35% of the production has been over 5 ct, with nearly one third of these in the 10–20 ct range. The author has even seen the occasional faceted peridot from Pakistan that exceeded 100 ct. As an additional example of the prolific nature of this mine, the author recently examined a beautiful, well-matched Pakistani peridot necklace, ring, and earring suite comprising 16 faceted peridots with a total weight of more than 400 ct. The continued production of large, fine pieces of

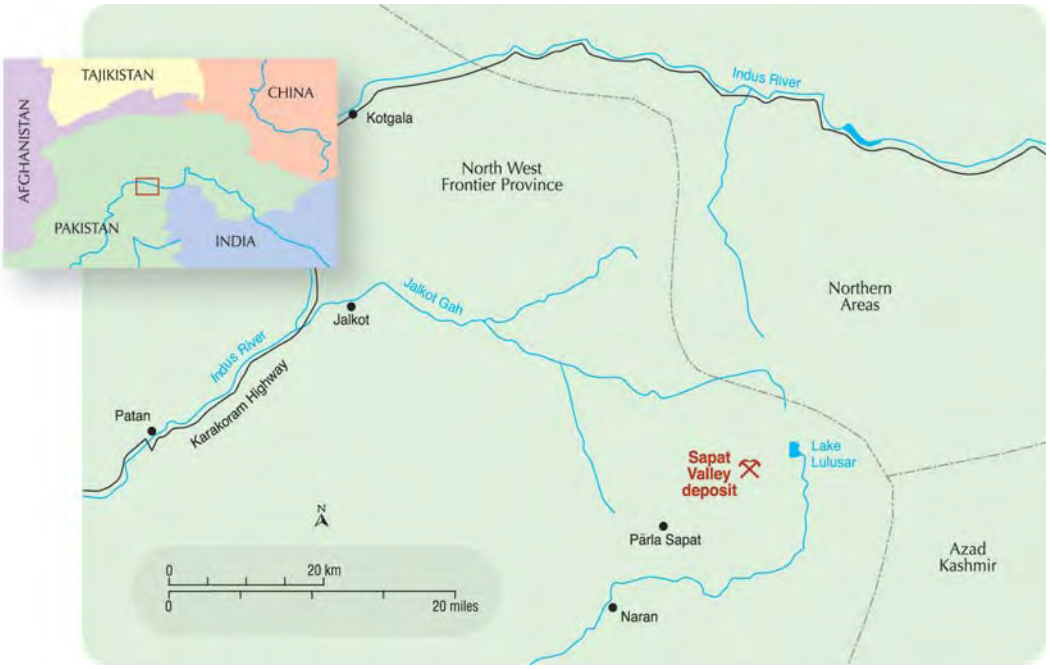

Figure 2. The peridot deposit is located in the Sapat Valley, Mansehra district, North West Frontier Province, Pakistan, about 240 km (by air) north-northeast of Peshawar. The route through Jalkot Valley is dangerous and is not recommended for nonlocals. Note that certain borders in this area are in dispute.

rough from Pakistan has had a significant impact on the jeweler's ability to create attractive designs containing numerous large matched peridots.

GEMOLOGY OF PERIDOT FROM PAKISTAN

As noted above, peridot from Pakistan often occurs as large gemmy crystals. With the exception of the occasionally occurring black acicular inclusions of ludwigite-vonsenite, which are unique to peridot from Pakistan (Koivula et al., 1994b; Milisenda et al., 1995; Peretti and Gübelin, 1996), the gemological properties of Pakistani peridot are consistent with those of peridot from other geographic localities. They are summarized in table 1.

ASSESSMENT AND ACQUISITION OF THE PERIDOT ROUGH

Eight kilograms (40,000 carats) of gem-quality peridot rough from the Sapat Valley, Pakistan, was purchased in February 2004 by an experienced manufacturer. Figure 3 shows some of the larger pieces from this parcel, which yielded a number of the gems in the jewelry suite. Sellers of gem rough typically start with a high asking price, recognizing that they will have to negotiate down. The purchaser must carefully study each piece in the parcel, determining the shape, size, and cutting yield, as well as market demand and the potential selling price of the cut gems, before making an offer. An accurate assessment and a little luck can produce a profit; a miscalculation can result in a loss.

Many of the steps in determining the yield and potential value of the faceted gemstones expected from a rough parcel overlap and are repeated during the sawing and preforming stages (see below). Once the identity of the gem mineral is established (again, see table 1), the rough is examined for color, transparency, and inclusions. Some dealers use a lightbox (again, see figure 3), while others use only a portable, high-intensity flashlight such as one utilizing a xenon light bulb and lithium batteries. The latter produces reliable results in either the field or the office. (For more information on identifying gems in the field, see Boehm, 2002.)

TABLE 1. Properties of peridot from Pakistan[a].

Property	Description
Refractive indices[b]	n_x = 1.648–1.653 n_y = 1.663–1.671 n_z = 1.683–1689
Birefringence[b]	0.035–0.038
Specific gravity[b]	3.29–3.37
Spectroscope spectra	Typical peridot Fe^{2+} absorption[b]: distinct, yet diffuse absorption bands at about 453, 477, and 497 nm, as well as a weaker band at about 529 nm (the last often seen only in large stones)[c]
Internal features	Acicular inclusions of ludwigite-vonsenite[b,c,d]; veils (fingerprints, feathers) composed of tiny fluid inclusions, and growth structures[b]

[a]*The gemological properties of Pakistani peridot are consistent with those of peridot from other geographic localities, with the exception of the ludwigite-vonsenite inclusions (which have not been reported in peridot from any other locality).*
[b]*Milisenda et al., 1995.*
[c]*Koivula et al., 1994b.*
[d]*Peretti and Gübelin, 1996.*

It is important to note that while artificial light is ideal for assessing inclusions, natural daylight is vital when judging color quality. Estimating the color of the completed faceted gem requires a thorough understanding of the relationship between the color observed in the rough crystal and the final face-up color. An excellent discussion on this difficult and complicated subject, as well as other aspects of evaluating gem rough, can be found in Sevdermish and Mashiah (1996). However, when assessing gem rough, there is no substitute for years of experience.

By carefully studying the 8 kg of peridot rough, it was estimated that a 20% recovery of faceted gems (or 8,000 carats) could be produced. Although there were many large pieces of rough (up to 35 g), the presence of inclusions and fractures in nearly all the large crystals meant they would need to be sawn into smaller pieces. Therefore, it was expected that 8–10% of the cut gems would weigh under 1 ct; 10–15% would weigh 1–2 ct, 40–50% would weigh 2–5 ct, and the remaining approximately 25–40% would be stones in the 5–20 ct range. The final average yield of approximately 6,500 ct of faceted stones was 16.2%, slightly lower than the original estimate. Of special significance to this article, the author and the manufacturer decided that an extraordinarily well-matched suite of gems could be cut from the parcel due to the uniformity of color.

Figure 3. This representative selection shows 330 g (1,650 ct) of the larger peridot pieces from the 8 kg (40,000 ct) parcel, from which some of the gems seen on the cover and in figure 1 were cut. The rough has been placed on a light-box (typically composed of a translucent white plastic top, illuminated from below with fluorescent lighting), which is often used to evaluate colored gem rough. Photo by Jeff Scovil.

DESIGNING THE GEMS

If properly executed, the cut of a gemstone showcases the gem's inherent beauty in vibrant color and radiating brilliance. A skilled cutter, or lapidary, can take a seemingly unattractive piece of rough and transform it into a beautiful gemstone. Likewise, an unskilled lapidary can ruin a stone with poor cutting and color orientation, resulting in a dull, unattractive, misshapen gem. Excellent cutting—in both planning and execution—is therefore essential to bringing out the maximum beauty of a gemstone.

A good gem cutter typically fashions a piece of rough for maximum weight retention, while also trying to maximize beauty. This is frequently an ongoing struggle, as the cutter must strike a balance between beauty—which depends on proper cutting proportions, symmetry, and color orientation—and the higher price that a greater weight may bring. Preforming (or pre-shaping), the process of grinding a piece of rough into the approximate shape of the finished stone, is a critical step in maximizing the value of a parcel of rough. In fact, many successful buyers of gem rough are exceptional preformers, and will often personally pre-shape most or all of the parcels of rough they purchase.

The initial steps in the processing of colored stones and diamonds differ significantly. In the "manufacture" of diamonds, a master cutter (or marker) marks the precise cleaving and/or sawing locations on the exterior of the rough diamond crystal using indelible ink ("India ink"). Thereafter, the various processing steps are carried out by different individual professionals, such as the sawyer, cleaver, bruter, and polisher (see, e.g., Watermeyer 1991; Sevdermish and Mashiah, 1996; Caspi, 1997).

In contrast, the colored stone preformer or designer alone typically undertakes nearly all of the processing steps. With many colored gems, this includes breaking (cobbing) or cleaving (of those gems having cleavage), sawing, preforming, and girdling (shaping). Once the preform is produced, it is turned over to the master cutter. He or she is responsible for the placement of the facets and achieving the final polish.

Most of the original 8 kg of peridot rough was preformed in the United States by the manufacturer, who is also a master preformer. The peridots prepared for the jewelry suite described in this article, as well as many other large and important stones

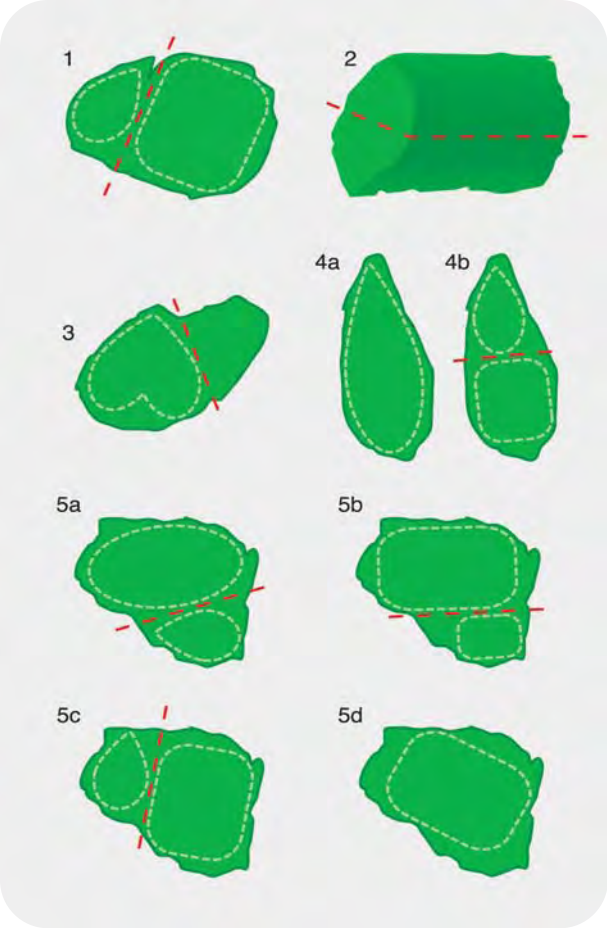

Figure 4. These diagrams illustrate various preform decisions that might be made during the sawing process. The red dashed lines show where the stones would be marked for saw cuts; the white dashed lines indicate the shapes of the gems that would be fashioned from the resulting pieces. Image 1 shows the sawing direction through a veil. Image 2 shows a thick crystal that could be sawn into two pieces from which matching emerald cuts might be faceted. In diagram 3, the red dashed line indicates where this piece would be sawn to remove the included section on the right. The elongated pear shape in 4a might be difficult to sell, so the preformer could decide to cut two smaller gems (4b). In diagram 5, four possible choices are shown for the same piece of rough; factors such as depth, cavities or indentations, and inclusions could influence the final decision. Adapted from Sevdermish and Mashiah (1996).

from the same parcel, were faceted by a European-trained master cutter with 30 years of faceting experience, who now lives in the U.S. Most of the remaining stones were cut in China.

The major design element of the matched peridot suite—the shape, size, and number of gems—was decided early in the preforming process. The Asscher cut (an early emerald cut with very wide corners, a high crown, and a deep pavilion) was selected for its classic look. Although this cutting style accentuates color and brilliance, it also highlights any inclusions present in the gem. Therefore, it was critical that only loupe-clean pieces of rough be used. As the necklace suite neared completion, a trapezoid shape was added as the "center" stone to add interest to the design.

Examination and Marking of the Peridot Rough. The peridot rough was first sorted into parcels based on size. Each size-specific parcel was next examined on a fluorescent light-box and sorted again for clarity using the unaided eye. Then, each piece of peridot rough was held very close to an intense incandescent light source. A bright, bare light bulb can be used for this last step, but many professionals prefer a fiber-optic light. Gently rotating the piece of rough, the preformer observes the colors from different directions; locates fractures and solid inclusions; and visualizes the final shape, size, and table location of the finished gem. The location of the table is critical in determining the face-up color of many faceted gems, because in pleochroic gem materials different colors are seen in the different crystallographic directions.

From this initial evaluation, the preformer can often predict the final weight and monetary value of the completed gemstone—in many cases, even

Figure 5. Sawing is one of the most important steps in gem cutting. The first series of cuts are made through cracks or veils ("fingerprints") in the rough. Here, the preformer uses a high-speed, liquid-cooled saw with a 0.2 mm thick diamond blade on one of the peridots. Photo by Jeff Scovil.

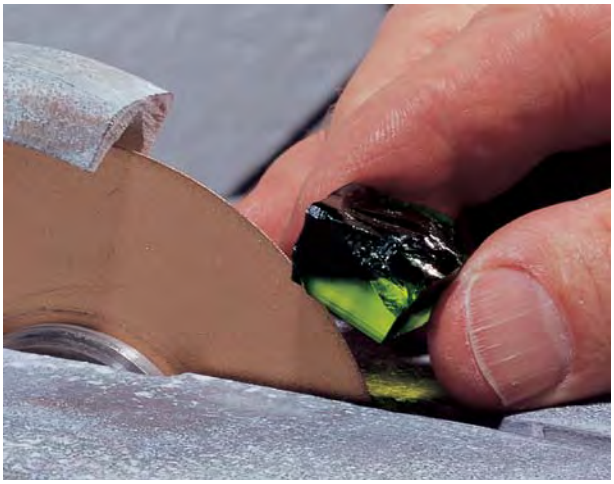

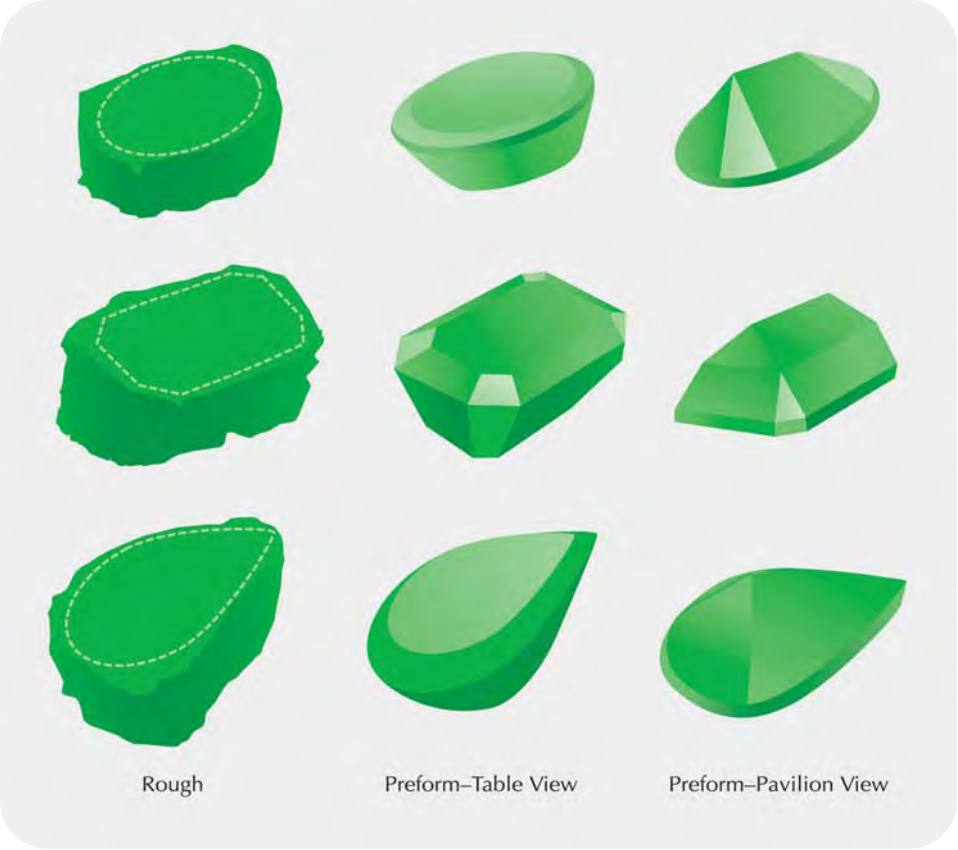

Figure 6. At the preforming stage, the preformer visualizes the shape, proportions, and table location of the finished gem. These idealized diagrams illustrate the transition from rough to finished preform for three popular shapes. Adapted from Sevdermish and Mashiah (1996).

before the first saw cut or grinding. Much of this assessment is done without the aid of magnification, although some preformers use a head-loupe, such as an OptiVisor. During this process, the preformer uses indelible ink to mark areas containing inclusions, deep indentations, and cavities that need to be sawn away, usually directly along fractures and veils, and to plan the final gems (figure 4).

Cobbing of Gem Rough. Another method of removing poorly colored, opaque, included, and/or fractured material (as well as other adhering minerals or matrix) from facetable gem rough is *cobbing*. This can be done by striking the rough with a small metal hammer to remove unwanted areas (Epstein, 1988) or by using a specially designed pair of steel pliers. If the unwanted area does not traverse the piece of rough, pliers are not used because facetable areas may be accidentally crushed or removed. These situations call for the use of a trim-saw (Sevdermish and Mashiah, 1996). Many preformers prefer to use only a saw with expensive gem rough, because it is far more controllable. All of the peridot rough described in this project was trimmed with a saw.

Sawing the Peridot Rough. Following the ink markings (again, see figure 4), the lapidary makes the first cuts using a high-speed, liquid-cooled saw with a sintered diamond blade (figure 5). The blades used for the peridot were a mere 0.2 mm thick. Although somewhat difficult to maneuver (they bend very easily, causing the saw cut to stray off the marked line), these thin blades save material and improve yield.

Next, the preformer evaluates each piece of sawn rough to determine if additional saw-cuts are necessary to produce finished stones with a minimum of weight loss. This is done by again holding the sawn piece up to a bright light to check for any remaining inclusions. If inclusions are still present, the preformer decides whether to remove them by sawing or grinding. Some rough requires multiple saw cuts to produce the desired shape.

Most gem cutters believe that sawing is the most important step in controlling the yield of the rough. Once the sawing of the peridots was completed, all the pieces that lent themselves to Asscher cuts were selected out of the parcel.

Grinding the Preforms. At this stage, the preformer again examines each piece of sawn rough to determine the ideal shape and proportions that can be cut from it (figure 6). As has been pointed out, in many cases this is an ongoing struggle and compromise between weight retention and beauty. In

Figure 7. The sawn piece of rough is then ground against a diamond-impregnated wheel to produce the approximate shape and proportions of the finished gemstone. This step is crucial to the design of the final gem. Photo by Jeff Scovil.

creating the peridot jewelry suite, weight retention was much less of a consideration, since the intent was to create the most precisely matched set possible from the original parcel. The beauty, uniqueness, and rarity of such a suite would more than compensate for the reduced yield.

Figure 8. As the preforms were completed, they were laid out to check for consistency of color (hue, tone, and saturation) from one stone to the next and, for the necklace, to ensure the smooth graduation from large to small sizes. This photo shows the beginning stages of this process; as more preforms were completed they were added, and some (including a few of those shown here) were removed. Photo by Jeff Scovil.

The next step in the preforming process involves grinding the sawn rough into the approximate shape of the finished gem (figures 7 and 8). In this case, three diamond-impregnated wheels—coarse, medium, and fine grit—were used to preform the peridot rough.

Some of the questions the preformer must consider are: Will the culet meet the edge of the rough so as to have the proper total depth, while not wasting too much material? (If not, another shape must be created from this particular piece of rough, and another sawn piece must be chosen for the jewelry suite.) Will the face-up color orientation match the color of the rest of the suite? Is there enough material under the proposed table to enable cutting the proper angles, so that the gem will not be too shallow or windowed? (If not, a smaller stone must be shaped.)

If the stone has great value—for example, a large natural-color ruby—the preformer may first grind the table into place and give the rough to the cutter to polish the table. This enables a clear view into the stone so that a better assessment of color, including distribution and clarity, can be made before the rest of the stone is preformed.

After the table is in place, the sawn rough is ground into the desired shape. While it does not have to be perfect, it does need to follow closely the shape and proportions desired for the final faceted gem (again, see figures 6 and 8). With the peridot suite, care was taken to ensure that the opposing sides of the preforms were parallel. The preformer also made certain that all the proportions (such as crown and pavilion angles, crown height and pavilion depth, table size, even girdle thickness, etc.) were consistent from one preform to the next. Minor corrections needed for these proportions could be made later by the faceter.

Any cracks and inclusions not removed during the sawing process are dealt with at this stage. The peridot suite required very clean stones, so all (or nearly all) inclusions were sawn or ground out of the preforms. However, with gem material for which some inclusions are allowable (such as emeralds), or with very expensive material (such as natural-color Mogok rubies), inclusions are left in the preforms, but the cut is designed to make them as inconspicuous as possible. For example, the performer tries not to place inclusions at or near the culet because they will reflect throughout the fin-

Figure 9. Once preformed, the pieces were delivered to the master cutter. Shown here is the slightly modified, classic Swiss jam-peg system that was used to facet the peridot suite. Photo by Jeff Scovil.

ished stone when viewed in the face-up position.

Some shapes are easier to sell than others, so it is often better to choose a more popular shape even if it results in a greater weight loss from the original rough. The girdles can be rough-cut by hand on the preforming grinder (again, see figure 7), or they can be cut using a girdle-grinding machine. The initial girdling (shaping) of the peridots in this suite was done during the preforming stage.

Once the peridot suite preforms were completed, they were laid out to be sure that the hue, tone, and saturation of the stones matched and, for the necklace, that the transition from large to small sizes was smooth (again, see figure 8). The preforms for the necklace were then sorted into "matched" pairs and delivered to the master cutter with instructions that each pair of opposing stones must have parallel sides and be precisely matched.

Placement and Polishing of the Facets. Several different kinds of faceting approaches and equipment choices exist (see, e.g., Sinkankas, 1984; Sevdermish and Mashiah, 1996). A slightly modified version of the classic Swiss jam-peg faceting system (with copper laps charged with diamond powder) was used to facet this peridot suite (figure 9). Although the jam-peg system is primitive in appearance, an experienced lapidary can produce extraordinarily well-cut gemstones with it, and various versions have long been used by many of the finest cutters in the world. The beauty of the system lies in the fact that it allows flexibility in choosing facet angles and, for the experienced jam-peg cutter, it is faster than the protractor-type (index) system, in which the dop is held mechanically at specific angles (Sinkankas, 1984).

The jam-peg system used to facet the peridot suite includes a dop-stick that is held in the cutter's hand. The flat end of the dop-stick, or rod, has the preformed stone attached by either cold or hot cementing (wax also can be used, as was the case with the peridot suite). The cutter presses the end holding the gem against the diamond-charged, horizontally rotating cutting lap, while the other (pointed) end of the dop-stick is "jammed" into a chosen hole (actually a shallow depression) that corresponds to a particular facet angle relative to the cutting wheel. These holes are precisely placed in a solid surface called an arc (A in figure 10), which was curved metal in the case of the peridot suite project, although other systems employ a flat-surfaced arc, which may be made of either wood or metal. The arc is attached to the table by a vertical support. By positioning the pointed end of the dop-stick into different holes of the jam-peg arc, the cutter determines the angles and position of the facets.

The dividing head (C in figure 10) determines the circumferential angles, as well as additional angles of altitude. A simple octagonal dividing head is adequate for square and rectangular emerald cuts (and was used in the cutting of the peridot suite), whereas a more complex dividing head is required for other shapes (see, e.g., Sevdermish and Mashiah, 1996).

The first step is to facet the crown. The facets are initially formed using a rough-textured lap to remove material quickly. This generates heat, so the rotating lap is cooled with water. The next step is undertaken with a final cutting lap, or pre-polish lap, which removes much less material but produces a slightly smoother, yet still rough surface. This allows the cutter to create all the facets at the

desired angles and sizes. Once the crown is faceted, an ultra-high polish is achieved using a copper lap charged with very fine diamond powder (up to 50,000 grit). Because very little material is removed during the polishing process, much less heat is generated, so water for cooling is not necessary during this final step (for the peridots, however, oil was mixed with the fine diamond powder).

After faceting of the crown is complete, the stone is removed from the dop-stick and cleaned of all adhesive. It is then remounted with the dop-stick perpendicular to the table, so that the uncut pavilion is exposed and the stone is centered on the dop's longitudinal axis. Once the stone is attached and centered on the dop, the cutter repeats the process of placing and polishing facets. The polishing of the girdle is the final stage in the faceting process while the stone is still on the dop-stick.

Sorting, Matching, and Slight Re-Cutting of the Suite. As each matched pair (opposing stones) in the necklace was completed, they were carefully checked to ensure that the color and all proportions were essentially the same. Minor deviations in proportions were remedied by slight re-cutting. Any other objectionable differences would cause the stone to be rejected, and another would be cut to replace it in the suite. The same quality-control process was undertaken for the stones in the bracelet and earrings. As the finished gems were completed, they were positioned to simulate the actual jewelry set (figure 11). The layout was then evaluated to ensure that hues, tones, saturations, and shapes matched, and that there was a smooth transition in sizes in the necklace.

Once we were satisfied with the 54 faceted peridots (which ranged from 3.57 to 18.30 ct, for a total of 350.40 ct), the suite was ready for the next major phase: the design of the jewelry, the cutting of the diamonds, and the manufacture of the finished pieces.

THE DESIGN AND MANUFACTURE OF THE JEWELRY SUITE

The completed matched suite of unset peridots was sold to an American client, who desired well-designed and finely crafted jewelry. Suwa (2001) stated that the highest quality of jewelry fabrication (representing just a few percent of the total market) is accomplished by marrying a well-planned design concept to the highest standards of craftsmanship using the finest materials and taking the necessary time. A superior design is not only aesthetically pleasing, but it also results in a finished piece that is comfortable to wear while it holds the gems securely. For these peridots, the client chose Van Cleef & Arpels to design and manufacture the jewelry.

A Brief History of Van Cleef & Arpels. The venerable firm of Van Cleef & Arpels began in 1896, with the marriage of Estelle Arpels, daughter of Leon, a gem trader, and Alfred Van Cleef, the son of a diamond merchant from Amsterdam. Alfred joined his new brothers-in-law to create a jewelry house. The success of this collaboration allowed them to move,

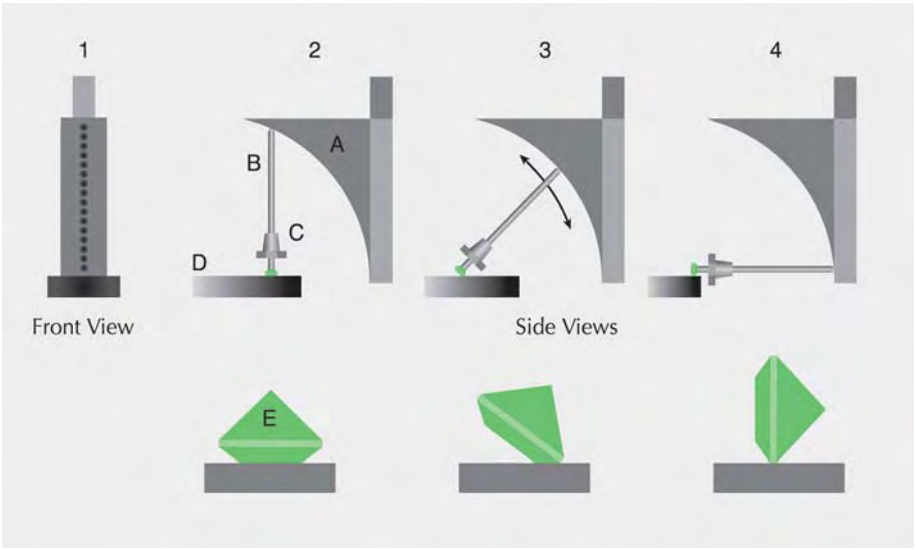

Figure 10. With the jam-peg system, the cutting angles are achieved by using the arc as illustrated here. Image 1 is a front view of the arc, showing the precisely placed holes into which the pointed end of the dop-stick is "jammed." Images 2–4 show the jam-peg process from the side, with A *the arc,* B *the dop-stick,* C *the octagonal dividing head,* D *the cutting lap, and* E *the gem. The position of the dop-stick when cutting the table of a stone is illustrated in image 2, with 3 showing the position for cutting the crown facets (with a similar position, but different angles, for the pavilion facets), and 4 the position used for the girdle. Adapted from Sevdermish and Mashiah (1996).*

in 1906, to the Place Vendôme in Paris, an area renowned for its elegance and luxury, and the headquarters remains located there today.

Van Cleef & Arpels's clients have included royalty and Hollywood legends, as well as other discriminating clientele. In 1956, VCA was designated "official supplier to the Principality" of Monaco, and a decade later their designs were selected from more than 50 proposals for the crown to be used at the coronation of Farah Pahlavi, who was to marry the Shah of Iran.

To this day, Van Cleef & Arpels is renowned for its innovative designs and techniques such as the "invisible setting," in which the prongs are hidden beneath the crown of the gemstone. The company prides itself on using only the highest-quality gems in their superbly crafted jewelry.

Creation of the Design at the Van Cleef & Arpels Paris Atelier. A designer at the Paris atelier was commissioned to produce two very simple yet sophisticated design renderings. The goal was to create a distinctive and attractive suite of jewelry to showcase the peridots. The degree of manufacturing difficulty was not considered as important as the final design.

The first illustration consisted of a modern design composed of uneven lateral baguette diamonds set between the Asscher-cut peridots. The second rendering, the one ultimately chosen by the client, consists of paired baguette diamonds set parallel to one another between the main gemstones in the necklace, and single baguette diamonds between the peridots in the bracelet and earrings, as well as in the back of the necklace. The ring contains two rows of baguette diamonds on each side of the shank, and baguettes on the peridot gallery (figure 12).

Handcrafting the Jewelry at the Van Cleef & Arpels New York Atelier. After the design was approved, the director of production in the New York atelier consulted his foreman to determine which jewelers would work on which pieces of the suite (i.e., the necklace, bracelet, earrings, or ring). The selection was made based on each jeweler's particular area of expertise. The jewelers selected to manufacture various parts of the suite specialized in hand fabrication and, with the exception of the ring, were the in-house experts for making hinges and joining mechanisms. Five different master jewelers worked on the suite, spending a combined total of more than 900 hours.

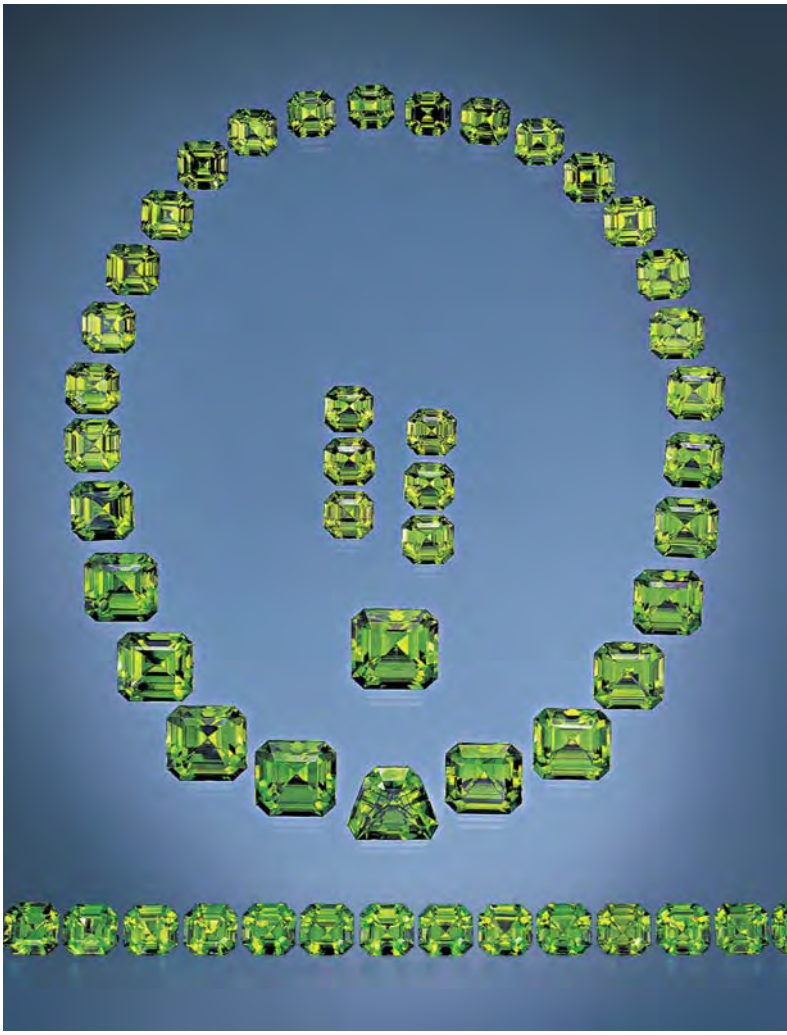

Figure 11. The final selection of cut peridots resulted in this matched suite comprising a total weight of 350.40 ct, with the 54 pieces ranging from 3.57 to 18.30 ct. Photo by Harold & Erica Van Pelt.

Making the Settings. The suite was handmade from a standard platinum alloy consisting of 95% platinum and 5% ruthenium. Pure platinum is soft, whereas platinum alloys are more durable and thus increase the wearability. The settings for all of the peridots include upper and lower galleries (sometimes referred to as bezels) that are joined by four prongs (figure 13). The outside measurements of the upper galleries were made smaller than the outer dimensions of the peridot—so that when finished, no metal would be visible from a top view except for the top portions of the tapered prongs. The upper and lower galleries were made from platinum sheet. Then, the prongs were made by hand using rectangular wire to fit the gallery to the peridot at the appropriate angle.

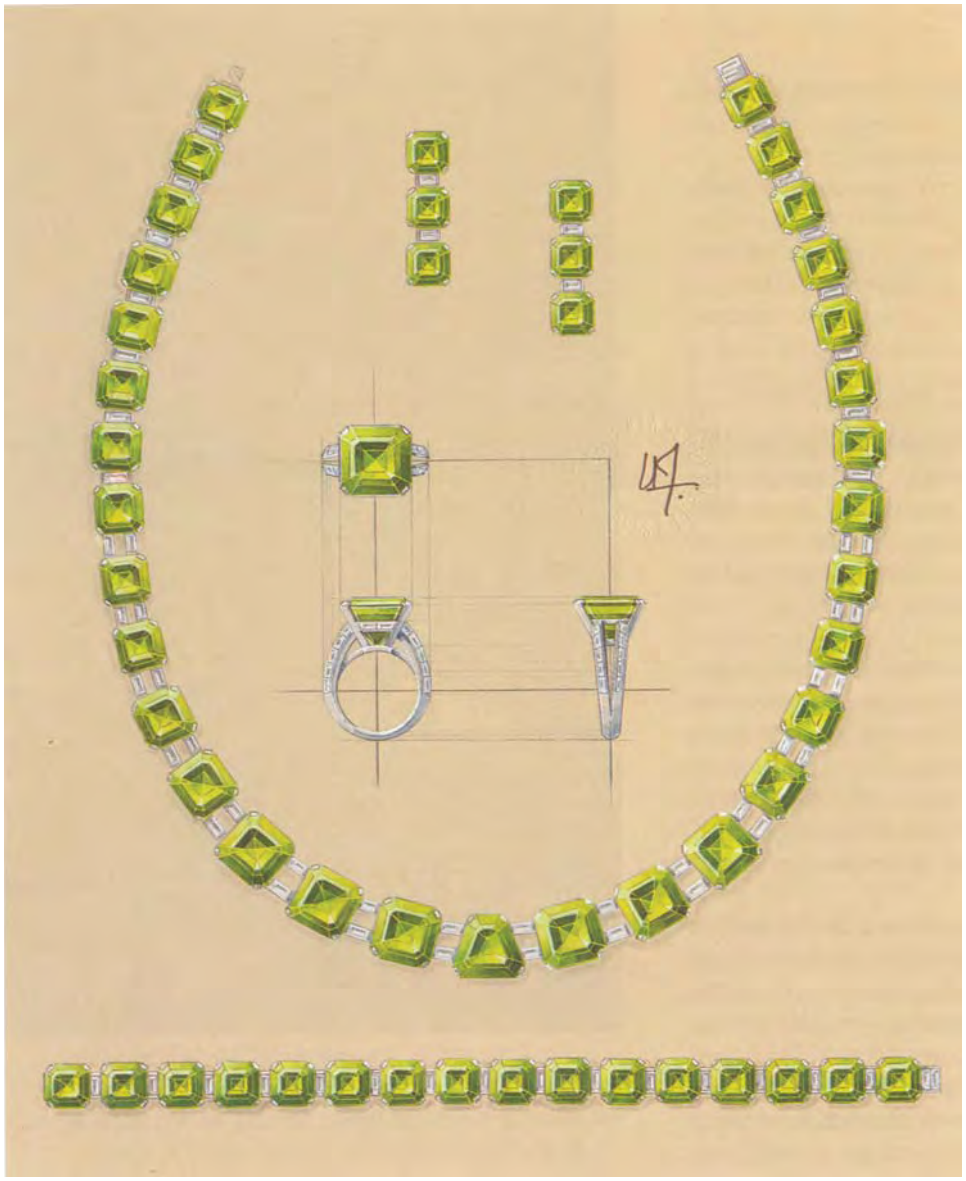

Figure 12. A color rendering of the jewelry suite was created by the Van Cleef & Arpels design team in Paris. This composite image of the designs shows the plans for the necklace, bracelet, ring, and earrings. © Van Cleef & Arpels.

After the gallery pieces and prongs were formed, they were filed, pre-polished, and assembled (figure 14). In contrast to gold, platinum is much more resistant to polishing because of its extreme density. However, platinum also holds its luster through assembly and soldering, so the settings required minimal additional polishing during the finishing process.

The jewelers then made the settings for the baguette diamonds in the necklace, earrings, and bracelet. The metal consisted of two precisely formed pieces of platinum placed on either side of the diamond to secure it, with a channel-type setting running the length of the narrow ends of the baguettes (that, again, was the only metal visible from the top view).

Creating the Hinges and Connectors. Next, the jewelers hand-fabricated the hinges and connectors (figure 15). The connection in a piece of jewelry actually marries the stones and metal. It is extremely important in couture craftsmanship to hide the connections as much as possible, so they are not visible to the unaided eye and do not detract from the essence of the design.

To construct the bracelet, two platinum tubes were attached to the peridot settings and one to the setting for each of the baguette diamonds. Platinum hinge wires were inserted through the tubes to join the bracelet segments. After the bracelet was joined, it was flexible and smooth, moving laterally with no play and evenly following the contour of the wrist when worn.

For the necklace and earrings, special connections were used that when joined can move in two directions, so the necklace lies comfortably on the contour of the neck and the earrings move and dangle freely.

Figure 13. The peridot settings were hand fabricated from sheet and wire platinum. They are composed of upper and lower galleries, and four prongs. The base of the setting, or the lower gallery, is cut out with a jewelers saw. The bearing—a notch cut in each prong with a setting burr—serves as a "seat" for properly positioning and securing the gem. (Note that this schematic diagram is to clarify terminology only; it does not represent the actual peridot settings.)

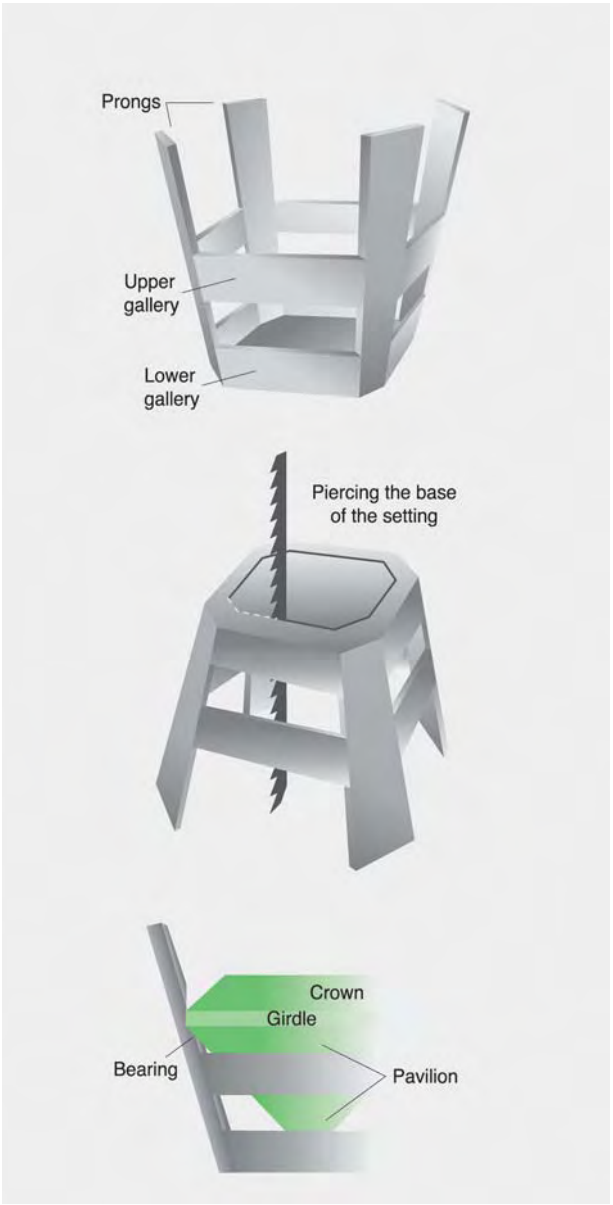

Figure 14. The setting (gallery and prongs) for each of the peridots was handmade to fit that stone. This photo shows the process underway. One tray holds the actual stones placed table-down over a color copy of the rendering; above this is a second tray with another copy of the rendering on which the settings have been placed in their proper position. The master jeweler then files and shapes each setting by hand to ensure the proper fit of the specific gem (inset). Photos by Robert Weldon.

Figure 15. The jeweler hand-fabricates the hinges and connectors for the suite. For the bracelet, two platinum tubes were attached to the peridot settings and one to the settings for the baguette diamonds. Platinum hinge wires were inserted through the tubes to "join" the bracelet; the ends were then flanged. Photo by Robert Weldon.

Figure 16. To set the peridots, a bracelet section comprising three main settings, with baguette diamonds separating the peridots, was put into a shellac stick on the end of a wooden handle. This stick allows the jeweler to firmly hold the section in one hand, while setting the gems using the appropriate tools. Photo by Robert Weldon.

The Finishing Steps. After the fabrication and assembly were completed, the jewelry items were detailed, polished, and finished by the in-house finishing expert. This was done before the peridots and diamonds were set, because polishing various parts prior to assembly enables the jeweler to achieve a mirror finish on areas that would not be easily accessible once all the gems were set.

Upon completion of the individual jewelry settings for the peridot suite, VCA turned to the diamonds. To supply the precisely cut diamonds required, the company either had existing baguettes recut to their specifications or had them specially cut from the rough. Not only were the diamonds cut to the proper length, but in areas where the necklace curves (essentially, the front half) and in the ring, the ends of many of the diamonds also had to be fashioned to the proper angle so they would fit perfectly into the settings. Incorporated into the suite's various jewelry pieces are more than 90 diamonds, with a total weight of approximately 21 carats. All are D-E color and VVS or better clarity.

After the finishing process, the settings, diamonds, and peridots were given to two different setters—one for the diamonds and another, who specializes in large colored stones, for the peridots (figure 16). More time and care is required to set peridots—than, for example, sapphires—because of their only fair to good toughness and $6\frac{1}{2}$–7 hardness.

The colored stone setter begins by vertically tapering the outside of the prongs; the bearings are then cut with a setting burr, and the peridot is placed at the proper height and evenly in the prong bearings (figure 17). At this point, the prongs are

Figure 17. Using a sanding wheel on a flexible shaft-motor, the setter vertically tapers the outside of the prongs holding the peridots (left). Bearings are then meticulously cut in each prong slightly above the upper gallery wire where the peridot will finally be seated (center), and the peridot is carefully positioned in the prong bearings (right). Photos by Robert Weldon.

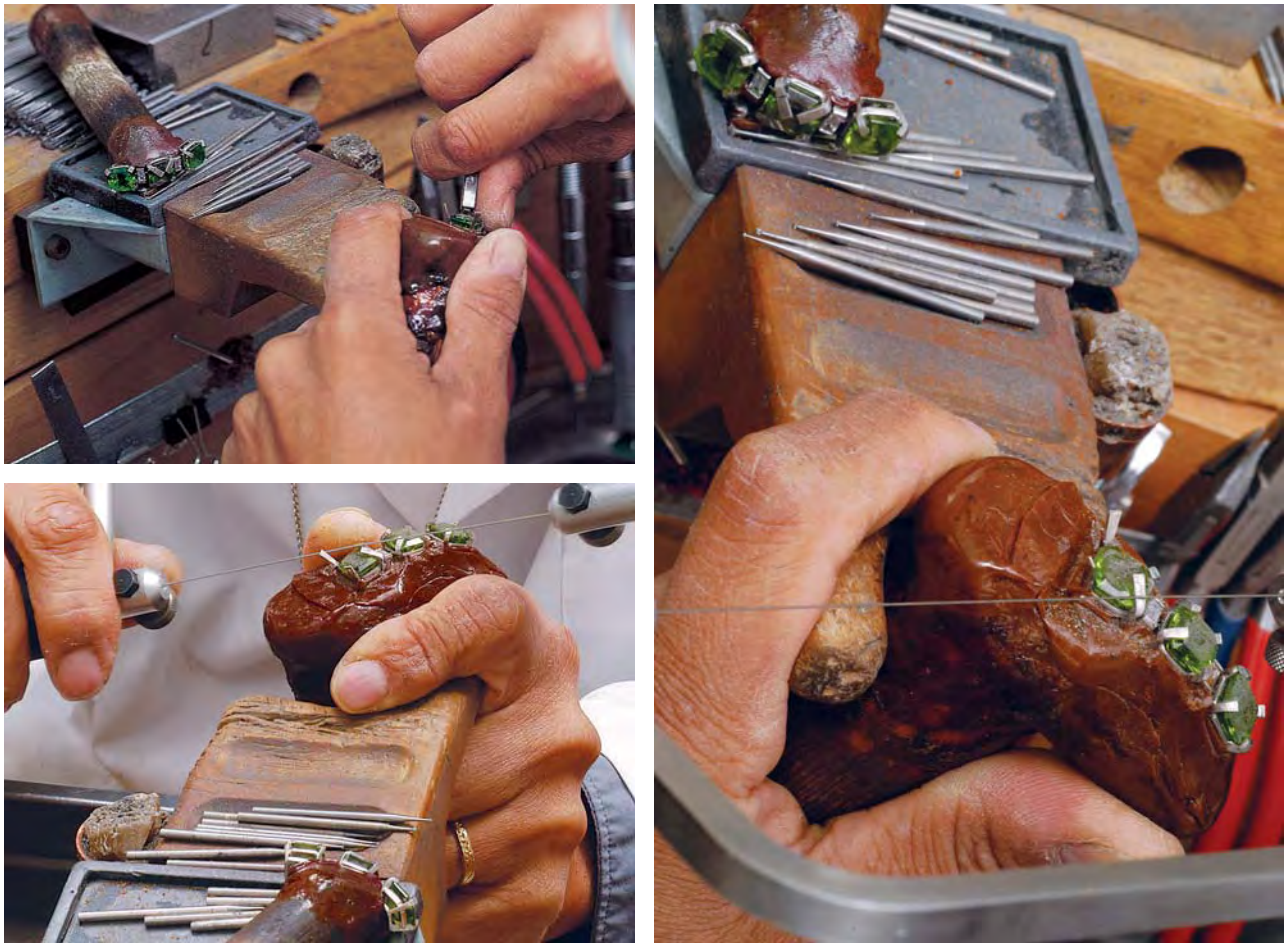

Figure 18. The setter uses a prong-pusher to bend the prongs one at a time over the crown at each corner (upper left). The prongs are then carefully shortened using a jeweler's saw (lower left and right). Photos by Robert Weldon.

pushed, one at a time, over the corners of the crown. A jeweler's saw is used to cut the prong to the correct length (figure 18). Great care is taken to keep the saw blade from touching the peridot, as this would damage it. Last, the prongs are filed and polished.

The primary goal was to set the peridots as low as possible without letting the culets extend below the bottom gallery. After setting, they were perfectly even and at the same height in each multistone piece.

Making the Ring. Although the above procedure was applied for the necklace, earrings, and bracelet, a somewhat different process was used for the ring. This mounting started with a model that was precisely hand-carved from a special wax used exclusively for items with intricate detail. The master wax model was then cast in platinum and the platinum perfected by filing and polishing. To create the sharpest and most precise details, which are not possible with lost wax casting, the ring was completed by hand fabricating the remaining components. Sheet and wire platinum were used to create the upper and lower galleries and the four prongs that would encase the peridot. The upper portion of the inside ring shank was then carefully crafted (figure 19). After the components were soldered, the peridot and all 24 specially cut diamonds were fitted prior to pre-finishing, polishing, and then setting.

CONCLUDING THOUGHTS

During the past 30 years, the gem and jewelry industries have been blessed with a plethora of new gem deposits around the world, yielding extraordinary qualities and quantities of a wide variety of gemstones. The discovery in the early 1990s of the Sapat Valley peridot deposit is an exceptional example. The consistent availability of large, fine pieces of rough from Pakistan has had a significant impact on the jeweler's ability to create beautiful designs

Figure 19. The main component of the ring was lost wax cast in platinum. The setting for the peridot (comprising the upper and lower galleries, and four prongs) was hand-fabricated from platinum sheet and wire. The upper inside-shank section was carefully fit to the ring (inset), before soldering and trimming. Photo by Robert Weldon.

with important stones. The added benefit of an expert preformer and faceter, as well as the talented designers and craftspeople at Van Cleef & Arpels, enabled the creation of the matched necklace, bracelet, ring, and earring suite described in this article. If the gem dealer, cutter, and jeweler are innovative and look for such opportunities, extraordinary jewelry can be produced.

ABOUT THE AUTHOR

Mr. Kane is a noted research gemologist and president of Fine Gems International, Helena, Montana (finegemsintl@msn.com).

ACKNOWLEDGMENTS: The author thanks the staff of Van Cleef & Arpels (in Paris and New York) for their extraordinary professionalism and kind cooperation. He also thanks Mark and Lainie Mann for very useful information regarding the manufacture of jewelry, and Erica and Harold Van Pelt, Jeff Scovil, and Robert Weldon for their exceptional photographs. The author holds a shared copyright with the photographers and GIA on all the photographs in this article.

REFERENCES

Boehm E. (2002). Portable instruments and tips on practical gemology in the field. *Gems & Gemology*, Vol. 38, No. 1, pp. 14–27.

Caspi A. (1997) Modern diamond cutting and polishing. *Gems & Gemology*, Vol. 33, No. 2, pp. 102–121.

Epstein D.S. (1988) Amethyst mining in Brazil. *Gems & Gemology*, Vol. 24, No. 4, pp. 214–228.

Federman D. (1992) Gem profile: Arizona peridot: Desert green. *Modern Jeweler*, Vol. 90, No. 5, pp. 39–40.

Federman D. (1995) Gem profile: Pakistan peridot. *Modern Jeweler*, Vol. 94, No. 8, p. 14.

Frazier S., Frazier A. (1997) The perils of peridot pursuit. *Lapidary Journal*, Vol. 50, No. 12, pp. 18–23.

Hammer V.M.F. (2004) The many shades of Pakistan's green gemstones. In *ExtraLapis English No. 6: Pakistan—Minerals, Mountains & Majesty*, Lapis International, LLC, pp. 64–71.

Jan M.Q., Khan M.A. (1996) Petrology of gem peridot from Sapat mafic-ultramafic complex, Kohistan, NW Himalaya. *Geological Bulletin, University of Peshawar*, Vol. 29, pp. 17–26.

Kausar A.B., Khan T. (1996) Peridot mineralization in the Sapat ultramafic sequence, Naran-Kohistan, Pakistan. *Geologica*, Vol. 2, pp. 69–75.

Koivula J.I., Kammerling R.C., Fritsch E., Eds. (1994a) Gem News: Peridot from Pakistan. *Gems & Gemology*, Vol. 30, No. 3, p. 196.

Koivula J.I., Kammerling R.C., Fritsch E., Eds. (1994b) Gem News: More on peridot from Pakistan. *Gems & Gemology*, Vol. 30, No. 4, pp. 271–280.

Milisenda C.C, Bank H., Henn A. (1995) Peridot aus Pakistan. *Zeitschrift der Deutschen Gemmologischen Gesellschaft*, Vol. 44, No. 2/3, pp. 33–42.

Peretti A., Gübelin E.J. (1996) New inclusions in Pakistani peridot: Vonsenite-Ludwigite needles. *Jewel Siam*, Vol. 6, No. 6, pp. 68–69.

Revere A. (2001) *The Art of Jewelry Making: Classic & Original Designs*. Sterling/Chapelle, New York, 144 pp.

Sevdermish M., Mashiah A. (1996) *The Dealer's Book of Gems and Diamonds*, Vols. I and II. Kal Printing House, Israel, 1004 pp.

Sinkankas J. (1984) *Gem Cutting: A Lapidary's Manual*, 3rd ed. Van Nostrand Reinhold Co., New York, 365 pp.

Suwa Y. (2001) *Gemstones: Quality and Value, Volume 3—Jewelry* (English edition). Sekai Bunka Publishing Inc., Tokyo, 144 pp.

Untracht O. (1982) *Jewelry Concepts and Technology*. Doubleday Books, New York, 864 pp.

Watermeyer B. (1991) *Diamond Cutting*, 4th ed. Publ. by the author, Johannesburg, South Africa, 405 pp.

AN UPDATED CHART ON THE CHARACTERISTICS OF HPHT-GROWN SYNTHETIC DIAMONDS

James E. Shigley, Christopher M. Breeding, and Andy Hsi-Tien Shen

A new chart, supplementing the one published in the Winter 1995 issue of *Gems & Gemology*, summarizes the features of both as-grown ("non-modified") and treated ("modified") synthetic diamonds currently in the gem market (that is, those grown by the high pressure/high temperature technique). It includes photographs of visual features, information about visible-range absorption spectra, and illustrations of growth-structure patterns as revealed by ultraviolet fluorescence imaging. The chart is designed to help gemologists recognize the greater variety of laboratory-created diamonds that might be encountered today.

Almost a decade ago, Shigley et al. (1995) published a comprehensive chart to illustrate the distinctive characteristics of yellow, colorless, and blue natural and synthetic diamonds. The accompanying article reviewed synthetic diamond production at the time, and discussed how the information presented on the chart was acquired and organized. It also included a box that provided a "practical guide for separating natural from synthetic diamonds." The chart was distributed to all *Gems & Gemology* subscribers, and a laminated version was subsequently made available for purchase.

Since that time, and especially within the past several years, the situation of synthetic diamonds in the jewelry marketplace has become more complicated. Lab-created colored diamonds are now being produced in several countries (including Russia, the Ukraine, Japan, the U.S., and perhaps China and elsewhere), although the quantities continue to be very limited. And today they are being sold specifically for jewelry applications (figure 1), with advertisements for synthetic diamonds seen occasionally in trade publications and other industry media. Recent inquiries to three distributors in the U.S.—Chatham Created Gems of San Francisco, California; Gemesis Corp. of Sarasota, Florida; and Lucent Diamonds Inc. of Lakewood, Colorado—indicate that their combined production of crystals is on the order of 1,000 carats per month (mainly yellow colors), a quantity that does not meet their customer demand.

The synthetic diamonds currently in the gem market are grown at high pressure and high temperature (HPHT) conditions by the temperature-gradient technique using several kinds of high-pressure equipment (belt, tetrahedral, cubic, and octahedral presses as well as BARS apparatuses), and one or more transition metals (such as Ni, Co, and Fe) as a flux solvent/catalyst. Typical growth temperatures are 1350–1600°C. Some lab-grown diamonds are being subjected to post-growth treatment processes (such as irradiation or annealing, or both) to change their colors (and, in some cases, other gemological properties such as UV fluorescence). Thus, the gemologist is now confronted with the need to rec-

See end of article for About the Authors and Acknowledgments.
GEMS & GEMOLOGY, Vol. 40, No. 4, pp. 303–313.

Figure 1. HPHT-grown Synthetic diamonds are now available in the gem and jewelry marketplace, as is evident from this attractive 1.00–1.25 ct synthetic yellow diamond jewelry provided by Gemesis Corp. (the colorless diamonds are natural) and the (each under 1 ct) loose synthetic diamonds from Lucent Diamonds and Chatham Created Gems. Composite photo: jewelry images courtesy of Gemesis Corp.; loose diamond photos by Harold & Erica Van Pelt.

ognize faceted synthetic diamonds with colors that are not only "as-grown" (yellow to yellow-brown to brown, blue, green, and colorless), but also result from post-growth treatment processes (yellow, yellow-brown, brown, pink, red, purple, green, or blue-green), as described in Shigley et al. (2004).

While the information presented in the 1995 chart remains valid, the contents of the updated chart reflect the wider variety of HPHT-grown synthetic diamonds now in the marketplace[1]. However, this new chart is not a comprehensive guide to the identification of as-grown and treated synthetic diamonds; rather, it provides an overview of the common characteristics of these materials, which can be helpful in separating them from their natural counterparts.

Recently, synthetic diamonds suitable for jewelry use have also been produced in small numbers at high temperatures but low pressures by the chemical vapor deposition (CVD) process. This material, which is not yet commercially available for jewelry purposes, has very different gemological properties from HPHT-grown samples and, therefore, is not included in this new chart. For further information on CVD-grown material, see Wang et al. (2003) and Martineau et al. (2004).

[1]Reports in the scientific literature indicate that as-grown synthetic diamonds with a green color can also be produced when growth occurs from a nickel solvent-catalyst along with a component in the flux that actively combines with nitrogen (i.e., a nitrogen "getter"; see Chrenko and Strong, 1975; Kanda, 1999). To the best of our knowledge, this kind of synthetic diamond is not presently available in the market.

CONTENTS OF THE NEW CHART

The new chart is organized differently from the one published in 1995 (figure 2). Given the greater amount of information and broader variety of material available, the present chart focuses entirely on synthetic diamonds and does not include entries for natural diamonds. (The reader is directed to the references cited in Shigley et al., 1995—and information provided on that chart—for information on natural as well as early synthetic diamonds. Also, during the past decade, several books and articles have described many of the features of both natural and lab-created diamonds; these are listed in the Additional Reading section at the end of this article.)

Regardless of their color, synthetic diamonds grown by the HPHT technique from a molten metal flux have some common characteristics as a result of their growth conditions. These include their cuboctahedral crystal shape (figure 3), growth features (such as surface markings, color zoning, and graining), and metallic inclusions. Representative photos and photomicrographs illustrating these three types of characteristics are grouped together across the upper portion of the new chart as a way to emphasize their common occurrence in HPHT-grown synthetic diamonds from all current manufacturers.

The lower portion of the chart is divided into two sections—one for information on synthetic diamonds with as-grown (or "non-modified") colors, and the other for those with treated (or "modified") colors (figure 4). For the latter, the entries are divid-

Figure 2. The chart published by Shigley et al. in 1995 included information on natural diamonds as well as on the kinds of HPHT-grown synthetic diamonds available at that time.

ed into the following four categories: (1) HPHT annealing, (2 and 3) irradiation plus annealing at two different temperatures, and (4) irradiation only. Organizing information in this way is not meant to imply that the distinction of untreated and treated colors in synthetic diamonds is important. Rather, it is designed to help the gemologist who must test an unknown sample with a color that might not at first be considered typical of synthetic diamonds. In addition, in some cases—such as yellow or green—the color may be either as-grown or treated.

In this lower portion of the chart, the entries are presented in a column format by color and diamond type (a grouping of diamonds into one of several categories based on their physical and spectral properties; see, e.g., Fritsch and Scarratt, 1992; Wilks and Wilks, 1994, pp. 62–82). Presenting information in this way provides a basis for better understanding the properties of the samples in each category. The visual features summarized in these two sections are supplemented by representative visible-range absorption spectra, as well as by ultraviolet fluorescence images of growth structure obtained with the Diamond Trading Company (DTC) DiamondView instrument (Welbourn et al., 1996). Such data are increasingly important to confirm the identity of some synthetic diamonds. Information obtained by nondestructive chemical analyses for transition metals (such as Ni and Fe), as well as by other spectroscopic (infrared and photoluminescence), cathodoluminescence, and analytical techniques available in the larger gemological laboratories, may also be useful for synthetic diamond recognition.

The information presented in the chart is based on data collected at GIA over the past 25 years on approximately 500 synthetic diamonds from all known sources of production. The photos and photomicrographs were selected to illustrate those visual features of lab-grown diamonds useful for identification purposes.

We do not indicate the manufacturer or distributor of the synthetic diamonds illustrated on the chart for two reasons. First, we know that once a synthetic diamond is sold in the trade, such information may no longer be available (unless a distinctive marking visible with magnification is placed on the girdle surface

Figure 3. HPHT-grown synthetic diamond crystals are usually cuboctahedral in shape, as illustrated by these colored synthetic diamonds from Chatham Created Gems, which weigh between 0.44 and 1.74 ct. Photo by Maha Tannous.

Figure 4. Synthetic diamonds currently sold for jewelry purposes display a range of as-grown and treated colors. The as-grown yellow crystal (2.43 ct) and three yellow faceted samples (0.28–0.84 ct) shown on the left represent the most common kind of synthetic diamond produced today. The colors of the green-to-blue faceted samples (0.20–0.40 ct) shown in the center also were produced during growth. In contrast, the pink-to-pinkish purple colors of the faceted samples (0.16–0.50 ct) shown on the right result from post-growth treatment processes. Photos by Maha Tannous.

by the manufacturer [see below]). Second, since each commercial source uses the same basic HPHT growth technique (although, possibly, with different equipment and procedures), all synthetic diamonds created with this method have many similar gemological properties that do not necessarily allow for a differentiation of the products of various manufacturers.

The visible absorption spectra included in the chart (collected at liquid nitrogen temperature) illustrate the general pattern of spectral features for each kind of synthetic diamond. These features correspond in some instances to those that might be seen using a desk-model spectroscope, and they give rise to the colors of the synthetic diamonds. Specific sharp absorption bands shown on the chart may or may not be present in the spectrum of a particular sample for several reasons (i.e., the type of sample, the method of growth, the flux metals used during growth, and the manufacturer, as well as the type of spectrometer and the data collection conditions). Conversely, other synthetic diamonds may exhibit additional spectral features not shown here. The interested reader is referred to the more complete descriptions of diamond spectra that have been published (see Wilks and Wilks, 1994; Collins, 2000, 2001; and Zaitsev, 2001).

The organization of information in the chart requires some clarification. First, in both natural and synthetic diamonds there are variations in nitrogen and boron contents, and in the degree of nitrogen atom aggregation. Both these factors define diamond type (i.e., type I, type II). Thus, the various type designations actually fall along a continuum, rather than being completely distinct categories as implied by the columnar organization of the lower portion of the chart. Also, with regard to "non-modified" (or as-grown) versus "modified" (or treated) colors, in reality, HPHT growth conditions and HPHT treatment conditions may in some instances (e.g., "yellow/brown," as-grown and as treated with HPHT annealing) be very similar. Consequently, one might see a corresponding similarity in the properties of some synthetic diamonds of the same color listed on the lower left and lower right portions of the chart. Last, the information given represents a consensus of observations on the synthetic diamonds that GIA has documented to date. In some cases (for example, irradiated green synthetic diamonds), only a limited number of samples were available to us for examination. As we study more samples in specific color groups, certain information may need to be expanded or modified.

It should be emphasized that we have not observed all the features shown on the chart in every synthetic diamond we have examined. Rather, all synthetic diamonds we have documented exhibited one or more of the distinctive properties listed here. This reinforces the importance of basing identification conclusions on as wide a variety of properties as possible rather than on just one or two features.

SYNTHETIC DIAMOND IDENTIFICATION

The ability to recognize a synthetic diamond first requires an understanding of the kinds of as-grown and treated materials that are now available. Overall production of gem-quality crystals remains very limited—to the best of our knowledge, perhaps 12,000 carats per year. Almost all are colored crystals up to about 2 ct (with faceted material up to about 1 ct). It is now possible to produce synthetic diamonds that contain little nitrogen and, as a result, might not be strongly colored. However, growth of type IIa colorless material continues to be difficult to achieve in the laboratory, and we do not believe it is available in significant quantities for jewelry purposes. GIA has documented only a few faceted colorless synthetic diamonds obtained from the gem trade during the past decade (see, e.g., Rockwell, 2004).

In recent years, improvements in growth technology and techniques have resulted in colored synthet-

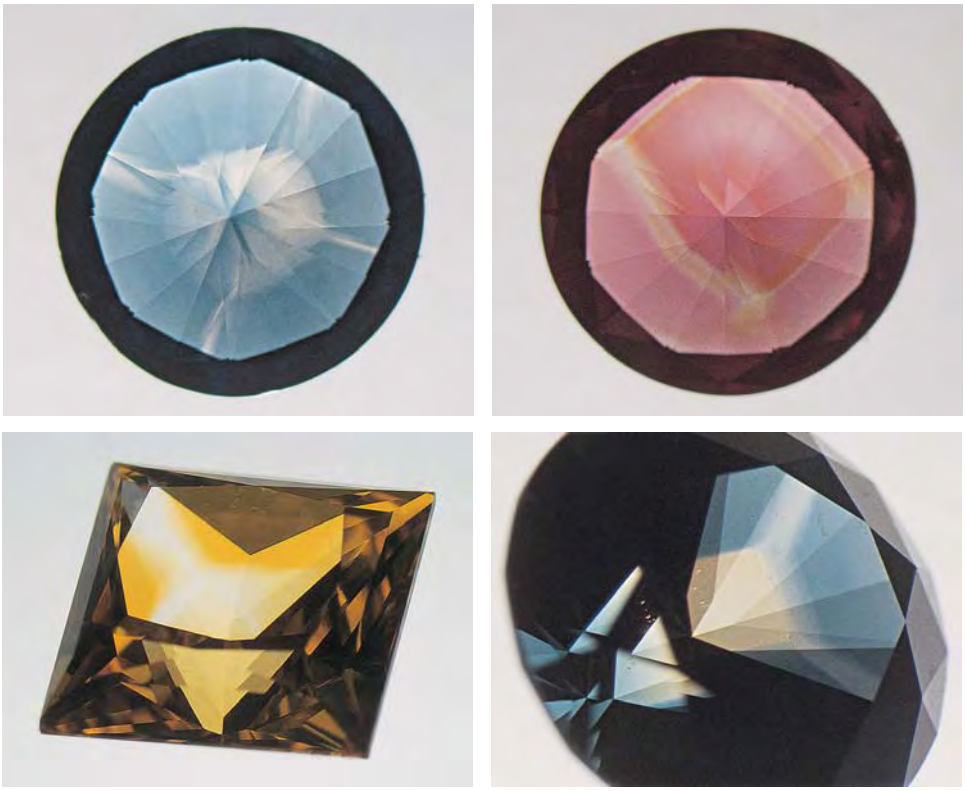

Figure 5. Colored synthetic diamonds often exhibit distinct color zoning due to differences in impurity contents between internal growth sectors. These four examples (0.17–0.68 ct) illustrate how these zoning patterns often appear as seen through the crown and pavilion facets. Immersing the material in a liquid (here, water) can aid in the observation of these patterns. Photos by J. E. Shigley; magnified 20×.

ic diamond crystals that are larger, have lower impurity contents, and are better quality. This finer quality is evident in the presence of few if any metallic inclusions and flaws, as well as less obvious color zoning in some cases. Nonetheless, lab-created diamonds can still be recognized by a variety of methods. Numerous articles (including the present one) and shorter reports describing these methods, which were published in *Gems & Gemology* over the past 30 years, have been collected together for a special volume that will be made available by GIA in early 2005 (Shigley, in preparation). By reviewing this information, as well as what is presented on this chart, the gemologist will be better prepared to recognize this material. The key identifying features of synthetic diamonds are summarized below.

Crystal Shape and Growth Structure. Natural diamond crystals typically exhibit an octahedral form, with many variations due to growth and/or dissolution (Orlov, 1977, pp. 59–106; Wilks and Wilks, 1994, pp. 108–126). In contrast, synthetic diamonds usually have a cuboctahedral form (again, see figure 3), which overlies a geometric arrangement of octahedral, cubic, and dodecahedral internal growth sectors. In a vertical orientation, these sectors radiate upwards and outwards from the seed location at the base of the crystal (see Welbourn et al., 1996, p. 162, figure 5). Diamond crystallization is accompanied by the incorporation of different amounts of impurities in these sectors—thus leading to a segregation of these impurities between sectors. Differential incorporation of impurities gives rise to the distinctive zoning of color, graining, and luminescence seen in many synthetic (as compared to natural) diamonds. When present, boundaries between adjacent color zones are usually sharp and planar (figure 5); they also may intersect to form angular patterns. Adjacent zones may be distinguished merely by lighter and darker appearances of the same color, or by zones of very different color. For example, certain lab-grown green samples now being sold by Chatham Created Gems exhibit both yellow and blue growth sectors when examined with a microscope (see Shigley et al., 2004). Post-growth color treatment processes do not obscure or remove these distinctive visual features, although it may be possible to lessen the visibility of the color zoning during growth (especially if one growth sector predominates within the crystal, while other sectors of differing color are smaller and thus less obvious).

Careful examination using a gemological microscope and different lighting techniques is the best way to see this growth sector–related color zoning in lab-grown diamonds. Immersion of the sample in a liquid (even water) for better observation is also

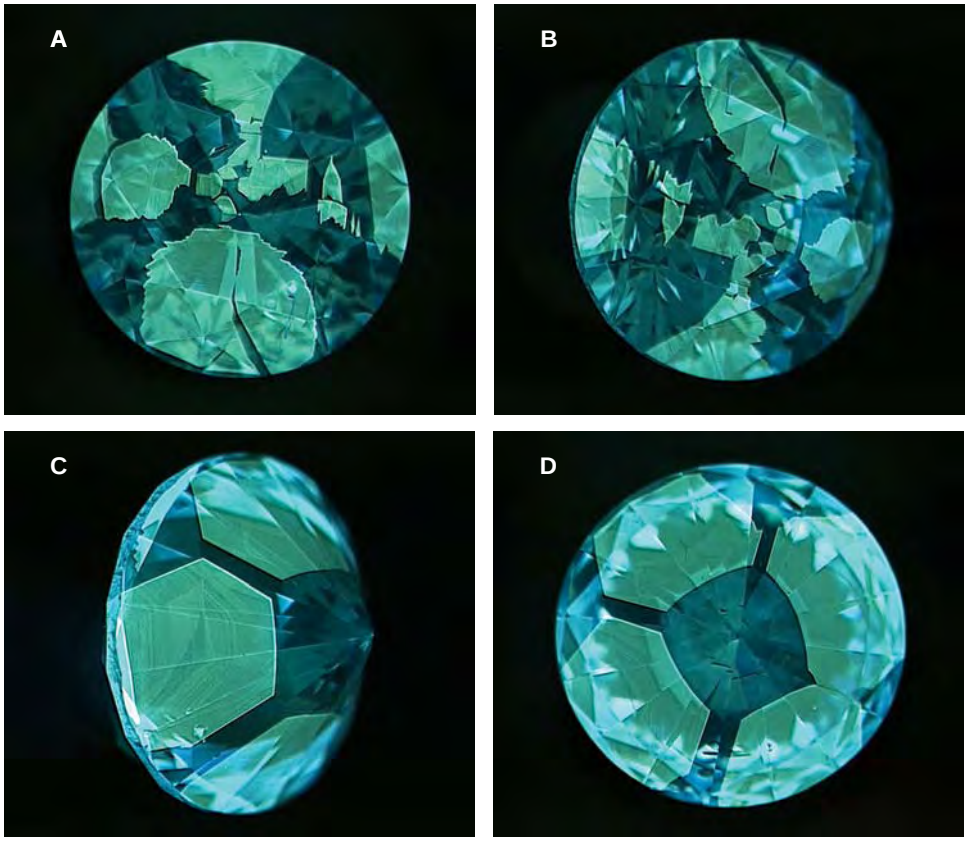

Figure 6. These four DTC DiamondView images of a 0.43 ct blue synthetic diamond illustrate the changing pattern of fluorescent and nonfluorescent growth sectors seen as the sample is rotated. The face-up view (A) shows the four-fold, cross-shaped fluorescence pattern typical of HPHT-grown synthetic diamonds, although in this orientation the sample displays a slightly complicated arrangement of growth sectors. As the sample is rotated toward the pavilion (B and C), the growth sector arrangement becomes more regular in structure. Fine growth striations (resulting from slight variations in impurity contents during growth) are visible within the yellowish fluorescing sectors in the pavilion views (C and D). Images by Andy Shen.

helpful. Such zoning should be evident as well when the sample is examined with a standard UV fluorescence unit or the DTC DiamondView. Depending on the viewing orientation, the zoning can display two-, three-, or four-fold patterns related to the diamond's cubic crystal symmetry. In most cases, the table facet of a polished sample is oriented approximately parallel to the cube face of the original crystal for maximum weight retention during faceting. Therefore, it is often best to look for any four-fold color or fluorescence zoning pattern by observing through the table or crown facets—or, alternatively, nearly parallel to the girdle facets—while rotating the sample. The key is to examine a sample in several orientations to look for changes in color or fluorescence separated by distinct planar boundaries (figure 6).

Inclusions, Graining, and "Strain" Patterns. Unless they are prevented from forming during growth, or are physically removed during faceting, metallic inclusions are a common feature in many polished synthetic diamonds. They may be rounded, elongate, or irregular in shape, and will appear opaque in transmitted light and dark gray-to-black (sometimes with a metallic luster) in reflected light. They may occur singly or in groups, and can vary in size. In some cases, their large size makes them virtually eye-visible (figure 7); whereas in other instances, they are so tiny as to be described as "pinpoint" inclusions, which are often seen in diffuse, cloud-like arrangements (figure 8). (Note that although some of these pinpoint inclusions may be metallic, others may represent different phases formed during synthesis.) Some of these inclusions may even be

Figure 7. Metallic inclusions, such as those shown in this 0.26 ct pink sample, are a distinctive visual feature of many HPHT-grown synthetic diamonds. Photomicrograph by Shane McClure; magnified 25×.

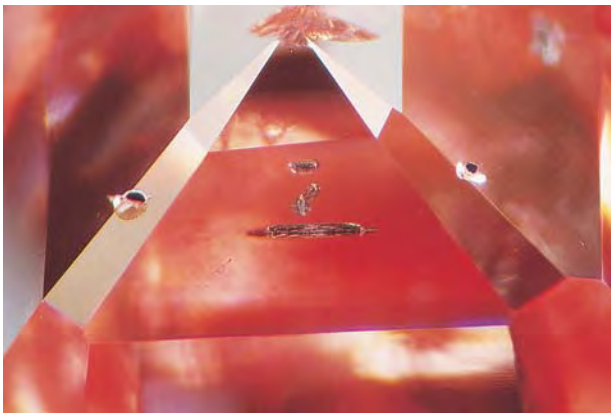

invisible with the magnification of a standard gemological microscope. Because the flux inclusions often contain iron, they can result in the synthetic diamond being attracted to a magnet.

Natural diamonds may display linear, cross-hatched, or irregular ("mosaic") internal graining patterns (Kane, 1980). In synthetic diamonds, internal graining in linear or intersecting geometric patterns appears to be the result of slight differences in refractive index between adjacent growth sectors, or between successive parallel "layers" of material beneath the crystal faces. It is best seen along the boundaries between sectors, or in planes that parallel the outer shape of the original crystal. Since the cuboctahedral crystals are often faceted in square or rectangular shapes for weight retention, one good place to check for graining in faceted samples is near the corners of the table facet (and adjacent crown facets) with magnification (a fiber-optic illuminator can be quite helpful).

Most natural diamonds exhibit anomalous double refraction (ADR) in banded, cross-hatched, or mottled patterns with bright interference colors (when observed through crossed polarizing filters; see Orlov, 1977, pp. 109–116). In comparison, our experience is that synthetic diamonds display much weaker, cross-like "strain" patterns with subdued interference colors (black or gray).

Luminescence. Given the wide variety of synthetic diamonds now available, their reactions to long- and short-wave UV radiation can differ greatly in terms of fluorescence intensity, color, distribution pattern, and phosphorescence. While it has been widely reported that most lab-grown samples display stronger fluorescence to short-wave UV than to long-wave, the opposite reaction has also been observed (as well as the same intensity reaction to both UV lamps), and some samples are inert to both UV excitations. To check for weak UV fluorescence reactions, it is best to observe the sample while in a darkened room, after the eyes have had time to adjust to low light levels. In more recent years, we have noticed an increasing number of synthetic diamonds that display only weak UV fluorescence, or no fluorescence reaction at all.

As mentioned, fluorescence colors can also vary, but typically they range from green to blue to yellow to orange or orange-red. More importantly, however, this fluorescence is often unevenly distributed, so that some portions of the sample fluoresce whereas others do not (or they fluoresce with different colors; see figure 9). This uneven distribution is again a reflection of the arrangement of internal growth sectors with their differing impurity contents, so there is a direct spatial relationship between color, graining, and UV fluorescence patterns. In the most obvious cases, this uneven fluorescence is seen as a square and/or cross-shaped geometric pattern. Again, the orientation of the faceted shape with respect to the original crystal will influence how color, graining, and fluorescence patterns appear, so it is important to examine a sample in several orientations.

Figure 8. In some cases, synthetic diamonds display "clouds" of pinpoint inclusions of uncertain identity. Since some natural diamonds also exhibit similar cloud-like arrangements, these pinpoint inclusions do not provide a reliable means of separation. Photomicrograph by Shane McClure; magnified 30×.

Similar fluorescence patterns in synthetic diamonds can be observed using the cathodoluminescence technique (where the sample is exposed to a beam of electrons while being held in a vacuum chamber). The DTC DiamondView, where fluorescence reactions are excited by exposure of the sample to UV radiation with wavelengths shorter than 230 nm, also provides an excellent tool for viewing surface-related fluorescence and phosphorescence patterns in a sample at different orientations (see Welbourn et al., 1996, and figure 6).

Colorless synthetic diamonds, and any colored samples that contain boron as an impurity, frequently display persistent greenish or yellowish phosphorescence (for up to 60 seconds or longer) when the UV lamp is turned off (see Shigley et al., 1997). Since phosphorescence is a phenomenon that decreases in intensity over time, it is again important to check for this kind of luminescence by viewing the samples in a darkened room. A good technique is to close one's eyes, and then open them at the same time the UV lamp is turned off. Blue (and some near-colorless) synthetic samples containing boron will exhibit electrical conductivity and, interestingly,

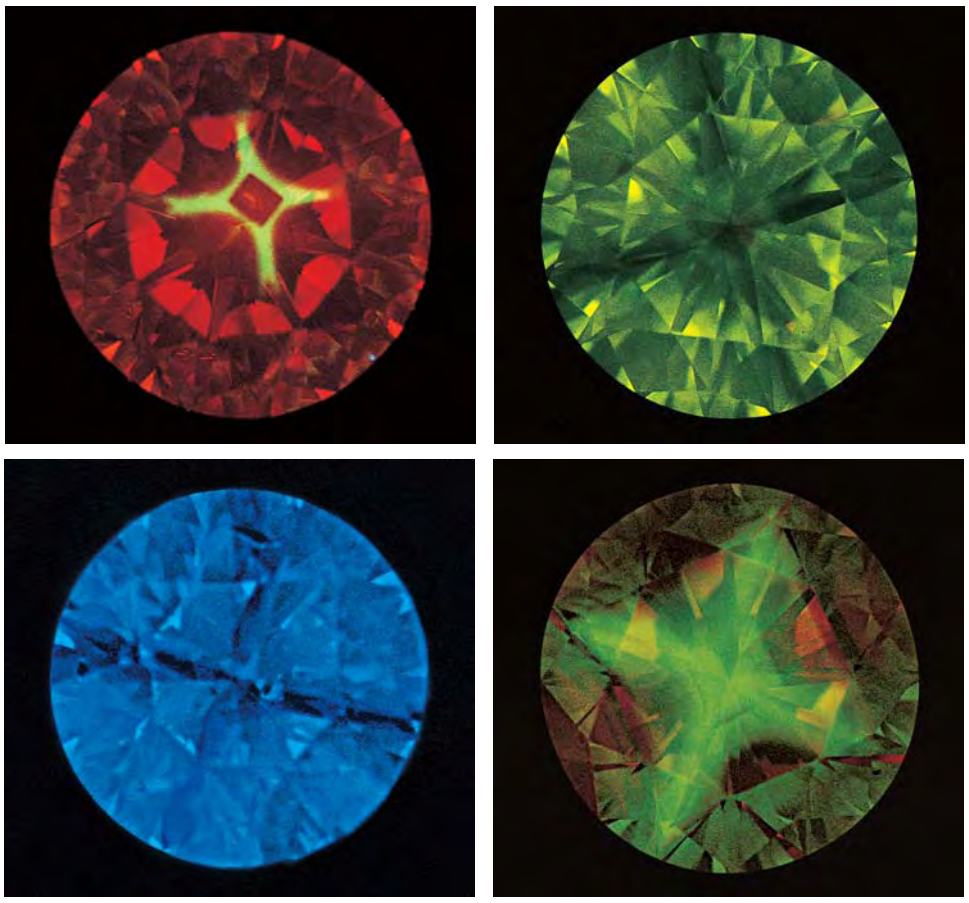

Figure 9. These four synthetic diamonds exhibit typical zoned fluorescence reactions when exposed to long-wave (top left, treated) and short-wave (remaining three images, as grown) ultraviolet radiation. In our experience, the fluorescence is usually stronger to short-wave UV than long-wave for as-grown synthetic diamonds, whereas it can be of equal intensity or stronger to long-wave UV for treated synthetic diamonds. In each instance shown here, certain growth sectors are fluorescing while others are not, resulting in a four-fold cross-shaped pattern. It is important to examine the sample both face-up and face-down, since the fluorescence may be emitted from just a localized area. Photos by Shane Elen and John I. Koivula.

will often display visible electroluminescence in the form of momentary tiny flashes of white to bluish white light when the samples are touched by the conductometer probe.

Chemical and Spectroscopic Analysis. Nondestructive methods of chemical analysis provide another rapid means of identifying synthetic diamonds by detecting flux metals (Ni, Co, and Fe) that are used in diamond growth. Particularly useful in recognizing lab-created diamonds, especially those that lack distinctive visual features, are several spectroscopy techniques that are found today in many gemological laboratories. Because diamond is relatively transparent from the infrared through the visible and ultraviolet regions of the electromagnetic spectrum, numerous absorption and emission features can be detected by these techniques (Zaitsev, 2001, lists the spectral features individually along with a brief description of what is known about them). Specific bands caused by the presence of transition metals are valuable for detecting either as-grown or treated synthetic diamonds by visible spectroscopy (for example, those at 494, 658, and 732 nm, as well as several others, which are all due to nickel; see again Zaitsev, 2001). Caution must be exercised, however, as we now know that some natural diamonds contain small amounts of nickel (see, e.g., Chalain, 2003; Lang et al., 2004; Hainschwang and Notari, 2004). Photoluminescence (PL) spectroscopy is increasingly important for gem laboratories, since many of the optical centers in diamond have associated sharp PL bands that are useful for identification purposes. The interested reader is referred to articles cited in the reference list for examples of the application of these and other spectroscopy methods to diamond characterization (see, e.g., Lawson et al., 1996; Collins, 2000, 2001; Zaitsev, 2000, 2001; Yelisseyev et al., 2002). Additional analytical techniques for detecting synthetic diamonds may become useful in the future.

Other features. As an aid to identification and disclosure, some manufacturers are inscribing a distinctive

mark or other information on the girdle facets of their polished synthetic diamonds; such a mark is easily visible with 10× magnification. In addition, certain gem-testing laboratories have agreed to issue grading reports on synthetic diamonds along with a clearly worded statement that they are laboratory grown.

CONCLUSION

The chart accompanying this article presents characteristics of both as-grown and treated synthetic diamonds produced under HPHT conditions using a metal or metal-alloy flux. While visual features such as color zoning and metallic inclusions remain valuable identification criteria, efforts to produce better-quality synthetic diamonds have resulted in such features becoming less evident (or even absent) in some recently grown material. Therefore, the recording of visible-range absorption and other spectra, and the observation of UV fluorescence patterns, have become increasingly important for synthetic diamond identification.

Particularly problematic for jewelers and gemologists are small stones. It is easier, faster, and cheaper to grow synthetic diamonds in the form of melee, but the small size means that the visual identifying features usually are more difficult to see with the microscope, and the large numbers make individual testing of whole parcels impractical. The best solution for parcels of melee is to submit representative samples to a gem-testing laboratory where the material can be fully characterized.

As one looks toward the future, continued research on diamond growth—and the possibility that more and larger synthetic diamonds will be produced—could pose further challenges for the jewelry industry. Although not yet a commercial process, the chemical vapor deposition (CVD) technique could yield larger synthetic diamonds that might lack, for example, growth sector–related color and UV fluorescence zoning patterns (in addition, they would not contain metallic inclusions). The absence of these features would make identification in a standard gemological laboratory more difficult, especially in colorless material, although the evidence from samples examined to date indicates that such material is clearly identifiable with advanced techniques such as the DTC DiamondView.

Scientific efforts are also underway to grow diamonds using flux materials other than transition metals (such as carbonate or silicate compounds; see, e.g., Arima et al., 2002: Litvin et al., 2002; Okada et al., 2002; Pal'yanov et al., 2002; Yamaoka et al., 2002). So far, only microscopic diamond crystals have been produced in this way. However, crystallization from these fluxes under HPHT conditions may eventually yield larger synthetic diamonds that lack some of the diagnostic features (such as metallic inclusions) seen in the HPHT material currently being marketed. Again, there is no evidence to date that such a growth process has been devised that can yield a synthetic diamond crystal of sufficient size and quality to make it suitable for faceting.

Improvements in diamond growth capabilities are an inevitable result of the ongoing scientific interest in diamond as a desirable high-technology material. As new kinds of synthetic diamonds are produced, gemological research must continue to develop practical means of identifying them using both standard and more sophisticated techniques. The goal is to create detection methods that can be applied to all synthetic diamonds—even those of melee size, where the rapid screening of large numbers of diamonds of unknown origin will be important.

ABOUT THE AUTHORS

Dr. Shigley is director of research, and Dr. Breeding and Dr. Shen are research scientists, in the GIA Gem Laboratory, Carlsbad, California.

Acknowledgments: The following individuals at GIA contributed to the collection of the information and photographic images used in this chart: Dino DeGhionno, Thomas Gelb, Scott Guhin, Shane Elen, Matthew Hall, John King, John Koivula, Dr. Taijin Lu, Shane McClure, Sam Muhlmeister, Elizabeth Quinn, Dr. Ilene Reinitz, Christopher Smith, Maha Tannous, and Dr. Wuyi Wang. We thank Chatham Created Gems of San Francisco, California, the Gemesis Corporation of Sarasota, Florida, and Lucent Diamonds Inc. of Lakewood, Colorado, for their loans of recent samples for study.

REFERENCES

Arima M., Kozai Y., Akaishi M. (2002) Diamond nucleation and growth by the reduction of carbonate melts under high-pressure and high-temperature conditions. *Geology*, Vol. 30, No. 8, pp. 691–694.

Chalain J-P. (2003) Gem News International: A natural yellow diamond with nickel-related optical centers. *Gems & Gemology*, Vol. 39, No. 4, pp. 325–326.

Chrenko R.M., Strong H.M. (1975) *Physical Properties of Diamond*. Report No. 75CRDO89, General Electric Co.,

Schenectady, New York.
Collins A.T. (2000) Spectroscopy of defects and transition metals in diamond. *Diamond and Related Materials*, Vol. 9, Nos. 3/6, pp. 417–423.
——— (2001) The colour of diamond and how it can be changed. *Journal of Gemmology*, Vol. 27, No. 6, pp. 341–359.
Fritsch E., Scarratt K. (1992) Natural-color nonconductive gray-to-blue diamonds. *Gems & Gemology*, Vol. 28, No. 1, pp. 35–42.
Hainschwang T., Notari F. (2004) Gem News International: A natural diamond with very high Ni content. *Gems & Gemology*, Vol. 40, No. 4, pp. 334–336.
Kanda H. (1999) Growth of high pressure synthetic diamond. *Journal of the Gemmological Society of Japan*, Vol. 20, Nos. 1/4, pp. 37–44.
Kane R.E. (1980) The elusive nature of graining in gem quality diamonds. *Gems & Gemology*, Vol. 16, No. 9, pp. 294–314.
Lang A.R., Yelisseyev A.P., Pokhilenko N.P., Steeds J.W., Wotherspoon A. (2004) Is dispersed nickel in natural diamonds associated with cuboid growth sectors in diamonds that exhibit a history of mixed-habit growth? *Journal of Crystal Growth*, Vol. 263, Nos. 1/4, pp. 575–589.
Lawson S.C., Kanda H., Watanabe K., Kiflawi I., Sato Y. (1996) Spectroscopic study of cobalt-related optical centers in synthetic diamond. *Journal of Applied Physics*, Vol. 79, No. 8, pp. 1–10.
Litvin Y.A., Butvina V.G., Bobrov A.V., Zharikov V.A. (2002) First synthesis of diamond in sulfide-carbon systems: The role of sulfides in diamond genesis. *Doklady Earth Sciences*, Vol. 382, No. 1, pp. 40–43.
Martineau P.M., Lawson S.C., Taylor A.J., Quinn S.J., Evans D.J.F., Crowder M.J. (2004) Identification of synthetic diamond grown using chemical vapor deposition (CVD). *Gems & Gemology*, Vol. 40, No. 1, pp. 2–25.
Okada T., Utsumi W., Shimomura O. (2002) In situ x-ray observation of the diamond formation process in the C-H_2O-MgO system. *Journal of Physics: Condensed Matter*, Vol. 14, No. 44, pp. 11331–11335.
Orlov Y.L. (1977) *The Mineralogy of the Diamond*. John Wiley & Sons, New York.
Pal'yanov Y.N., Sokol A.G., Borzdov Y.M., Khokhryakov A.F., Sobolev N.V. (2002) Diamond formation through carbonate-silicate interactions. *American Mineralogist*, Vol. 87, No. 7, pp. 1009–1013.
Rockwell K. (2004) Lab Notes: Unusual near-colorless synthetic diamond. *Gems & Gemology*, Vol. 40, No. 4, pp. 326–327.
Shigley J.E., Ed. (2005) *Synthetic Diamonds*. Gemological Institute of America, Carlsbad, California (in preparation)
Shigley J.E., Fritsch E., Reinitz I., Moses T.E. (1995) A chart for the separation of natural and synthetic diamonds. *Gems & Gemology*, Vol. 31, No. 4, pp. 256–264.
Shigley J.E., McClure S.F., Breeding C.M., Shen A.H-T., Muhlmeister S.M. (2004) Lab-grown colored diamonds from Chatham Created Gems. *Gems & Gemology*, Vol. 40, No. 2, pp. 128–145.
Shigley J.E., Moses T.M., Reinitz I., Elen S., McClure S.F., Fritsch E. (1997) Gemological properties of near-colorless synthetic diamonds. *Gems & Gemology*, Vol. 33, No. 1, pp. 42–53.
Wang W., Moses T., Linares R.C., Shigley J.E., Hall M., Butler J.E. (2003) Gem-quality synthetic diamonds grown by a chemical vapor deposition (CVD) method. *Gems & Gemology*, Vol. 39, No. 4, pp. 268–283.
Welbourn C.M., Cooper M., Spear P.M. (1996) De Beers natural versus synthetic diamond verification instruments. *Gems & Gemology*, Vol. 32, No. 3, pp. 156–169.
Wilks J., Wilks E. (1994) *Properties and Applications of Diamond*. Butterworth-Heinemann, Oxford.
Yamaoka S., Shaji Kumar M.D., Kanda H., Akaishi M. (2002) Crystallization of diamond from CO_2 fluid at high pressure and high temperature. *Journal of Crystal Growth*, Vol. 234, No. 1, pp. 5–8.
Yelisseyev A., Babich Y., Nadolinny V., Fisher D., Feigelson B. (2002) Spectroscopic study of HPHT synthetic diamonds, as grown at 1500°C. *Diamond and Related Materials*, Vol. 11, No. 1, pp. 22–37.
Zaitsev A.M. (2000) Vibronic spectra of impurity-related optical centers in diamond. *Physical Review B*, Vol. 61, No. 19, pp. 12909–12922.
——— (2001) *Optical Properties of Diamond: A Data Handbook*. Springer Verlag, Berlin.

ADDITIONAL READING (1996–PRESENT)

Antsygin V.D., Gusev V.A., Kalinin A.A., Kupriyanov I.N., Pal'yanov Y.N., Rylov G.M. (1998) Some aspects of the transformation of synthetic diamond defects under the action of high temperatures and high pressures. *Optoelectronics, Instrumentation, and Data Processing*, No. 1, pp. 9–15.
Attrino T. (1999) U.S. scientists, Russians produce new synthetic diamonds. *Rapaport Diamond Report*, Vol. 22, No. 36, pp. 88–89.
Babich Y.V., Feigelson B.N., Fisher D., Yelisseyev A.P., Nadolinny V.A., Baker J.M. (2000) The growth rate effect on the nitrogen aggregation in HTHP grown synthetic diamonds. *Diamond and Related Materials*, Vol. 9, Nos. 3/6, pp. 893–896.
Bates R. (2000) Color bind. *JCK*, Vol. 171, No. 6, pp. 294–296.
——— (2004) Getting real about synthetics. *JCK*, Vol. 175, No. 6, pp. 92–98.
Borzdov Y.M., Sokol A.G., Pal'yanov Y.N., Khokhryakov A.F., Sobolev N.V. (2000) Growth of synthetic diamond monocrystals weighing up to six carats and perspectives on their application. *Doklady Earth Sciences*, Vol. 374, No. 7, pp. 1113–1115.
Burns R.C., Kessler S., Sibanda M., Welbourn C.M., Welch D.L. (1996) Large synthetic diamonds. In *Advanced Materials '96: Proceedings of the 3rd NIRIM International Symposium on Advanced Materials*, National Institute for Research in Inorganic Materials (NIRIM), Tsukuba, Japan, pp. 105–111.
Burns R.C., Hansen J.O., Spits R.A., Sibanda M., Welbourn C.M., Welch D.L. (1999) Growth of high purity large synthetic diamond crystals. *Diamond and Related Materials*, Vol. 8, Nos. 8/9, pp. 1433–1437.
Campbell I.C.C. (2000) An independent gemmological examination of six De Beers synthetic diamonds. *Journal of Gemmology*, Vol. 27, No. 1, pp. 32–44 and Vol. 27, No. 2, p. 124.
Caveney R. (2003) 50th anniversary of first successful diamond synthesis. *Industrial Diamond Review*, No. 1, pp. 13–15.
Chatham T.H. (1998) Created gemstones: Past, present and future. *Canadian Gemmologist*, Vol. 19, No. 1, pp. 8–12.
Chepurov A.I., Fedorov I.I., Sonin V.M. (1998) Experimental studies of diamond formation at high *PT*-parameters. *Russian Geology and Geophysics*, Vol. 39, No. 2, pp. 234–244 [in Russian].
Choudhary D., Bellare J. (2000) Manufacture of gem quality diamonds: A review. *Ceramics International*, Vol. 26, No. 1, pp. 73–85.
DeVries R.C., Badzian A., Roy R. (1996) Diamond synthesis: The Russian connection. *MRS [Materials Research Society] Bulletin*, Vol. 21, No. 2, pp. 65–75.
De Weerdt F. (2000) Synthetic gem quality diamonds—Historical overview and newest developments. *Antwerp Facets*, No. 37, pp. 6–14.
Federman D. (1996) Growing pains. *Modern Jeweler*, Vol. 95, No. 11, pp. 36–44.
——— (2000) Hot off the presses. *Modern Jeweler*, Vol. 99, No. 4, pp. 12–13.
Ferro S. (2002) Synthesis of diamond. *Journal of Materials Chemistry*, Vol. 12, No. 10, pp. 2843–2855.
Fisher D., Lawson S.C. (1998) The effect of nickel and cobalt on the aggregation of nitrogen in diamond. *Diamond and Related Materials*, Vol. 7, Nos. 2/5, pp. 299–304.
Gorbatova M.S., Vins V.G. (2002) Comparison of the color of synthetic polished diamonds with the concentration of basic diamond lattice impurity defects. *Gemological Bulletin*, No. 7, pp. 29–31 [in Russian].
Haines J., Léger J.M., Bocquillon G. (2001) Synthesis and design of superhard materials. *Annual Review of Materials Research*, Vol.

31, pp. 1–23.
Halevi V. (2004) Has the Apollo really landed? *Idex*, Vol. 19, No. 165, pp. 100–115.
Johnston K., Mainwood A. (2002) Modelling transition metals in diamond. *Diamond and Related Materials*, Vol. 11, Nos. 3/6, pp. 631–634.
Kanda H. (2000) Large diamonds grown at high pressure conditions. *Brazilian Journal of Physics*, Vol. 30, No. 3, pp. 482–489.
Kanda H., Jia X. (2001) Change of luminescence character of Ib diamonds with HPHT treatment. *Diamond and Related Materials*, Vol. 10, Nos. 9/10, pp. 1665–1669.
Kaneko J., Yonezawa C., Kasugai Y., Sumiya H., Nishitani T. (2000) Determination of metallic impurities in high-purity type IIa diamond grown by high-pressure and high-temperature synthesis using neutron activation analysis. *Diamond and Related Materials*, Vol. 9, No. 12, pp. 2019–2023.
Kiefer D.M. (2001) The long quest for diamond synthesis. *Today's Chemist at Work*, Vol. 10, No. 7, pp. 63–64.
Kiflawi I., Kanda H., Fisher D., Lawson S.C. (1997) The aggregation of nitrogen and the formation of A centres in diamond. *Diamond and Related Materials*, Vol. 6, No. 11, pp. 1643–1649.
Kiflawi I., Kanda H., Lawson S.C. (2002) The effect of growth rate on the concentration of nitrogen and transition metal impurities in HPHT synthetic diamonds. *Diamond and Related Materials*, Vol. 11, No. 2, pp. 204–211.
Kiflawi I., Kanda H., Mainwood A. (1998) The effect of nickel and the kinetics of aggregation of nitrogen in diamond. *Diamond and Related Materials*, Vol. 7, Nos. 2/5, pp. 327–332.
Lerner E.J. (2002) Industrial diamonds gather strength. *Industrial Physicist*, Vol. 8, No. 4, pp. 8–11.
Lindblom J., Hölsä J., Papunen H., Häkkänen H., Mutanen J. (2003) Differentiation of natural and synthetic gem-quality diamonds by luminescence properties. *Optical Materials*, Vol. 24, Nos. 1/2, pp. 243–251.
Meng Y., Newville M., Sutton S., Rakovan J., Mao H-K. (2003) Fe and Ni impurities in synthetic diamond. *American Mineralogist*, Vol. 88, No. 10, pp. 1555–1559.
Nadolinny V.A., Yelisseyev A.P., Baker J.M., Twitchen D.J., Newton M.E., Feigelson B.N., Yuryeva O.P. (2000) Mechanisms of nitrogen aggregation in nickel- and cobalt-containing diamonds. *Diamond and Related Materials*, Vol. 9, Nos. 3/6, pp. 883–886.
New detectors separate "man-made" from "natural" diamonds (1996) *Mazal U'Bracha*, No. 84, pp. 54–62.
Pal'yanov Y.N., Borzdov Y.M., Sokol A.G., Khokhryakov A.F., Gusev V.A., Rylov G.M., Sobolev N.V. (1997) Dislocation-free monocrystals of synthetic diamond. *Transactions of the Russian Academy of Sciences, Earth Science Section*, Vol. 353, No. 2, pp. 243–246.
——— (1998) High-pressure synthesis of high-quality diamond single crystals. *Diamond and Related Materials*, Vol. 7, No. 6, pp. 916–918.
Pal'yanov Y.N., Khokhryakov A.F., Borzdov Y.M., Sokol A.G., Gusev V.A., Rylov G.M., Sobolev N.V. (1997) Growth conditions and real structure of synthetic diamond crystals. *Russian Geology and Geophysics*, Vol. 38, No. 5, pp. 920–945.
Pal'yanov Y.N., Sokol A.G., Borzdov Y.M., Khokhryakov A.F., Gusev V.A., Sobolev N.V. (1997) Synthesis and characterization of diamond single crystals up to 4 carats. *Transactions of the Russian Academy of Sciences, Earth Science Section*, Vol. 355A, No. 6, pp. 856–858.
Rapaport M. (2003) Cultured diamonds. *Rapaport Diamond Report*, Vol. 26, No. 37, pp. 1, 15–16.
Reinitz I., Shigley J. (1997) How to identify synthetics. *Jewellery News Asia*, No. 150, pp. 150–156.
Roskin G. (2001) A new market for colored synthetics? *JCK*, Vol. 172, No. 1, pp. 64–65.
——— (2004) Jewel of the month: Gem-quality synthetic diamond. *JCK*, Vol. 175, No. 2 , pp. 72–74.
Russian synthetic diamonds: Finally on the way to market? (1996) *New York Diamonds*, Vol. 35, June/July, pp. 62–63.
Scarratt K., Dunaigre C.M., DuToit G. (1996) Chatham synthetic diamonds. *Journal of the Gemmological Association of Hong Kong*, Vol. 19, pp. 6–12.
Shelementiev Y.B., Gorbenko O.Y., Saparin G.V., Obyden S.K., Chukichev M.V. (2001) Gemological characterization of gem quality synthetic diamonds manufactured in Russia. *Gemological Bulletin*, No. 1, pp. 4–8 [in Russian].
Shigley J.E., Abbaschian R., Clarke C. (2002) Gemesis laboratory-created diamonds. *Gems & Gemology*, Vol. 38, No. 4, pp. 301–309.
Shor R. (1997) De Beers deploys synthetic diamond testers—Just in case. *New York Diamonds*, Vol. 38, pp. 56–60.
Sirakian D. (1997) Diamants: la synthèse a une historie. *Revue de Gemmologie a.f.g.*, No. 131, pp. 6–10.
Smith C.P., Bosshart G. (1999) Synthetic blue diamonds hit the market. *Rapaport Diamond Report*, Vol. 22, No. 20, pp. 114–116.
Sumiya H., Satoh S. (1996) High-pressure synthesis of high-purity diamond crystal. *Diamond and Related Materials*, Vol. 5, No. 11, pp. 1359–1365.
Sumiya H., Toda N., Nishibayashi Y., Satoh S. (1997) Crystalline perfection of high purity synthetic diamond. *Journal of Crystal Growth*, Vol. 178, No. 4, pp. 485–494.
Sumiya H., Toda N., Satoh S. (2000) High-quality large diamond crystals. *New Diamond and Frontier Carbon Technology*, Vol. 10, No. 5, pp. 233–251.
——— (2002) Growth rate of high-quality large synthetic diamond crystals. *Diamond and Related Materials*, Vols. 237/239, No. 2, pp. 1281–1285.
Sung J.C. (2003) The eastern wind of diamond synthesis. *New Diamond and Frontier Carbon Technology*, Vol. 13, No. 1, pp. 47–61.
Synthetic diamonds launched at JCK Show in June (1996) *Diamond World Review*, No. 92, pp. 78–80.
Synthetic diamonds meet the challenge (2000) *Mining Journal*, Vol. 334, No. 8571, pp. 146–147.
Vins V. (2002) Color changing in synthetic diamonds: Influence of growth conditions. *Gemological Bulletin*, No. 4, pp. 28–36 [in Russian].
——— (2002) Change of colour produced in synthetic diamonds by βHT-processing. *Gemological Bulletin*, No. 5, pp. 26–32.
Wakefield S. (1996) Synthetic diamond jewelry: Are you prepared? *Jewelers' Circular Keystone*, Vol. 167, No. 3, pp. 47–51.
Watanabe K., Lawson S.C., Isoya J., Kanda H., Sato Y. (1997) Phosphorescence in high-pressure synthetic diamond. *Diamond and Related Materials*, Vol. 6, No. 1, pp. 99–106.
——— (1998) Spectroscopic study of boron-doped diamond. *Proceedings 5th NIRIM International Symposium on Advanced Materials (ISAM '98)*, National Institute for Research in Inorganic Materials, Tsukuba, Japan, March 1–5, 1998, pp. 101–104.
Welbourn C.M., Cooper M., Spear P.M. (1997) Instruments de vérification de la De Beers pour distinguer les diamants naturels des synthétiques. *Revue de Gemmologie a.f.g.*, No. 131, pp. 11–20.
Weldon R. (1998) Growing carats. *Professional Jeweler*, Vol. 1, No. 2, pp. 47–48.
——— (1999) With a tweak and a smile. *Professional Jeweler*, Vol. 2, No. 3, pp. 26–29.
——— (1999) Phenomenal synthetic. *Professional Jeweler*, Vol. 2, No. 4, p. 28.
——— (2004) Gemesis gemological markers. *Professional Jeweler*, Vol. 7, No. 2, pp. 30–32.
——— (2004) Gemesis: The retail marketing plan. *Professional Jeweler*, Vol. 7, No. 2, pp. 23–24.
Yin L-W., Zou Z-D., Li M-S., Liu Y-X., Cui J-J., Hao Z-Y. (2000) Characteristics of some inclusions contained in synthetic diamond single crystals. *Materials Science and Engineering*, Vol. A293, Nos. 1/2, pp. 107–111.
Yin L-W., Li M-S., Sun D-S., Li F-Z., Hao Z-Y. (2002) Some aspects of diamond crystal growth at high temperature and high pressure by TEM and SEM. *Materials Letters*, Vol. 55, No. 6, pp. 397–402.
Yuan J.C.C. (2000) Russian colourless synthetic diamond. *Australian Gemmologist*, Vol. 20, No. 12, pp. 529–533.

A NEW METHOD FOR DETECTING BE DIFFUSION–TREATED SAPPHIRES: LASER-INDUCED BREAKDOWN SPECTROSCOPY (LIBS)

Michael S. Krzemnicki, Henry A. Hänni, and Roy A. Walters

This article describes the first application of laser-induced breakdown spectroscopy (LIBS) to gemology. So far, the detection of Be-diffused sapphire and ruby has been based on LA-ICP-MS or SIMS, neither of which is readily available to most laboratories. In this study, we use LIBS to detect beryllium in corundum at very low concentrations (down to ~2 ppm). This technique is a reliable tool for identifying Be diffusion–treated sapphires, and is affordable for most commercial gemological laboratories. As with other laser-based techniques, LIBS may cause slight damage to a gemstone, but this can be minimized by choosing appropriate instrument parameters.

Sapphires treated by beryllium diffusion entered the gem trade in mid-2001, and the first laboratory alert on this treatment was issued by the American Gem Trade Association in New York on January 8, 2002 (Scarratt, 2002). This treatment modifies various colors of corundum into stones of more attractive hues, usually yellow or orange to orangy red (figure 1). Some of these colors are rather rare in untreated or traditionally heated corundum, so the stones may be very valuable, especially the orangy pink variety ("padparadscha"). Several studies of Be-diffused corundum have revealed that the presence of low concentrations of beryllium (i.e., ~5–10 ppm) in the corundum lattice may result in a distinct yellow-to-orange coloration (Hänni and Pettke, 2002; Peretti and Günther, 2002; Emmett et al., 2003; Pisutha-Arnoud et al., 2004). In contrast, untreated or traditionally heated sapphires of similar color contain no Be or have only minute traces (i.e., parts-per-billion [ppb] levels) of this light element (Emmett et al., 2003; D. Günther, pers. comm., 2004).

Unfortunately, the detection of Be-diffused sapphires has proved difficult, because testing by traditional nondestructive analytical methods (e.g., energy-dispersive X-ray fluorescence [EDXRF]) cannot detect light elements such as Be. Although some Be-diffused sapphires can be identified by a yellowish orange rim when observed in immersion (see, e.g., Hänni and Pettke, 2002; McClure et al., 2002; Peretti and Günther, 2002; Emmett et al., 2003), often no such diffusion feature is present. Until now, the reliable detection of Be diffusion has usually required highly sophisticated methods, such as laser ablation–inductively coupled plasma–mass spectrometry (LA-ICP-MS) or secondary ion mass spectrometry (SIMS). Both techniques are slightly destructive, as they vaporize a minute quantity of the sample for analysis with a mass spectrometer (Guillong and Günther, 2001).

Since the two analytical techniques described above are quite expensive, time consuming, and only rarely at the disposal of gemological laboratories, we investigated a more affordable technology. In July 2003, we began to evaluate the potential of

See end of article for About the Authors and Acknowledgments.
GEMS & GEMOLOGY, Vol. 40, No. 4, pp. 314–322.

Figure 1. The attractive colors of the Umba Valley (Tanzania) sapphires in this composite photo were produced by Be diffusion. The loose stones range from 1.27 to 7.91 ct, and the sapphires in the 18K white gold jewelry are 3.19 ct (ring center stone) and 3.52 ct total weight (leaf pendant). Photo by Myriam Naftule Whitney; courtesy of Nafco Gems, Scottsdale, Arizona.

laser-induced breakdown spectroscopy (LIBS) for gemstone analysis. As in the other methods mentioned above, LIBS analysis also is slightly destructive, as a small portion of the sample is ablated by a laser. Our initial results revealed the potential of LIBS to detect Be-diffused corundum (Hänni and Krzemnicki, 2004). In April 2004, SSEF became the first laboratory to install a LIBS instrument that was specially designed for gemstone analysis. Since July 2004, SSEF has offered Be detection in corundum as a regular service to its clients. In this article, we present the first detailed results obtained by LIBS on beryllium-diffused corundum, as analyzed with the SSEF GemLIBS system (table 1).

LIBS BACKGROUND

LIBS can provide qualitative to semiquantitative chemical data. Initial studies on laser spark spectroscopy (Brech and Cross, 1962; Allemand, 1972; Corney, 1977) were further developed in the early 1980s, mainly by scientists at Los Alamos National Laboratory in New Mexico. Radziemski et al. (1983) showed the ability of LIBS to detect trace concentrations of Be (in air) as low as 0.5 ppm. Recently, major improvements in laser and spectrometer technology have dramatically expanded the possibilities and applications of LIBS for military uses, environmental monitoring, process control, and material analysis (Bogue, 2004); these include remote in-situ testing of fine particulate matter (Carranza and Hahn, 2002) and real-time analysis of steel composition during production (Gruber et al., 2004). The use of LIBS in the gem industry has so far been rather limited, and has involved analyzing the composition of jewelry metal alloys (e.g., García-Ayuso et al., 2002) as well as Be-diffused corundum (Krzemnicki and Hänni, 2004).

The principle behind LIBS is the interaction of a laser with a sample to produce an optical emission spectrum that is specific to that sample. A pulsed laser focused onto a sample (solid, liquid, or gas) vaporizes a small portion for analysis. The superheated, ablated material is transformed into a plasma, a form of matter in which the original chemical bonds of the substance are broken apart and the resulting atoms are converted into a mixture of neutral atoms, ions, and electrons. The atoms and ions within the expanding plasma lose some of their energy by emitting light, which produces a characteristic emission spectrum in the ultraviolet, visible, and near-infrared spectral range. The spectrum is then recorded with a spectrometer. Due to complex plasma dynamics, LIBS does not yield quantitative data. By using reference standards of known composition, it is sometimes possible to calibrate the instrument to generate semiquantitative data, such as for Be in a corundum matrix (Krzemnicki and Hänni, 2004).

MATERIALS AND METHODS

In this study, we present data on 21 well-characterized faceted natural sapphires and rubies, as well as three synthetic corundums (figures 2 and 3; table 2). Six of the natural corundums were Be-diffused (Be-1–Be-6). Fifteen of the natural samples were

Figure 2. These are some of the corundum samples that were analyzed by LIBS for this study. The faceted stones on the left are Be-diffused sapphires (Be-1 to Be-4). On the bottom right are samples that have been heated by traditional methods with no Be-diffusion (NBe-1, NBe-6, and NBe-14). In the background are a split boule of orange flame-fusion synthetic sapphire that was doped with Be (sample BeS-1) and a faceted flame-fusion synthetic ruby without Be (sample NBeS-1). Photo by M. S. Krzemnicki, © SSEF.

not Be-diffused (NBe-1–NBe-15), but nine of them were heated by traditional methods. The natural samples were compared to a flame-fusion synthetic orange sapphire (BeS-1) that was doped with a minute amount of Be (2–3 ppm measured by LA-ICP-MS) to investigate the detection limit of our particular LIBS configuration. In addition, a flame-fusion synthetic ruby (NBeS-1) and a flame-fusion synthetic color-change sapphire (NBeS-2) were analyzed to study possible peak interference by chromium and vanadium with the Be emission doublet at 313 nm in the LIBS spectra.

All samples were chemically analyzed by EDXRF spectrometry, using a Tracor Spectrace 5000 instrument, to determine semiquantitative concentrations of Ti, V, Cr, Fe, and Ga. Additional elements (such as Na, Mg, Si, Ca, Mn, Ni, Cu, and Zn) were typically below the EDXRF detection limit. As EDXRF spectrometry is not capable of analyzing light elements such as Be, only by using methods such as LIBS, LA-ICP-MS, or SIMS is it possible to detect them in corundum. We used LA-ICP-MS to obtain quantitative data on Be (and other trace elements) in all six Be-treated samples (Be-1–Be-6), in three of the stones treated by traditional heating (NBe-1, NBe-6, and NBe-14), and in the Be-doped synthetic sapphire (BeS-1), for comparison with the LIBS spectra. The LA-ICP-MS analyses were obtained using a pulsed Excimer ArF laser with a characteristic wavelength of 193 nm for sample ablation, combined with special optics to homogenize the energy distribution across the laser beam (Günther et al., 1997; now commercially available as the GeoLas system). The ICP-MS was a quadrupole instrument from PerkinElmer, the ELAN 6100. The size of the ablated laser pits was about 100 µm in diameter and a few tens of micrometers deep. In contrast to many other commercially available LA-ICP mass spectrometers, this instrument is characterized by a perfectly flat laser beam geometry, which enables drilling of very

Figure 3. These are the additional non-Be-diffused natural corundum samples that were analyzed for this study. From left to right, top row: NBe-9 (Umba, Tanzania), NBe-15 (Luc Yen, Vietnam), NBe-5 and NBe-3 (Sri Lanka), NBe-10 (Tunduru, Tanzania); and bottom row: NBe-8 and NBe-7 (Tanzania), NBe-13 (Ilakaka, Madagascar), NBe-4 and NBe-2 (Sri Lanka), NBe-11 and NBe-12 (Tunduru, Tanzania). As expected, the LIBS analyses for all of these samples revealed no evidence of beryllium. Photo by H. A. Hänni, © SSEF.

TABLE 1. Characteristics of the SSEF GemLIBS system.

Laser: Single-pulsed Nd:YAG laser	
Pulse duration	7 nanoseconds
Wavelength	1064 nm
Energy	100 millijoules
Frequency	3 Hz
Focus lens	35 mm
Spectrometer: Ocean Optics LIBS2000+	
Range	200–980 nm broadband spectrum
Q-switch delay	2 microseconds
Analysis	Simultaneous, real-time
Resolution	0.1 nm FWHM (full width at half maxium)
Sample chamber	
Dimensions	17 × 22 × 14 cm (width × height × depth)
Protection	Laser safety plastic, 180° visibility
Conditions	Measured in air
Sample holder	Manual x-y-z sample stage

precise flat round laser holes. More details about this setup will be provided in an article on the application of LA-ICP-MS in gemology (M. S. Krzemnicki et al., in preparation)

The SSEF GemLIBS system used for the LIBS analyses consists of an Ocean Optics LIBS 2000+ instrument that was modified for gemological purposes with an x-y-z sample holder for precise targeting (see table 1 and figures 4 and 5). The sample was fixed to a glass plate with some Blu-Tack and positioned under the laser. The system uses a single-pulse 1064 nm Nd:YAG laser (pulse duration of 7 nanoseconds with an energy of 100 millijoules [mJ]) from BigSky Quantel. A series of overlapping high-resolution fiber-optic spectrometers enables the simultaneous recording of emission spectra in the range 200–980 nm, in which the emission lines of all elements are found. The peak resolution (full width at half maximum [FWHM]) is 0.1 nm. Thus, it is possible to detect emission lines that are very close to one another.

Laser safety is an important consideration when performing LIBS analysis or other laser-based experiments (e.g., Raman and LA-ICP-MS). The laser energy used for LIBS analysis is powerful, and reflection from gemstone facets may cause damage to the retina of the eye. The system comes with a transparent laser-protected sample chamber. LIBS analyses should only be carried out while the sample chamber is completely closed.

In our study, numerous emission lines from elements of the corundum matrix (Al, Cr, Fe, V, Ti) and the atmosphere (O, N) were encountered. In accordance with Radziemski et al. (1983), Be

TABLE 2. LIBS samples for this study on Be diffusion–treated corundum.[a]

Sample	Mineral	Treatment	Weight (ct)	Form	Origin	LA-ICP-MS Be (ppm)	LIBS Be detection
Be-1	Purple sapphire	Be diffusion	0.63	Faceted	East Africa	34–49	Positive
Be-2	Orange sapphire	Be diffusion	1.26	Polished slab	East Africa	5–21	Positive
Be-3	Orange sapphire	Be diffusion	1.00	Faceted	East Africa	8–11	Positive
Be-4	Orange sapphire	Be diffusion	0.85	Faceted	East Africa	8–10	Positive
Be-5	Orange sapphire	Be diffusion	0.98	Faceted	East Africa	4–10	Positive
Be-6	Yellow sapphire	Be diffusion	0.97	Faceted	Sri Lanka	9–11	Positive
BeS-1	Synthetic orange sapphire[b]	Be diffusion	242.17	Split boule	Flame fusion	2–3	Positive (very low)
NBeS-1	Synthetic ruby	None	5.47	Faceted	Flame fusion	na	Negative
NBeS-2	Synthetic V-corundum	None	2.64	Faceted	Flame fusion	na	Negative
NBe-1	Yellow sapphire	Heated	1.51	Faceted	Sri Lanka	bdl	Negative
NBe-2	Yellow sapphire	Heated	2.57	Faceted	Sri Lanka	na	Negative
NBe-3	Light yellow sapphire	Heated	2.18	Faceted	Sri Lanka	na	Negative
NBe-4	Orangy pink sapphire[c]	None	0.73	Faceted	Sri Lanka	na	Negative
NBe-5	Pink sapphire	None	2.10	Faceted	Sri Lanka	na	Negative
NBe-6	Sapphire	Heated	1.22	Faceted	Sri Lanka	bdl	Negative
NBe-7	Ruby	None	0.60	Faceted	Tanzania	na	Negative
NBe-8	Light purple sapphire	None	0.88	Faceted	Tanzania (Umba)	na	Negative
NBe-9	Slightly brownish pinkish orange sapphire	None	1.53	Faceted	Tanzania (Umba)	na	Negative
NBe-10	Pink sapphire	Heated	1.10	Faceted	Tanzania (Tunduru)	na	Negative
NBe-11	Pink sapphire	Heated	1.27	Faceted	Tanzania (Tunduru)	na	Negative
NBe-12	Light pink sapphire	Heated	1.47	Faceted	Tanzania (Tunduru)	na	Negative
NBe-13	Light pink sapphire	Heated	2.15	Faceted	Madagascar (Ilakaka)	na	Negative
NBe-14	Ruby	Heated	1.05	Faceted	Kenya	bdl	Negative
NBe-15	Ruby	None	2.40	Polished fragment	Vietnam (Luc Yen)	na	Negative

[a] *Abbreviations: bdl = below detection limit (0.3–0.8 ppm); na = not analyzed by LA-ICP-MS (only EDXRF), so Be was not quantified.*
[b] *Analyses performed near the rim of the cleaved Be-doped synthetic orange sapphire.*
[c] *Also referred to as the "padparadscha" variety of corundum.*

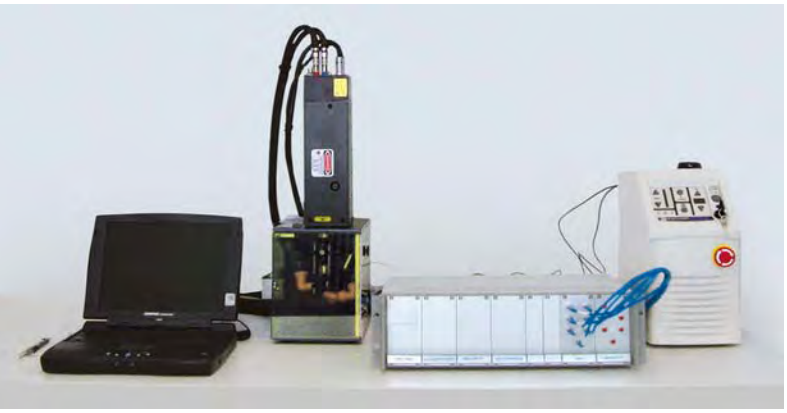

Figure 4. The SSEF GemLIBS system consists of a sample chamber with an attached pulsed Nd:YAG laser, a series of high-resolution fiber-optic spectrometers, the laser power supply, and a computer for controlling the system and analyzing the spectra. Photo by H. A. Hänni, © SSEF.

detection was based on the presence of the first-order ionic Be II doublet at 313.042 and 313.107 nm (NIST database). Using our LIBS system, this doublet was not resolved but appeared as a single peak centered at 313.08 nm. A weaker Be emission was found at 234.86 nm. However, this emission was not used, since Fe from the corundum matrix may produce overlapping peaks.

Repeated testing revealed that about 20 laser shots per LIBS analysis resulted in a high signal-to-background ratio for the Be emission at 313 nm. Additional laser pulses only slightly increased this ratio. The method was further improved by focusing the laser slightly above the surface of the sample. We found that the delay after the laser pulse, which is when the characteristic optical emission of an element is analyzed, is also an important factor. Immediately after the laser pulse, the plasma emission is dominated by continuous light emission. Only after a certain delay can the characteristic optical emission of the elements be detected. However, different elements may reveal maximum characteristic optical emissions at different delays after the laser

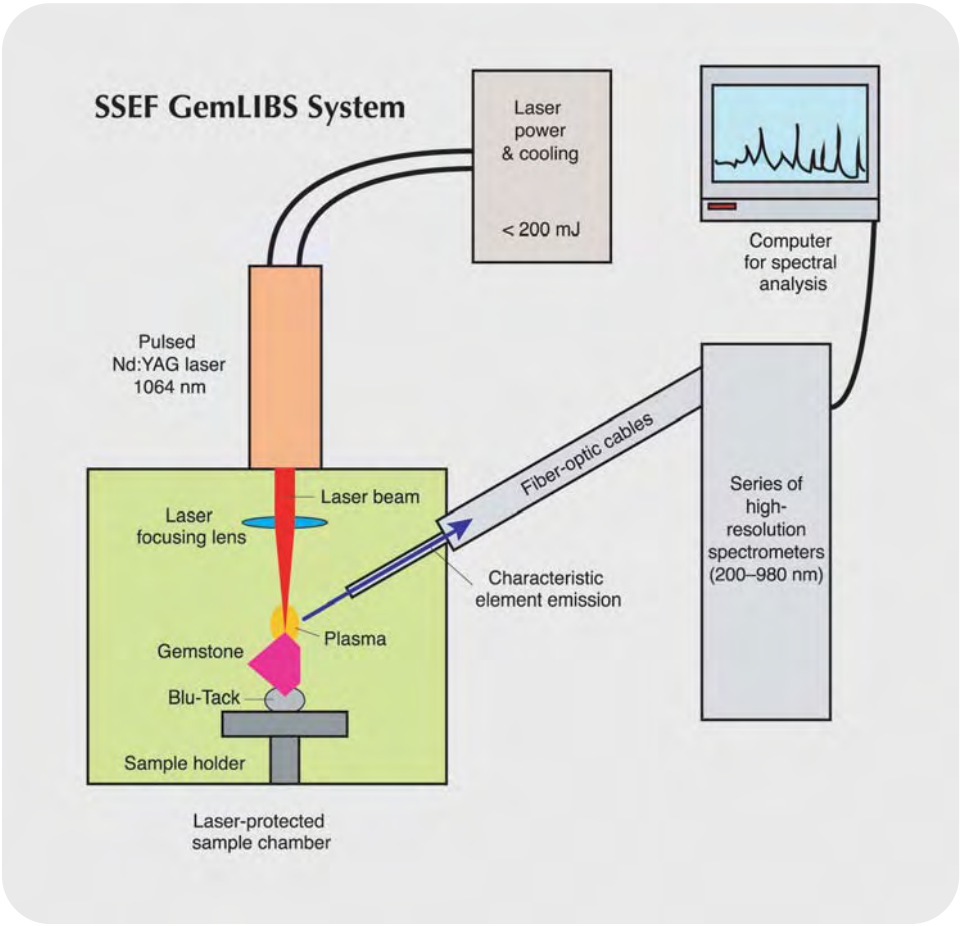

Figure 5. This schematic diagram shows the individual constituents of the SSEF GemLIBS system.

pulse. We found that a delay of 2 microseconds was ideal for beryllium detection in corundum.

We performed extensive testing to minimize the possibility of laser-induced internal damage to the gem sample. We established that a laser energy of 100 mJ is ideal for Be detection in a corundum matrix. At this energy, the laser ablation spot on the surface of the gemstone is minimized and internal damage is avoided. Higher energies (e.g., 150 or 200 mJ) may lead to damage, as part of the laser energy is transmitted through the sample, resulting in small disc-like tension cracks along the laser path. Note, too, that the analyzed spot should not be located close to a near-surface fracture or inclusion, as in rare cases this may cause a tiny tension crack. It is therefore recommended that a gemologist examine the sample with a microscope before choosing the spot for LIBS analysis.

With our optimized setup, the tiny laser spots on a sample's surface have a diameter of less than 0.1 mm (100 µm) and a maximum depth of 30–50 µm (figure 6). This is similar to the size of the laser holes generated by LA-ICP-MS. The LIBS laser spots may be detected by a close inspection of the sample with a 10× loupe, but they do not affect the overall appearance of the gemstone. As the vaporized portion of the sample is redeposited around the hole after the breakdown of the plasma, a small iridescent zone may be visible around the LIBS spot (about 2 mm in diameter). It can be easily removed with a slight repolishing. By analyzing faceted samples on or near their girdle, the tiny laser spots are inconsequential. The girdle also is of interest because it is usually rather poorly repolished after treatment, thus offering a better possibility of finding minute areas that are filled with residual Be-enriched flux material (Hänni and Pettke, 2002; Emmett et al., 2003). For the detection of Be-diffusion treatment by LIBS, a maximum of two or three spots is chosen for analysis.

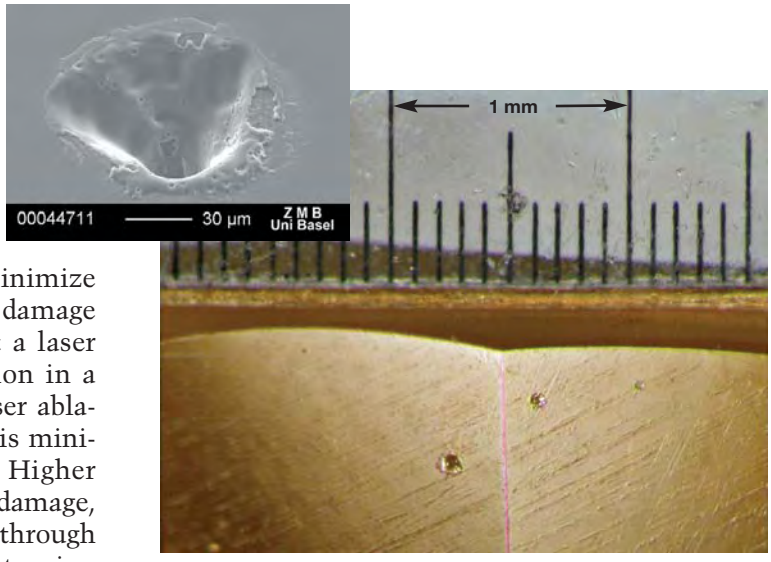

Figure 6. Two LIBS laser spots are visible near the girdle of this yellow sapphire. A micrometer scale is shown for comparison. The diameter of these tiny laser spots is less than 0.1 mm, similar to that of the holes produced by LA-ICP-MS. They are hardly visible with 10× magnification, and are particularly inconspicuous when located on or near the girdle (photo by H. A. Hänni, © SSEF). The SEM image in the inset shows a closer view of a LIBS laser hole, which in this case is about 0.03 mm deep (micrograph by M. Düggelin, © SEM Laboratory, University of Basel, Switzerland).

RESULTS

The LIBS spectra were averaged from 20 individual laser pulses to obtain the best counting statistics over the whole broad-band range from 200 to 980 nm (see, e.g., figure 7). The highest peaks in the ultraviolet to mid-visible spectral range are due to Al. The peaks in the upper spectral range (>600 nm) are mainly due to oxygen and some nitrogen from the atmosphere (air).

Figure 8 compares the LIBS spectra of the Be diffusion–treated sapphires (Be-1–Be-6 and BeS-1) to those of two Be-free flame-fusion synthetic

Figure 7. This LIBS spectrum of a purple Be-diffused sapphire (sample Be-1) shows the full spectral range between 200 and 980 nm. Numerous atomic and ionic emission lines are present, which may partially interfere with one another. The main peaks are due to aluminum. Emission due to beryllium produces a peak at approximately 313.08 nm.

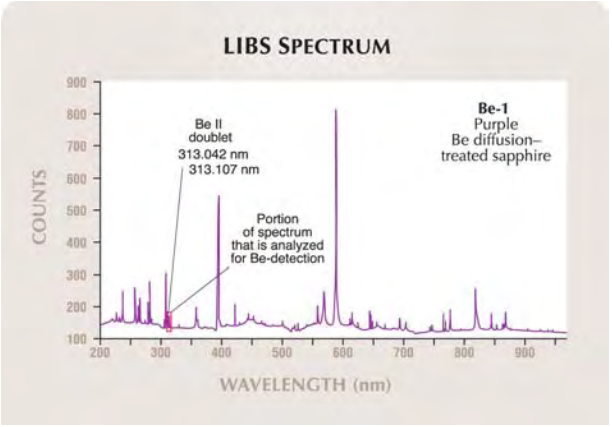

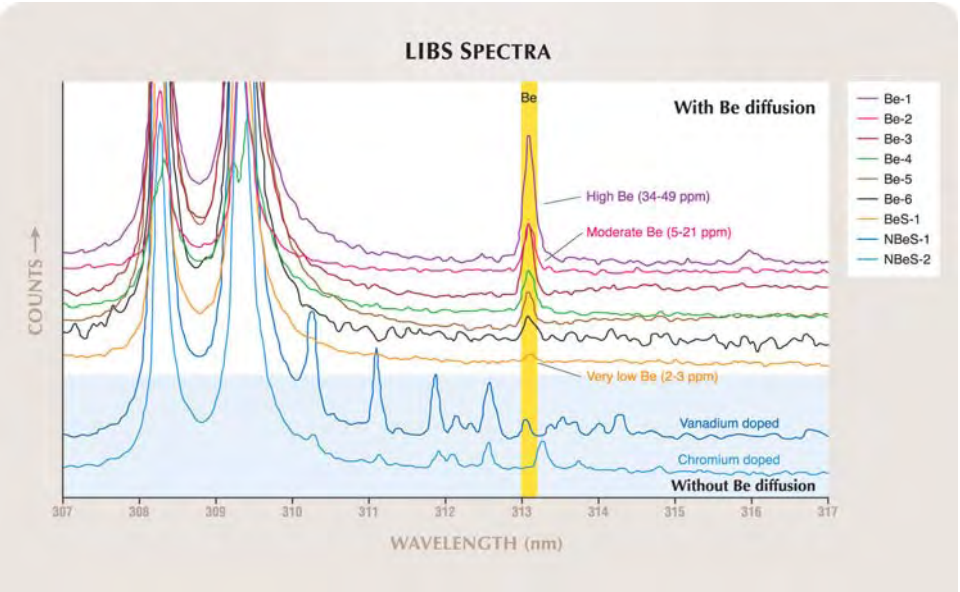

Figure 8. These LIBS spectra in the range of 307–317 nm are of Be-treated sapphires (Be-1 to Be-6) and an orange Be-doped flame-fusion synthetic sapphire (BeS-1) shown in comparison to the spectra of two Be-free flame-fusion synthetic samples (NBeS-1 and NBeS-2). The 313.08 nm Be peak is the basis for the detection of Be-treated sapphires. Fortunately, this peak does not exactly overlap any of the numerous Cr and V peaks in that region.

corundum samples (NBeS-1 and NBeS-2). The dominant (and truncated) peaks at about 308 and 309 nm are due to the Al in corundum. The spectra are shown without normalization of the Al II emission at 309.27 nm. Nevertheless, there is a distinct positive correlation between the height of the 313.08 nm Be peak and the beryllium concentration as measured by LA-ICP-MS. At a low concentration of 2–3 ppm (BeS-1), the Be peak is very small. The LIBS analyses on this cleaved Be-doped synthetic sample were taken close to the LA-ICP-MS spots, near the rim. Based on the analysis of this sample, we estimate that the detection limit for Be in corundum is ~2 ppm with our LIBS system.

At a much higher Be concentration (Be-1, 34–49 ppm), the Be peak measured with LIBS was much stronger. The range of Be indicated for each sample in table 2 is based on several LA-ICP-MS analyses and reflects the inhomogeneity of these samples (especially sample Be-2, with concentrations ranging from 5 to 21 ppm Be). As each spec-

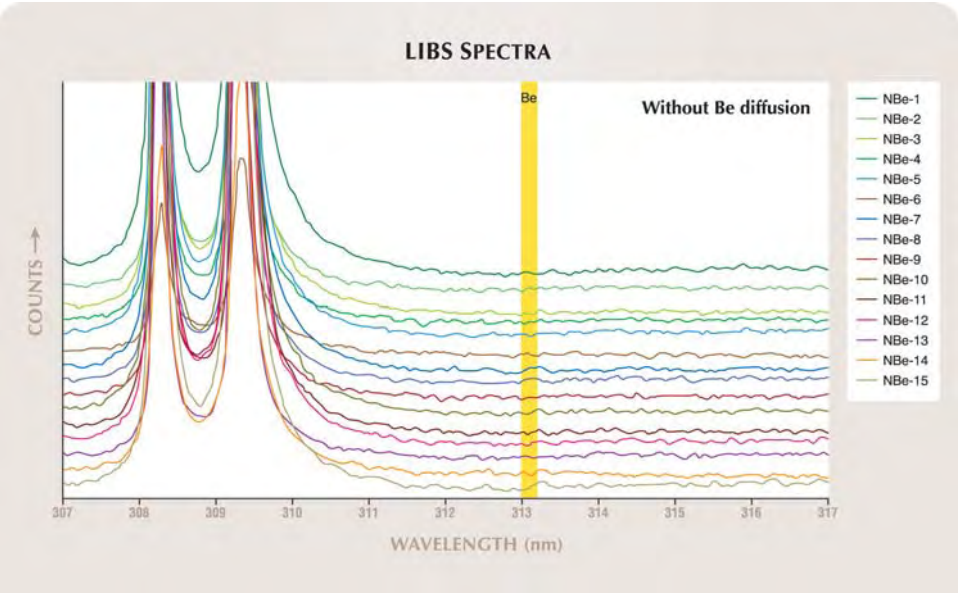

Figure 9. The LIBS spectra of the samples that were either untreated or heated by traditional methods (NBe-1 to NBe-15) do not show Be emission at 313.08 nm. The dominant peaks at about 308 and 309 nm are due to Al.

trum in figure 8 represents a single LIBS spot, it reflects only the Be concentration at that particular location. Consequently, to better characterize a sample with LIBS, it is often useful to analyze the stone in several places.

The spectra of two beryllium-free synthetic samples showed no Be peak at 313.08 nm, but they did show several peaks in the 310–314 nm region (figure 8) that are due to chromium (NBeS-1) and vanadium (NBeS-2).

Figure 9 presents the LIBS spectra of all the corundum samples that were not subjected to Be-diffusion treatment. The spectra are quite uniform, and none shows a Be peak at 313.08 nm. Although the composition of these samples varied (especially Cr and V), there do not appear to be any distinct chromium or vanadium emissions in the spectral range of 307–317 nm.

DISCUSSION

Our investigations show that Be-diffused sapphires can be reliably detected by LIBS. In one sample (BeS-1), our system was able to detect a Be concentration as low as ~2–3 ppm. As discussed by Pisutha-Arnoud et al. (2004), very low Be concentrations (on the order of 3 ppm) may result in the formation of a stable yellow (or brown, in Fe-free stones) color center in corundum, and this appears to be the case for the orange synthetic sapphire (BeS-1).

The Be diffusion–treated natural sapphires (Be-1 to Be-6) showed distinctly higher Be concentrations than the Be-doped synthetic sample. The levels of Be measured by LA-ICP-MS in these samples (4–49 ppm Be) are consistent with those reported for Be-diffused sapphires in the literature (see, e.g., Hänni and Pettke, 2002; Emmett et al., 2003). All the LIBS spectra from these samples showed a moderate to distinct Be emission peak centered at 313.08 nm.

A comparison of the Be-containing samples with the two untreated flame-fusion synthetics revealed no peak overlap at 313.08 nm from the corundum matrix. Chromium and vanadium peaks may be in the same range near 313 nm, as shown by the highly Cr- and V-doped synthetic samples (NBeS-1 and NBeS-2; figure 8), but they do not exactly overlap with Be emission. Potentially overlapping emissions from other elements were not observed; their emission intensity in the corundum matrix is too low to produce any interference with the Be emission at 313 nm.

In the natural untreated or traditionally heated corundum samples (NBe-1 to NBe-15), no Be emission at 313 nm could be detected. This was expected since LA-ICP-MS data on three of the samples (NBe-1, NBe-6, NBe-14) showed that beryllium was below the detection limit (generally <0.3–0.8 ppm).

CONCLUSIONS

Our investigations using the modified Ocean Optics LIBS 2000+ system (SSEF GemLIBS) were successful in detecting Be-diffusion of corundum. Based on extensive research, we have developed an analytical technique for routine testing of faceted corundum for the presence of beryllium.

Compared to other methods of Be detection, LIBS has several advantages. The sample preparation is very simple (i.e., attaching the stone to a glass plate with Blu-Tack), and no vacuum is needed for analysis. The LIBS instrument is much less expensive than SIMS or LA-ICP-MS, and it also is easier to maintain. (As a general rule, a LIBS system costs US$20,000–$90,000, whereas LA-ICP-MS ranges from $200,000 to $500,000 and SIMS may run from $750,000 to over $2,000,000.) When equipped with broad-band spectrometers, LIBS is capable of simultaneous multi-element detection (from low to high atomic weights). The detection limit for Be in corundum is quite low, at about 2 ppm (depending on the experimental parameters). After calibration and validation of a specific LIBS system, Be detection in corundum can be done by knowledgeable lab personnel without extensive training.

A disadvantage of LIBS is that it is slightly destructive. Even when it is properly used, the laser leaves small spots on the surface of the gemstone, similar to other Be detection methods such as LA-ICP-MS and SIMS. Also, the LIBS technique only yields qualitative to semiquantitative data, unlike the other two Be-detection techniques.

This article describes the first systematic use of LIBS in gemology, that is, for the detection of Be-diffused sapphires. LIBS may also have some potential for determining the geographic origin of gemstones and identifying color modification in pearls and other gem materials, since this technique can detect a full range of elements, even at trace levels. Moreover, its relatively low cost makes it a viable technique for many gemological laboratories.

ABOUT THE AUTHORS

Dr. Krzemnicki is a gemologist and director of education at the SSEF Swiss Gemmological Institute in Basel, Switzerland. Dr. Hänni is director of SSEF and professor at the University of Basel, Switzerland. Dr. Walters is vice president of research and development at Ocean Optics Inc., Orlando, Florida.

ACKNOWLEDGMENTS: The authors thank Kees Van De Steeg, Richard Grootveld, and all of the staff at Ocean Optics Inc. for their support during the installation of the LIBS instrument at SSEF. Further thanks go to Hans-Ruedi Rüegg of the Mineralogical Institute, University of Basel, for technical assistance. LA-ICP-MS analyses were carried out at the Institute of Mineral Resources at the Swiss Federal Institute of Technology (ETH) Zurich by Dr. Thomas Pettke, under the direction of Dr. Christoph Heinrich. Greatly appreciated are discussions with, and information provided by, Dr. Detlef Günther (ETH Zurich, Switzerland), Dr. Johannes Heitz (Johannes Kepler University, Linz, Austria), and Dr. John Emmett (Crystal Chemistry, Brush Prairie, Washington). We thank Werner Spaltenstein (Multicolor Ltd., Chanthaburi, Thailand) and Djeva S.A. (Monthey, Switzerland) for donating samples for this research.

REFERENCES

Allemand C.D. (1972) Spectroscopy of single-spike laser-generated plasmas. *Spectrochimica Acta Part B*, Vol. 27, pp. 185–188.

Bogue R.W. (2004) Boom time for LIBS technology. *Sensor Review*, Vol. 24, No. 4, pp. 353–357.

Brech F., Cross L. (1962) Optical microemission stimulated by a ruby maser. *Applied Spectroscopy*, Vol. 16, p. 59.

Carranza J.E., Hahn D.W. (2002) Assessment of the upper particle size limit for quantitative analysis of aerosols using laser-induced breakdown spectroscopy. *Analytical Chemistry*, Vol. 74, No. 21, pp. 5450–5454.

Corney A. (1977) *Atomic and Laser Spectroscopy*. Clarendon Press, Oxford, England.

Emmett J.L., Scarratt K., McClure S.F., Moses T., Douthit T.R., Hughes R., Novak S., Shigley J.E., Wang W., Bordelon O., Kane R.E. (2003) Beryllium diffusion of ruby and sapphire. *Gems & Gemology*, Vol. 39, No. 2, pp. 84–135.

García-Ayuso L.E., Amador-Hernández J., Fernández-Romero J.M., Luque de Castro M.D. (2002) Characterization of jewellery products by laser-induced breakdown spectroscopy. *Analytica Chimica Acta*, Vol. 457, No. 2, pp. 247–256.

Gruber J., Heitz J., Arnold N., Bäuerle D., Ramaseder N., Meyer W., Hochörtler J., Koch F., (2004) In-situ analysis of metal melts in metallurgic vacuum devices by laser-induced breakdown spectroscopy. *Applied Spectroscopy*, Vol. 58, No. 4, pp. 457–462.

Guillong M., Günther D. (2001) Quasi "non-destructive" laser ablation–inductively coupled plasma–mass spectrometry fingerprinting of sapphires. *Spectrochimica Acta Part B*, Vol. 56, No. 6, pp. 1219–1231.

Günther D., Frischknecht R., Heinrich C.A. (1997) Capabilities of an argon fluoride 193 nm excimer laser for a laser ablation inductively coupled plasma mass spectrometry microanalysis of geological materials. *Journal of Analytical Atomic Spectrometry*, Vol. 12, pp. 939–944.

Hänni H.A., Pettke T. (2002) Eine neue Diffusionsbehandlung liefert orangefarbene und gelbe Saphire. *Gemmologie: Zeitschrift der Deutschen Gemmologischen Gesellschaft*, Vol. 51, No. 4, pp. 137–152.

Hänni H.A., Krzemnicki M.S., Kiefert L., Chalain J.P. (2004) Ein neues Instrument für die analytische Gemmologie: LIBS. *Gemmologie: Zeitschrift der Deutschen Gemmologischen Gesellschaft*, Vol. 53, No. 2/3, pp. 79–86.

Hänni H.A., Krzemnicki M.S. (2004) A new tool in analytical gemology: LIBS. *29th International Gemological Congress*, Wuhan, China, p. 63.

Krzemnicki M.S., Hänni H.A. (2004) The potential of LIBS in gemstone testing: Detection of Be-diffusion treated corundum and determination of country of origin based on chemical fingerprinting. *3rd International Conference on Laser Induced Plasma Spectroscopy and Applications*, September 28–October 1, Malaga, Spain.

McClure S., Moses T., Wang W., Hall M., Koivula J.I. (2002) Gem News International: A new corundum treatment from Thailand. *Gems & Gemology*, Vol. 38, No. 1, pp. 86–90.

Peretti A., Günther D. (2002) Colour enhancement of natural fancy sapphires with a new heat-treatment technique (Part A). *Contributions to Gemmology*, Vol. 1, pp. 1–48.

Pisutha-Arnoud V., Häger T., Wathanakul P., Atichat W. (2004) Yellow and brown coloration in beryllium treated sapphires. *Journal of Gemmology*, Vol. 29, No. 2, pp. 77–103.

Radziemski L.J., Cremers D.A., Loree T.R. (1983) Detection of beryllium by laser-induced-breakdown spectroscopy. *Spectrochimica Acta Part B*, Vol. 38, No. 1/2, pp. 349–355.

Scarratt K. (2002) Orange-pink sapphire alert. American Gem Trade Association, www.agta.org/consumer/gtclab/orange-sapphirealert.htm.

LAB NOTES 2004

EDITORS

Thomas M. Moses, Ilene Reinitz,
Shane F. McClure, and Mary L. Johnson
GIA Gem Laboratory

CONTRIBUTING EDITORS

G. Robert Crowningshield
GIA Gem Laboratory, East Coast

Cheryl Y. Wentzell
GIA Gem Laboratory, West Coast

Faceted APOPHYLLITE With "Crop Circles"

Although apophyllite is found in beautiful transparent colorless to pale green tetragonal crystals of relatively good size, it is virtually unheard of as a faceted gemstone. On the one hand, its perfect basal {001} cleavage makes it difficult to cut. On the other, as a hydrated silicate [$(KCa_4Si_8O_{20}(OH,F)\cdot 8H_2O$], apophyllite is also very susceptible to heat damage, so even the friction from grinding and polishing on a lap can generate enough heat to cause cracking. It was therefore of interest to document gemologically the 6.28 ct near-colorless oval modified brilliant cut (13.11 × 11.48 × 9.31 mm) apophyllite shown in figure 1, the first faceted apophyllite we have seen in the laboratory. The gem, from Poona, India (a locality famous for apophyllite), was provided for examination by internationally known Scottish gemologist Alan Hodgkinson.

Figure 1. This 6.28 ct stone—from Poona, India—is the first faceted apophyllite we have encountered in the laboratory. Note the slight iridescence visible beneath the table facet.

True to its nature, this faceted apophyllite had a relatively large cleavage open to the surface (again, see figure 1), which was clearly visible through the table facet. The cleavage was oriented in a plane slightly off parallel to the table, an alignment that was probably intentional. Had the planes of the table and the cleavage been parallel, it would have been virtually impossible to get a good polish on the table facet.

Gemological identification was relatively straightforward, with only standard instruments needed. When the stone was examined through the table facet, a uniaxial optic figure was clearly visible in polarized light. The refractive index was recorded as n_o = 1.531 and n_e = 1.534 in monochromatic near-sodium equivalent light, with a corresponding birefringence of 0.003. The stone was inert to both long- and short-wave ultraviolet radiation, and the hydrostatic specific gravity was 2.38.

As seen in figure 2, the most striking feature of this gem was the condition of its internal cleavage surfaces when viewed with magnification. Rather than being more or less "feathery" in appearance, as is common on fresh cleavage surfaces, this particular cleavage was relatively smooth. It showed distinctive rectangular, circular, and square patterns, with some

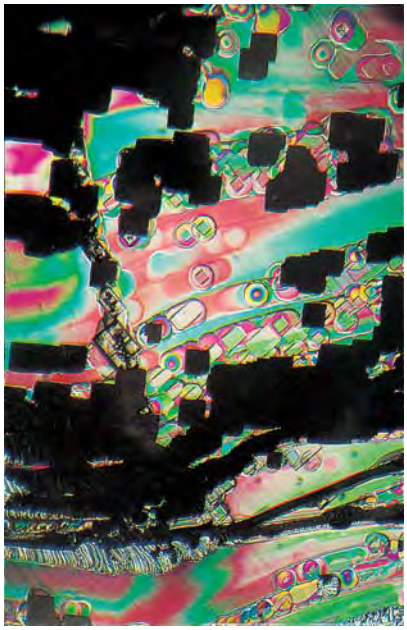

Figure 2. With 15× magnification, the apophyllite's perfect basal {001} cleavage shows a pleasing "crop circle" geometry colored by bright interference colors.

Editor's note: The initials at the end of each item identify the editor(s) or contributing editor(s) who provided that item. Full names are given for other GIA Gem Laboratory contributors.

GEMS & GEMOLOGY, *Vol. 40, No. 4, pp. 323–333*

squares being contained in the centers of the circles. This was somewhat reminiscent of the infamous and relatively controversial "crop circles" that have been found in some farm fields. From the overall appearance of the inner walls of the cleavage, we suspect that the interesting geometric forms were the result of regrowth, rather than post-growth etching.

John I. Koivula and Maha Tannous

DIAMOND

Luminescent "Hopper" Diamond

The vast majority of the diamonds graded by the GIA Gem Laboratory are polished goods, so we enjoy the opportunity to examine natural diamond crystals that exhibit attractive colors or shapes, as well as other features. Such crystals are "gems" in their own right, and because of their intriguing beauty they often remain in their natural state, uncut. It was therefore with interest that we recently examined a 2.03 ct transparent, near-colorless diamond cube that showed significant hopper growth (that is, where the faces have grown more at the edges and corners than in the center) and etching, with the center of each of the cube faces depressed and the edges and corners extended (figure 3).

The crystal, which measured 5.90 × 5.72 × 5.67 mm, was purchased in Antwerp by Chris Amo of CEO Enterprises, Amherst, New York. He spotted it at a diamond cutting factory as it was being checked for UV luminescence. The crystal stood out immediately because of its bright yellow fluorescence to long-wave UV radiation, and the fact it looked like a glowing star when viewed in a direction toward a corner point (figure 4). After purchasing the crystal, which was in a parcel of rough diamonds reportedly from the Democratic Republic of the Congo, Mr. Amo sold it to gem and mineral collector William W. Pinch of Rochester, New York, who in turn provided it to the laboratory for examination.

Figure 3. Note the cavernous appearance seen on the faces of this 2.03 ct "hopper" diamond crystal.

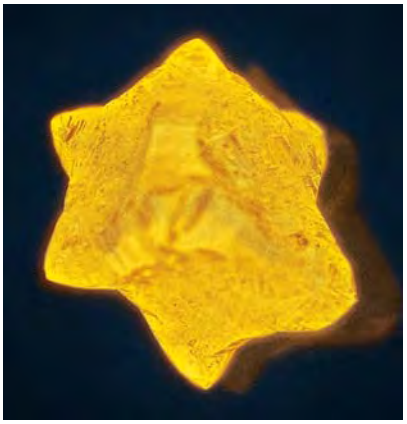

Figure 4. When viewed directly toward a corner, this 2.03 ct etched diamond cube showed an obvious stellate form that was further accentuated by the strong yellow fluorescence to long-wave UV.

Strain was visible in the diamond crystal when it was examined with magnification between crossed polarizers; the strain colors served to highlight the cubic etch figures and other surface contours (figure 5) visible on all the crystal's faces. Using the deep UV radiation of the Diamond Trading Company (DTC) DiamondView, we did not observe any growth zoning. Fourier-transform infrared (FTIR) spectrometry showed that the crystal was a type IaA, with significant amounts of both nitrogen and hydrogen.

It is not often that we see a crystal, such as this diamond from the Congo, that possesses all the attributes (beauty, durability, and rarity) required of a gem, as well as distinctive fluorescence and surface features.

Figure 5. Viewed between crossed polarizers with 10× magnification, intense strain colors in the 2.03 ct diamond highlight the cubic etch pits and related surface contours.

John I. Koivula, Maha Tannous, and Christopher M. Breeding

"Magnetic" Natural Pink Diamond

One interesting feature of some synthetic diamonds is their attraction to a simple magnet. (Strictly speaking, diamonds do not possess any magnetism.) This apparent "magnetism" is due to the existence of metallic inclusions—usually the flux materials, such as Fe, Ni, or Co, used in the growth process. While magnetism is a very good indication that a diamond is synthetic, some rare exceptions do exist.

Recently, a 0.12 ct Fancy Intense purplish pink diamond (figure 6) submitted to the West Coast laboratory demonstrated apparent magnetism (figure 7). In addition to pink graining, magnification revealed several inclusions, among them "feathers" and

Figure 6. This 0.12 ct Fancy Intense purplish pink natural diamond demonstrated apparent magnetism.

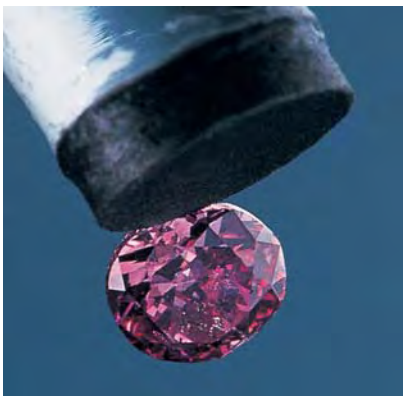

Figure 7. Because of iron-containing residue in surface cavities, this diamond could be suspended when touched by a magnet.

dark features, a few of which reached the surface. Some of these features had a platy habit, while others were irregular in shape. The diamond also had several cavities on the girdle and pavilion facets that were filled with a dark material. It had a few cloud-like patches of pinpoint inclusions, but their appearance was different from the clouds we have seen in synthetic diamonds. When observed with a desk-model spectroscope, the diamond showed only a 415 nm "Cape" line. It fluoresced blue to standard long-wave UV radiation, and yellow and blue to short-wave UV. When examined with the DTC DiamondView fluorescence imaging system (figure 8), it did not show the cross-shaped zoning typically seen in most synthetic diamonds. Last, no bands that could be attributed to Ni or other flux metals were observed in the photoluminescence spectrum. On the basis of these results, we concluded that the diamond was natural.

Figure 8. In this fluorescence image recorded with the DTC DiamondView, the cross-shaped zoning pattern typical of most synthetic diamonds is absent. The residue-filled surface cavities can be seen along the girdle on the left side of the diamond.

Figure 9. This photomicrograph shows the residue-filled surface cavities along the girdle of the diamond. Chemical analysis by EDXRF revealed the presence of Fe and Ca in the residue. Magnified 60×.

When a magnet was brought close to the diamond, however, it attracted the dark material that was exposed in cavities along the girdle (figure 9). When we analyzed this dark material using energy-dispersive X-ray fluorescence (EDXRF) spectroscopy, we found Fe and Ca to be the major components. We studied the exposed dark material further using Raman spectroscopy and found features that could be attributed to hematite, limonite (rust), and diamond. We concluded that this dark material was residue from the manufacturing process. Metallic fragments within the residue caused the magnetic behavior of this sample, while oxidation of the iron fragments generated the hematite and limonite peaks observed in the Raman spectra. We attempted to analyze the dark inclusions in the diamond with Raman spectroscopy, but the spectra did not reveal any recognizable features. Raman analyses of some of these inclusions where they reached the surface produced spectra similar to the spectrum of the dark material in the cavities, but this also may be from residue covering those inclusions.

The magnetic response of this natural diamond was similar in intensity to what we have seen in synthetic diamonds with metallic inclusions. Cleaning the diamond with acid would presumably dissolve this residue, and thereby render the diamond "nonmagnetic." Attraction to a magnet remains a useful way to check for synthetic diamonds, but as with other gem testing methods, this should not be the sole identification criterion.

Andy H. Shen and James E. Shigley

Diamond with Many Microscopic Carbonate Inclusions

Mineral and fluid inclusions in diamond have been studied extensively, because of the unique information they offer about diamond formation and the geochemistry of the Earth's mantle. Carbonate, phosphate, and water inclusions of microscopic scale also have been reported in the coatings on many of those natural diamonds

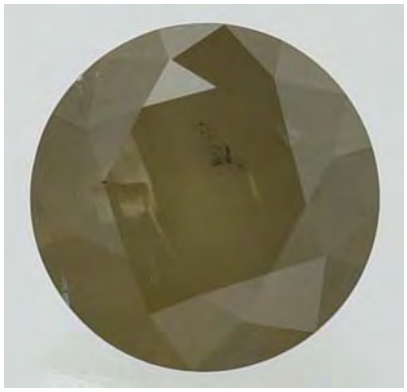

Figure 10. This 2.38 ct Fancy Dark brown–greenish yellow diamond contains numerous microscopic carbonate inclusions.

Figure 11. Micro-inclusions occur throughout the 2.38 ct diamond, and relatively large particles are aligned to form many nearly parallel bands. Width of the image is 3.2 mm.

that have a translucent outside "skin" and a transparent gem-quality core (see, e.g., O. Navon et al., "Mantle-derived fluids in diamond micro-inclusions," *Nature*, Vol. 335, 1988, pp. 784–789). Ranging up to 1 mm thick, these coatings generally are removed by the cutting and polishing process, although coatings on some (usually very small) cuboid opaque diamonds could extend to the central part of the crystals. The East Coast laboratory recently examined a faceted diamond (figure 10) that had dense microscopic carbonate inclusions similar to those found in such coatings; however, the micro-inclusions occurred throughout the entire stone, with relatively large particles aligned in many nearly parallel bands (figure 11). These inclusions also showed some interesting features in their composition.

The 2.38 ct round brilliant cut (8.63 × 8.66 × 5.27 mm) was color graded Fancy Dark brown–greenish yellow, and its clarity was at the bottom of the GIA clarity grading scale. Indeed, it was translucent due to the micro-inclusions. No transparent region was observed even with magnification. Infrared absorption spectroscopy showed that the diamond was a type IaA, with very low nitrogen but relatively high hydrogen concentrations (figure 12). Strong absorptions at 1471–1433 and 874 cm^{-1}, and a weak but sharp absorption at 729 cm^{-1}, from micro-inclusions of calcite and dolomite-ankerite were detected. These features are similar to those observed for micro-inclusions in diamond coatings. However, a strong and sharp peak at 3698 cm^{-1} also was observed, which is not present in coatings and rarely occurs in diamond. Another unusual feature of this diamond was that no water component was detected. Water is very common in diamond coatings, and the absence of water and the relatively large size of this diamond indicate that it crystallized in a stable carbonate-rich and water-poor environment.

Despite the low clarity, this diamond was of interest due to the numerous micro-carbonate inclusions and their uniform arrangement.

Wuyi Wang and TMM

Figure 12. The IR absorption spectrum of this unusual diamond revealed the presence of calcite and dolomite-ankerite (i.e., features at 1471–1433, 874, and 729 cm^{-1}). The absorption at 3698 cm^{-1} is rarely observed in diamond or its inclusions; its assignment is unclear.

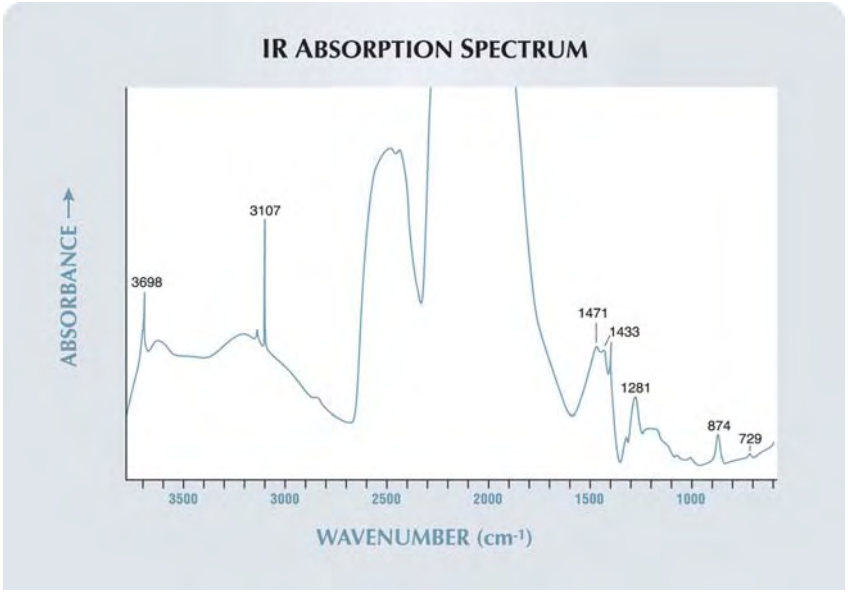

Unusual Near-Colorless SYNTHETIC DIAMOND

Recently, a 0.32 ct near-colorless round brilliant was submitted to the West Coast laboratory for a Diamond Dossier report. Gemological examination of the inclusions and spectroscopic analysis suggested that this was not a typical diamond. Further testing with the DTC DiamondView instrument strongly indicated that the diamond was, in fact, a synthetic. Although GIA does not provide color or clarity grading services for synthetic diamonds, had this been a natural

stone it would have been equivalent to the VS range in clarity, with only a few small inclusions in the crown, and approximately I color.

It is extraordinary to encounter such a high-quality near-colorless synthetic diamond in the marketplace, because this material is extremely difficult to grow by conventional high pressure/high temperature processes. Considerable effort and expense must be undertaken to prevent nitrogen (which causes yellow in diamonds) from being incorporated during diamond growth. Furthermore, the processes required to limit nitrogen almost always result in abundant, readily visible inclusions.

Previous researchers have described experimental synthetic diamonds from De Beers and General Electric Co. that showed properties similar to this sample (see, e.g., J. E. Shigley et al., "Gemological properties of near-colorless synthetic diamonds," Spring 1997 *Gems & Gemology*, pp. 42–53). Because of the rarity of this type of near-colorless synthetic diamond, a full description of its properties is presented here.

Microscopic examination revealed opaque metallic-appearing inclusions, pinpoint inclusions, and a number of very thin, translucent, parallelogram-shaped platelets that appeared gray-blue to brown and transparent in transmitted light (figure 13). Similar inclusions were described by Shigley et al.; however, those platelets were triangular. When viewed between crossed polarizing filters, anomalous birefringence ("strain") was observed to be associated with the platelets; but the cross-hatched, or "tatami," strain typical of natural type IIa diamonds was absent. A cloud of very fine pinpoint inclusions, similar to those often seen in synthetic diamonds, was evenly distributed throughout the sample, although it was not dense enough to have a significant effect on clarity. The opaque inclusions in this synthetic diamond appeared as fine black rods, needles, or sub-rounded particles in transmitted light. Several of these reached the surface and appeared metallic and "gold" colored in reflected light. The opaque inclusions were not attracted to a magnet, and Raman spectroscopy suggested that they consisted of non-diamond, carbon-rich material.

Figure 13. This 0.32 ct near-colorless synthetic diamond, submitted to the lab for a grading report, revealed opaque metallic-appearing inclusions, "pinpoints," and numerous parallelogram-shaped platelets. Reflected light, magnified 35×.

All known colorless and near-colorless synthetic diamonds are type IIa; that is, they are effectively nitrogen-free. While spectroscopic analysis usually indicates that natural type IIa diamonds do contain very small amounts of nitrogen, absorption and photoluminescence spectra showed no evidence of nitrogen in this sample. However, the mid-infrared absorption spectrum displayed a feature at 2803 cm^{-1}, which indicates the presence of small amounts of boron (figure 14). Consistent with this finding, the sample was electrically conductive in a few directions.

When examined with long-wave UV radiation, the synthetic diamond was inert and showed no phosphorescence. The short-wave reaction was an unevenly distributed weak yellowish green, with a weak to moderate greenish phosphorescence that lasted more than one minute. Cathodoluminescence and DiamondView

Figure 14. The mid-infrared absorption spectrum of this synthetic diamond indicates the presence of small amounts of boron, as demonstrated by the feature at 2803 cm^{-1}. As would be expected, the synthetic diamond was electrically conductive in some directions.

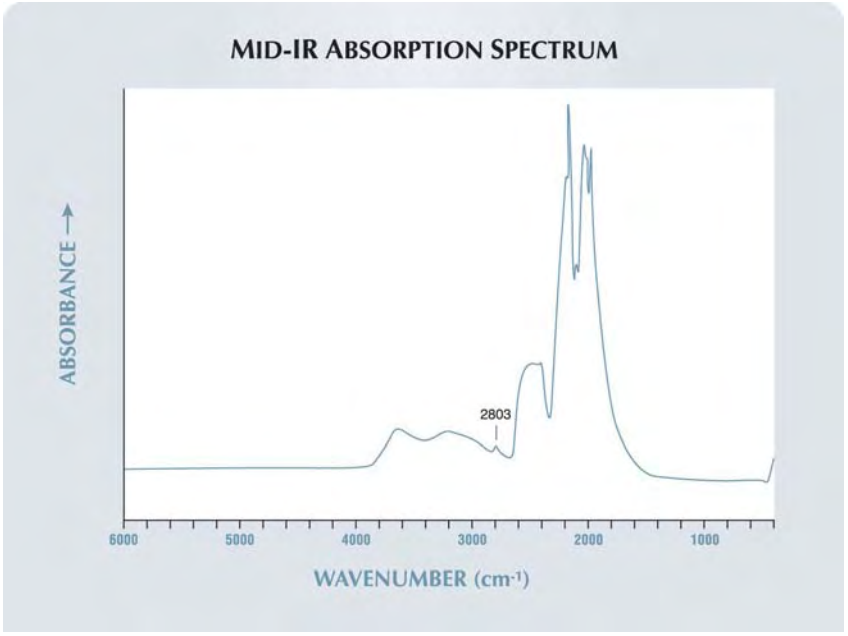

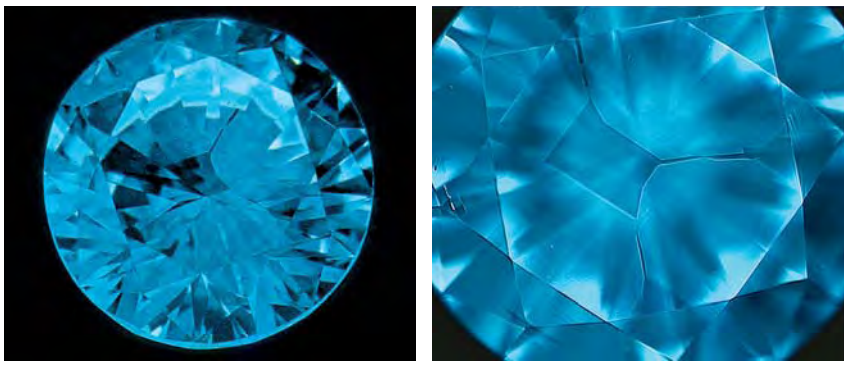

Figure 15. Cathodoluminescence (left) and DTC DiamondView (right) testing of the near-colorless synthetic diamond showed the cuboctahedral growth pattern and strong blue phosphorescence typical of synthetics.

reactions were pale blue and uneven, with a cuboctahedral growth pattern (i.e., square and cross-shaped zones) as well as strong blue phosphorescence, both of which are typical of synthetic diamonds (figure 15).

Although the rarity of high-quality colorless synthetic diamonds makes it easy to believe that one will not encounter such material in the trade, this sample serves as a strong reminder that these diamonds do exist and can be difficult for gemologists to identify without very careful examination of inclusions and fluorescence reactions.

Kimberly M. Rockwell

Orangy Brown IOLITE From Madagascar

A 4.45 ct transparent orangy brown oval modified brilliant was recently submitted to the West Coast laboratory for identification (figure 16) by Mark Kaufman of Kaufman Enterprises, San Diego, California. Gemological testing revealed that it was biaxial with R.I.'s of 1.532–1.541 (birefringence 0.009) and an S.G. of 2.57 (determined hydrostatically). It did not fluoresce to either long- or short-wave UV radiation and had only a weak-to-medium absorption band centered at 490 nm. The stone was represented as iolite from Madagascar, and the properties we recorded were consistent with those previously reported in the literature for this gem (see R. Webster, *Gems*, 5th ed., rev. by P. G. Read, Butterworth-Heinemann, Oxford, 1994, pp. 345–346). Due to its unusual color, we decided to perform Raman analysis, which confirmed that it was indeed iolite. Microscopic examination of the stone revealed fractures, iridescent dust-like particles throughout, "fingerprints," short needles, and spotty orange-brown color concentrations, along with unusual "roiled" growth zoning.

Most in the trade are familiar with the gem iolite (also known as cordierite) and its typical, attractive violetish blue color. It usually has strong pleochroism, consisting of deep violetish blue and near-colorless to light yellow-brown colors that can be observed without the aid of a polarizing filter (see Spring 2001 Gem News International, pp. 69–70). The iolite reported here also displayed fairly strong pleochroism, but the strengths of the individual colors were reversed. Whereas the violetish blue pleochroic color is typically the strongest in iolite, this orangy brown iolite's dominant pleochroic color was yellow-orange. It did have a grayish violet pleochroic component, but this was quite a bit weaker than the yellow-orange, so much so that it was not easily visible with the unaided eye.

Figure 16. This 4.45 ct orangy brown stone proved to be iolite. The color is very unusual for iolite, which is typically violetish blue.

In researching this material, we found very few references that listed brown as a possible color for iolite, and even the ones we found stated that this color was rare. None of the gemologists in the West Coast lab had previously seen an iolite of this color.

Elizabeth P. Quinn

Flashing LABRADORITE

Labradorite is a relatively common member of the feldspar group. It is so common, in fact, that large polished slabs of rock containing labradorescent phenocrysts of this mineral are used in the building and construction industries for walls and countertops. Like all gem materials, however, there is a very limited supply of fine-quality labradorite suitable for gem and jewelry applications.

The West Coast laboratory recently examined two well-polished labradorite gems, said to be from India, that were sent to us by lapidary Leon M. Agee of Deer Park, Washington. These stones displayed very attractive and dramatic banded labradorescence, which seemed to flash as the stones and/or overhead light source were moved back and forth in a direction perpendicular to the obvious lamellar twin structure.

The larger of the two stones was an 85.58 ct polished trapezoidal piece that measured 40.15 × 28.16 × 8.61 mm, while the other was a 34.98 ct

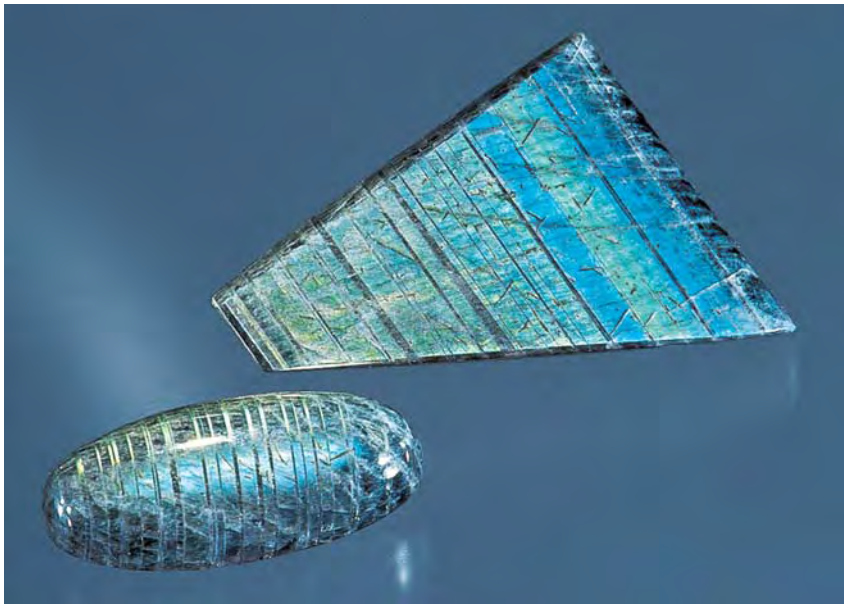

Figure 17. Accented by their characteristic labradorescent colors, these two phenomenal labradorites, weighing 85.58 and 34.98 ct, show distinct lamellar twinning. The cabochon also displays chatoyancy.

oval cabochon measuring 33.09 × 14.30 x 6.17 mm. As shown in figure 17, the labradorescence presented itself in relatively typical intense-to-muted shades of blue, green, and yellow. In addition to the labradorescent flash shown by both stones, the cabochon displayed a blue chatoyant band (also seen in figure 17), which seemed to be independent of the shift in color of the lamellar twin layers.

The labradorescent shift was particularly interesting when viewed with low magnification. As seen in figure 18 (left), almost the entire surface area displayed labradorescent interference colors; only a few thin bands appeared dark. When the light position was shifted 90° across the stone (figure 18, right), the broad colored areas went dark, while the once-dark thin twin layers showed bright labradorescence.

John I. Koivula and Maha Tannous

Figure 18. When examined with low (5×) magnification, almost the entire imaged surface of the trapezoidal labradorite displayed interference colors, with only a few thin twin bands remaining dark (left). When the incident light was shifted 90° (right), the thin twin layers showed labradorescence, while the rest of the stone went dark.

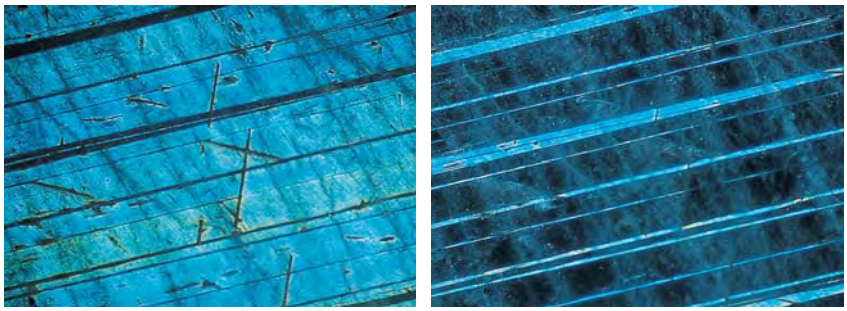

Natural Saltwater Mussel PEARLS

Nacreous saltwater pearls almost invariably originate from oysters (e.g., *Pinctada sp.* and *Pteria sterna*) or one of several species of abalone. Although there are some attractive non-nacreous "pearls" that originate from various mollusks (conch, melo melo, scallop, clam, etc.), it is rare to see attractive, colorful nacreous pearls from such an ordinary bivalve as a common saltwater mussel. The West Coast laboratory recently had the opportunity to examine two such natural pearls. The first was a 22.77 ct grayish purple and white baroque-shape pearl (figure 19) submitted by Jeremy Norris of Oasis Pearl in Albion, California. Mr. Norris reported that the pearl was recovered from the Pacific Coast of Baja California, Mexico. He also provided a shell of the saltwater mussel species from which he thought the pearl originated (again, see figure 19). Comparison to photos of various saltwater mussels and consultations with malacological experts indicated that the shell was that of *Mytilus californianus*, the California mussel (2004 pers. comms. from, e.g., Paul Valentich-Scott, Curator of Malacology, Santa Barbara Museum of Natural History).

The first task was to determine whether the specimen was a true nacreous pearl. This was readily proved by examination with magnification, which revealed a nacre platelet structure. However, the appearance of the overlapped "suture lines" (figure 20) differed from that seen in an oyster pearl, suggesting that it was from another type of mollusk.

X-radiography revealed a structure that was typical of natural pearls. Long-wave UV fluorescence was very weak dark brown to inert, mottled with weak light yellow and moderate to strong whitish areas that corresponded to the white areas on the pearl.

The pearl did not fluoresce to X-rays, which is typical for dark-colored pearls regardless of their freshwater or saltwater origin. EDXRF analysis, however, confirmed the absence of

Figure 19. This attractive grayish purple pearl (18.35 × 16.30 × 10.85 mm) is shown with a saltwater mussel shell from Mytilus californianus *(the California mussel). Both were recovered from the Pacific Coast of Baja California, Mexico.*

Mn, which proved the pearl was of saltwater origin.

With the saltwater mussel shell available, we decided to obtain UV-Vis and Raman spectra for both the pearl and the shell to see if there was a close correlation between the two. In fact, the UV-Vis reflectance spectra proved to be very similar, with a transmission maximum centered around 600 nm that would contribute to the reddish modifying component in the color of the pearl. Likewise, the Raman spectra for the pearl and the shell were nearly identical, with two distinct peaks at approximately 1094 and 1482 cm^{-1} that are consistent with the presence of carotenes.

These matching spectra would suggest that the pearl originated from this, or a closely related, type of mollusk. However, since it could not be confirmed that the pearl was produced by the type of mussel whose shell was provided, Mr. Norris sent us another darker, but very similar, 3.82 ct grayish purple mussel pearl with an accompanying shell that a local fisherman stated was the same as the host of that pearl (figure 21). Mr. Norris reported that these items also were recovered from the Pacific Coast of Baja California, where they are found in intertidal, estuary, and mangrove areas. Although the interior of the *M. californianus* shell contained a small patch of highly iridescent nacre toward its outer edge (again, see figure 19), the color of this area and the dark violet pigments in the colored part of the shell interior did not closely resemble that of the pearl's nacre. The second saltwater mussel shell, however, was smaller, slightly different from the first, and had an interior mother-of-pearl surface with a reddish purple color that closely matched that of the two pearls (again, see figure 21). Experts agreed that the smaller shell was that of *Modiolus capax* (e.g., P. Valentich-Scott, pers. comm., 2004). *M. capax*, the fat-horse mussel, has a

Figure 20. The suture lines of this mussel pearl are notably different from those of saltwater oyster pearls, with a textured zone along the leading edge that causes them to appear coarser and more broadly defined. Magnified 25×.

Figure 21. This smaller, darker grayish purple pearl (10.15 × 9.15 × 5.75 mm) rests on the shell of the saltwater mussel Modiolus capax *(also found in Mexico), which has an interior surface that more closely matches the appearance of both this pearl and the one in figure 19.*

reddish shell, a nacreous interior, and grows up to approximately 14 cm in length, a size capable of producing the large pearl shown in figure 19. Like *M. californianus*, it is also of the family *Mytilidae*.

UV-Vis and Raman spectra were collected for the second pearl and shell specimens to compare with the first. The UV-Vis reflectance spectra were all very similar to each other, and the Raman spectra were all nearly identical, with the same carotene absorption peaks. The Raman spectra also matched those for another common North American saltwater mussel that was found in Carlsbad, California, most likely a *Mytilus galloprovincialis* (European blue mussel or bay mussel). The similarities among these Raman spectra are in contrast to the distinct differences from those for a pink conch pearl, which had a $CaCO_3$ peak at 1085 cm^{-1} and carotene peaks at 1124 and 1512 cm^{-1}, as well as from those of several purple to pink freshwater pearls, which had a 1084 cm^{-1} $CaCO_3$ peak and carotene peaks at 1130 and 1523 cm^{-1}. The similarity in the data between the purple saltwater pearls and their accompanying mussel shells, along with the dissimilarity to data collected from more disparate species, strongly indicated that the purple pearls originated from one of a group of closely related mussels, probably of the *Mytilidae* family, and quite possibly from genus *Modiolus*.

CYW and Shane Elen

Treated-Color "Golden" South Sea CULTURED PEARLS

Determining the origin of color for "golden" South Sea cultured pearls has been an increasingly important challenge in recent years. The growing demand for these cultured pearls, for which natural-color supplies are limited, has led to a greater variety of treated-color products in the marketplace.

Two recent *G&G* articles by S. Elen addressed the identification of treated-color "golden" South Sea pearls ("Spectral reflectance and fluorescence characteristics of natural-color and heat-treated 'golden' South Sea cultured pearls," Summer 2001, pp. 114–123; "Update on the identification of treated 'golden' South Sea cultured pearls," Summer 2002, pp. 156–159). The 2001 article showed that the natural-color cultured pearls exhibit a broad absorption feature from 330 to 460 nm, which is the combination of two individual absorption features: 330–385 nm and 385–460 nm. The treated-color "golden" South Sea cultured pearls examined had UV-visible absorption features in the 330–385 nm region that were consistently weaker than those of their natural-color counterparts. Some—but not all—of the treated-color samples also exhibited color concentrations in nacre defects and/or around the drill holes.

Figure 22. These three strands of drop-shaped "golden" South Sea cultured pearls proved to be treated color.

The East Coast laboratory recently examined three strands containing a total of 87 drop-shaped "golden" South Sea cultured pearls (as indicated by X-radiography) ranging from 18.15 × 15.55 × 14.90 mm to 13.50 × 12.45 × 12.10 mm. The overall color was an unnatural orangy yellow with an unusual pinkish cast evident in some lighting conditions (figure 22). With 10× magnification, all these cultured pearls showed a slightly mottled nacre with small raised spots and patches. They also exhibited visible signs of dye, including an unevenly distributed color accompanied by small concentrations of a deep red dye. Some of the dyed areas were dendritic in shape, whereas others were visible below the surface, indicating the cultured pearls were dyed after drilling.

Reflectance spectra were collected for all 87 of the cultured pearls (figure 23). We then compared the reflectance spectra of these treated-color samples to the spectrum of a natural-color cultured pearl shown in Elen (2001, figure 8). The natural-color spectrum exhibited the characteristic broad absorption from 330 to 460 nm, with stronger absorption in the UV (330–385 nm) than in the blue (385–460 nm). The treated-color cultured pearls showed increased absorption (i.e., lower reflectance) at ~305 nm, in contrast to the well-defined reflectance feature in natural-color cultured pearls. A very weak ~345 nm absorption and a 415–430

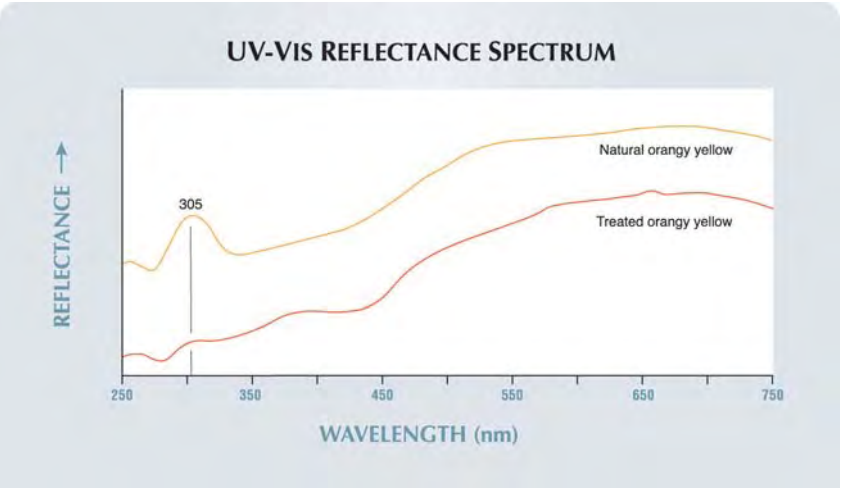

Figure 23. The South Sea cultured pearls in this study exhibited absorption features at ~345 and 415–430 nm that previously were reported in treated-color cultured pearls. The absence of a 305 nm reflectance feature is also consistent with treatment; natural-color cultured pearls show a well-defined 305 nm reflectance feature. (The spectrum of a natural-color orangy yellow pearl shown here is from Elen, 2001.)

nm absorption feature for 84 of the 87 treated-color cultured pearls were consistent with the Elen results, particularly for orangy yellow treated-color cultured pearls (see Elen, 2001, figure 9).

These results support Elen's conclusion that the absence of a 330–385 nm absorption is characteristic of treated-color "golden" cultured pearls. In addition, the absence of a well-defined reflectance feature at ~305 nm was characteristic of these treated-color "golden" cultured pearls. Differences between the spectra of the treated-color samples in Elen's studies and those described here probably result from differences in the pre-treatment characteristics of the cultured pearls and/or variations in the treatment method.

Carolyn van der Bogert

QUARTZ in Three Colors

In the Spring 2003 Lab Notes section (pp. 44–45), we discussed how some gem materials gain apparent bodycolor through the presence of brightly colored inclusions. The material featured in that note was quartz that was colored dark grayish blue by randomly scattered indicolite rods and needles. Apparent blue color in natural quartz was also mentioned as resulting from various other mineral inclusions, among them ajoite, a hydrated potassium sodium copper aluminum silicate hydroxide.

The West Coast laboratory recently had the opportunity to examine a freeform step-cut quartz (figure 24, left) that was colored a pleasing light blue by the presence of numerous fibers of ajoite (figure 25), which were identified by Raman analysis. This 3.52 ct gem (15.50 × 9.49 × 6.17 mm) was faceted by Art Grant of Coast to Coast Rare Gems in Martville, New York, who sent it to the laboratory for examination. The original rough material was from the Messina mine, Transvaal, Republic of South Africa, a locality well known among collectors for its specimens of quartz with inclusions of copper minerals.

At approximately the same time, the laboratory received for study two additional faceted quartzes that were colored by mineral inclusions. The largest of these was a 9.41 ct shield-shaped step cut (figure 24, center) that was fashioned from Russian "strawberry" quartz by Leon M. Agee. As expected for so-called strawberry quartz, and as shown in figure 26, this stone was colored by ultra-thin intense red inclusions of hematite (identified by Raman analysis), but it was unusual for the intensity and evenness of the color.

The third quartz (figure 24, right) was a 3.38 ct mottled dark green, pear-shaped step cut provided for examination by mineral collector Edward R. Swoboda of Beverly Hills, California, who reported that the locality was Kastamonu, in northern Turkey.

Figure 24. These three quartz gems are colored by mineral inclusions. Left to right, the color results from ajoite (3.52 ct), hematite (9.41 ct), and népouite (3.38 ct).

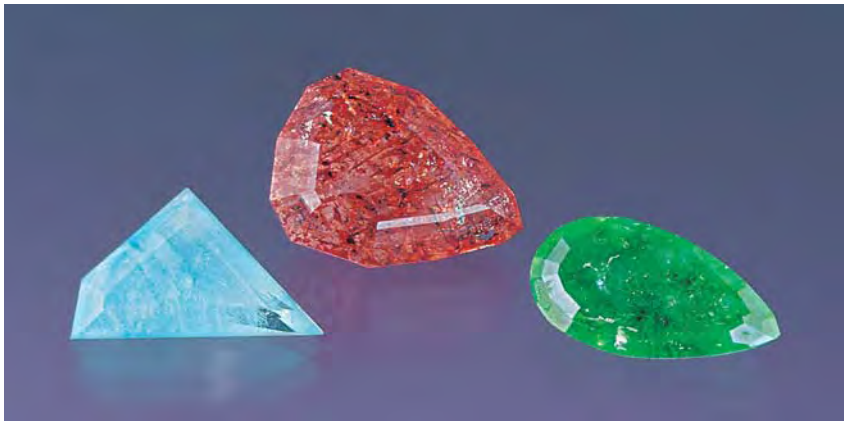

Figure 25. Colored by the presence of copper, these ajoite fibers are responsible for the blue face-up appearance of their otherwise colorless quartz host. Magnified 15×.

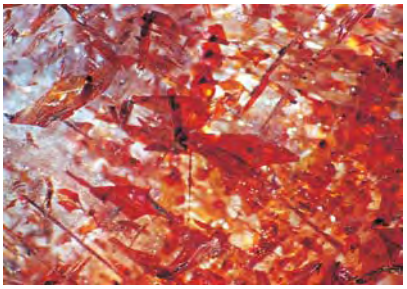

Figure 26. This quartz gained its color from the presence of numerous red transparent-to-translucent inclusions of hematite. Magnified 10×.

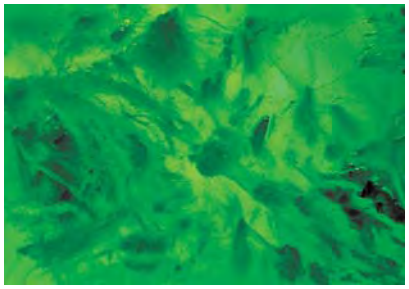

Figure 27. The green color of this quartz was provided by numerous dense sprays and compact masses of népouite, which in turn gets its color from nickel. Magnified 10×.

Magnification showed that the green bodycolor came from numerous dense sprays and compact masses of a green mineral (figure 27). X-ray powder diffraction analysis of a small amount scraped from the surface of the stone revealed the mineral to be a close match for népouite, a nickeliferous member of the kaolinite-serpentine group.

These three gems illustrate how mineral inclusions can provide very pleasing colors to stones that would otherwise be near-colorless. In all three cases, we were told, the color provided by the inclusions was the main reason these stones were cut.

John I. Koivula, Maha Tannous, and Dino DeGhionno

ERRATUM

The clarity-enhanced ruby entry in the Fall 2004 Lab Notes section (pp. 247–249) incorrectly stated that the glassy residue left by heat treatment of natural rubies can facilitate the partial healing of a fracture. It is *flux* that facilitates partial healing by dissolving the walls of a fracture, and then new crystallization (synthetic growth) occurs. The areas closest to the walls of a fracture are often synthetic corundum, and the center of the "filled fracture" is a noncrystalline glass byproduct.

PHOTO CREDITS
Maha Tannous—1, 3, 4, 6, 7, 15–17, and 24; John I. Koivula—2, 5, 18, 20, and 25–27; Andy Shen—8 and 9; Elizabeth Schrader—10 and 22; Wuyi Wang—11; Shane F. McClure—13; C. D. Mengason—19 and 21.

DIAMONDS

A natural diamond with very high Ni content. Nickel in diamond (as point defects and nickel-nitrogen complexes) is mainly known in synthetics that are grown from a Ni-containing catalyst. These synthetic diamonds may contain a large number of Ni-related absorption features in a wide region of the spectrum, from the UV to the NIR (S. C. Lawson, and H. Kanda, "An annealing study of nickel point defects in high-pressure synthetic diamond," *Journal of Applied Physics*, Vol. 73, No. 8, 1993, pp. 3967–3973). The presence of trace Ni impurities in natural diamonds has been known for years, but little has been published on the associated spectral features. K. Iakoubovskii and G. J. Adriaenssens ("Optical characterization of natural Argyle diamonds," *Diamond and Related Materials*, Vol. 11, 2001, pp. 125–131) and others have attributed a number of photoluminescence features detected in natural diamonds to nickel. More recently, the UV-Vis-NIR optical centers related to Ni and nickel-nitrogen complexes in a natural diamond were published by J.-P. Chalain (see the Winter 2003 Gem News International section, pp. 325–326).

The present contributors recently analyzed a saturated orangy yellow 1.33 ct natural diamond (figure 1) that contained elevated contents of Ni and exhibited very interesting properties. The diamond fluoresced pinkish orange to both long- and short-wave UV excitation, which is a very rare emission color for diamond. Yellow phosphorescence lasting several seconds also was observed, which was more distinct after short-wave UV excitation.

Internal features consisted of fractures and distinct etch channels, some with a tabular appearance (figure 1, inset). The morphology of these etch channels resembled that of the metallic flux inclusions in some HPHT-grown synthetic diamonds. These inclusions are sometimes dissolved during particular post-growth conditions, leaving behind hollow channels.

Infrared spectroscopy revealed that this was a low-

Figure 1. This 1.33 ct orangy yellow natural diamond displayed unusual Ni-related absorption features. The stone contains numerous hollow etch channels (see inset; magnified 25×), some of which appear dark in the photo of the diamond. Photos by F. Notari.

Editor's note: The initials at the end of each item identify the editor or contributing editor who provided it. Full names and affiliations are given for other contributors.

Interested contributors should send information and illustrations to Brendan Laurs at blaurs@gia.edu (e-mail), 760-603-4595 (fax), or GIA, 5345 Armada Drive, Carlsbad, CA 92008. Original photos will be returned after consideration or publication.

GEMS & GEMOLOGY, Vol. 40, No. 4, pp. 334–357

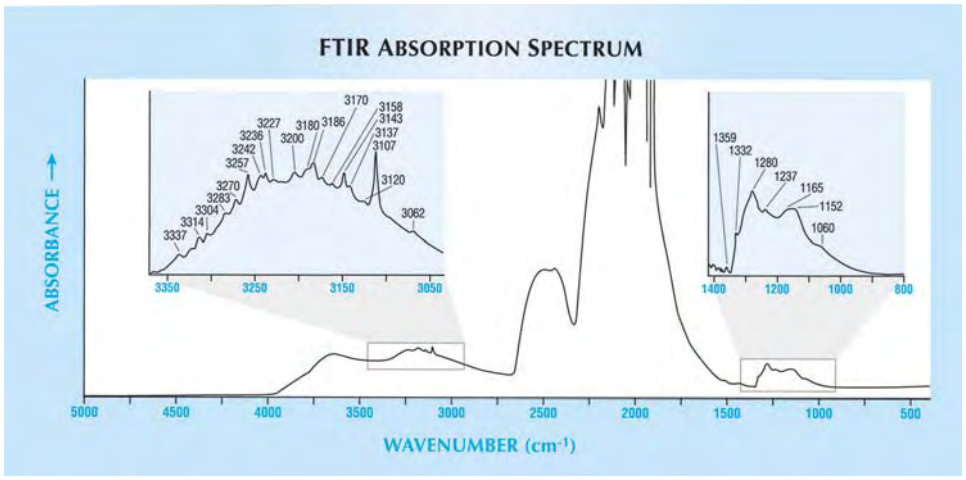

Figure 2. The FTIR spectrum indicates that the sample is a low-nitrogen type IaA natural diamond with a distinct Ib character, as shown by peaks at 1359 and 1237 cm^{-1} and several sharp absorptions between 3270 and ~3000 cm^{-1} (see insets). The spectrum proves natural origin, since most of these features are unknown in synthetic diamonds.

nitrogen type IaA diamond with a very distinct Ib character, as shown by peaks at 1359 and 1237 cm^{-1} and several sharp, weak absorptions between 3270 and ~3000 cm^{-1}, with main features at 3180 and 3143 cm^{-1} (figure 2; see G. S. Woods and A. T. Collins, "Infrared absorption spectra of hydrogen complexes in type I diamonds," *Journal of Physics and Chemistry of Solids*, Vol. 44, No. 5, 1983, pp. 471–475). This spectrum indicated natural origin, since most of the features recorded are unknown in synthetic diamonds.

A low-temperature Vis-NIR spectrum in the 400–1000 nm range was recorded to detect possible color treatment (figure 3). This spectrum was very unusual and exhibited at least 36 absorptions, with multiple oscillations between 600 and 720 nm. These oscillations are apparent as two distinct groups of absorptions with individual peaks that show regular spacing (i.e., 6–9 nm for the first group [610–647 nm] and about 8–9 nm for the second group [686–720 nm]). The oscillating nature of the second group is clearer than the first, which has rather variable spacing, intensity, and curve shapes (see figure 3, inset). Such spectral properties in diamond have been reported before, and the oscillating nature of the defects has been documented by I. M. Reinitz et al. ("An oscillating visible light optical center in some natural green to yellow diamonds," *Diamond and Related Materials*, Vol. 7, 1998, pp. 313–316). Those authors indicated that such a spectrum is extremely rare and possibly due to vibronic interactions of some unknown molecular species, particularly in green diamonds. In contrast, the saturated orangy yellow color of the 1.33 ct diamond described here can be explained by the absence of the two broad bands centered at ~700 and 600 nm, as seen in the spectrum of a green diamond published by Reinitz et al. The transmission window in the green part of the spectrum of the 1.33 ct diamond is distinctly weaker, so the stone appears yellow. There is no indication that the color of this diamond resulted from a treatment process.

A strong absorption at 891 nm (not mentioned by Reinitz et al., since their spectra did not extend above 850 nm) appeared to be a "normal" zero-phonon line, and thus

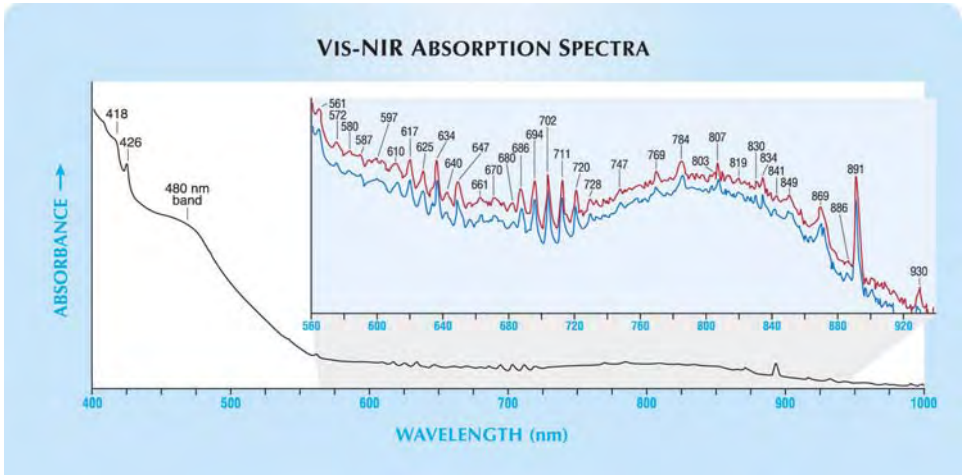

Figure 3. Numerous absorptions are evident in this low-temperature Vis-NIR spectrum of the diamond. The inset view of the 560–940 nm region shows two separately recorded spectra from this sample to demonstrate the reproducibility of the small absorptions. Besides the possibly oscillating nature of the defect(s) responsible for the 600–720 nm absorptions, the vibronic nature of the broad band at 800 nm with its zero phonon line at 891 nm is apparent.

the broad band centered at approximately 800 nm can be interpreted as the vibronic structure of this defect (again, see figure 3). To our knowledge, this is the first time that the 891 nm system has been documented in any diamond, natural or synthetic.

In our experience, the general appearance and positions of several absorptions in this spectrum have distinct similarities to the spectra of certain synthetic diamonds grown with a Ni catalyst, especially after annealing at high temperature. We have recorded Vis-NIR spectra of high-Ni synthetic diamonds with up to 25 sharp absorptions between 470 and 819 nm. Some of the absorptions seen in the spectrum of the 1.33 ct orangy yellow diamond were detected by us in a Ni-rich dark yellow-brown Gemesis synthetic diamond (i.e., at 572, 610, 617, 647, 661, 670, 694, 711, 747, and 819 nm). In contrast, the combination of bands at 426 and 480 nm is known in natural diamonds exhibiting a thermochroic and photochroic color change, the so-called "chameleon" diamonds (E. Fritsch, et al., "Examination of the twenty-two carat green chameleon diamond," in D. J. Content, Ed., *A Green Diamond: A Study of Chameleonism*, W. S. Maney & Son, Leeds, England, 1995, p. 25). Such diamonds also exhibit an 800 nm band, although they lack the vibronic structure seen in the spectrum of this sample. The 426 nm band provides additional proof that this is a natural diamond.

The low-temperature photoluminescence spectrum of the diamond provided further evidence of Ni-related defects (figure 4). The PL spectrum was very similar to those of chameleon diamonds analyzed by these contributors, and many of the observed emissions correspond to known features that are assigned to Ni point defects and nickel-nitrogen complexes. The features at 639, 657, 677, 690, 705, 723, 739, 800, and 884 nm seen in this diamond have been identified in Ni-catalyst synthetic diamonds and attributed to nickel defects (A. M. Zaitsev, *Optical Properties of Diamond: A Data Handbook*, Springer-Verlag, Berlin, 2001, pp. 140–197). In addition to these, the present authors know of emissions at 581, 590, 604, 616, 647, and 756 nm in synthetic diamonds grown from a Ni-containing catalyst.

Figure 4. The low-temperature photoluminescence spectrum of the diamond exhibits several emissions that appear to be Ni-related. The inset shows the weak Ni-related feature at 884 nm plus a weak 930 nm peak of unknown origin.

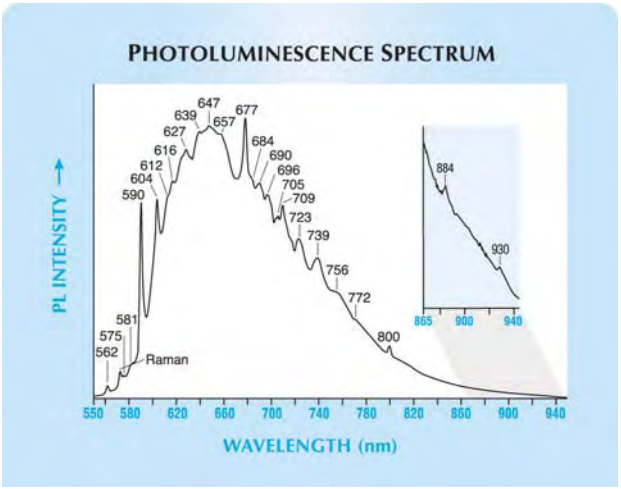

EDXRF spectroscopy of the diamond revealed distinct peaks for both Ni and Fe. From the spectrum we estimated the Ni content of the diamond at 30–50 ppm. While the Fe content was not too unusual for a natural diamond, the detection of Ni by EDXRF spectroscopy has so far been restricted to synthetic diamonds grown by the temperature gradient method using a Ni-containing catalyst (J. E. Shigley et al., "Gemesis laboratory-created diamonds," Winter 2002 *Gems & Gemology*, pp. 301–309). In natural diamonds, the Ni content is generally far too low to be detected by this method.

The same holds true for UV-Vis-NIR absorption spectroscopy, by which Ni point defects and nickel-nitrogen complexes can be identified in synthetic diamonds; in contrast, Ni-related features in natural diamonds are very rarely detected by this method. The only nondestructive method to effectively detect extremely low Ni contents in diamond is photoluminescence spectroscopy (see Zaitsev, 2001).

The complex Vis-NIR and PL spectra of this diamond are explained with high probability by the presence of an unusually high concentration of Ni-related defects. Our observation of many absorptions at approximately equal positions in the Vis-NIR and PL spectra of Ni-catalyst synthetic diamonds, combined with the detection of remarkable amounts of Ni in the 1.33 ct stone by EDXRF, lead us to propose that at least some of the many peaks in these spectra are due to naturally occurring Ni and/or nickel-nitrogen complexes. It would be very surprising *not* to detect Ni-related optical absorptions in the PL and Vis-NIR spectra of a diamond with such elevated Ni content, especially after the natural annealing this stone must have experienced, since substantial amounts of its nitrogen were aggregated. Further chemical analyses of diamonds exhibiting these spectral features will be performed to confirm these findings as we encounter the appropriate samples.

We thank Dr. Ilene Reinitz of the GIA Gem Laboratory in New York for reviewing this report.

Thomas Hainschwang (gemlab@adon.li)
Gemlab Gemological Laboratory
Vaduz, Principality of Liechtenstein

Franck Notari
GemTechLab Laboratory
Geneva, Switzerland

Figure 5. Violet chalcedony showing adularescence is being mined from the Qom area of central Iran. From left to right, Dr. Edib Dariush, two local miners, and Makhmout Douman are shown with some recent production; the mining pit can be seen in the background. The inset shows irregular nodules of the chalcedony that are partially covered by green glauconite. Photos courtesy of Makhmout Douman.

COLORED STONES AND ORGANIC MATERIALS

Adularescent chalcedony from Iran. Since 2003, violet chalcedony showing adularescence has been recovered from the Qom area near the Qom Salt Lake, about 150 km south-southwest of Tehran (figure 5). This area is underlain by Eocene andesite volcanic rocks. The chalcedony is found as irregular nodules that are mostly covered by glauconite, a green potassium-iron silicate (see figure 5, inset).

Mechanized mining is done by a group of geologists from Tehran, in an area measuring about 700 m^2. They produce approximately 800 kg of the chalcedony each month, but only a small portion (±150 kg) shows the violet color in moderate tones. Overall, the material ranges from light grayish violet to dark violet. In addition to the violet chalcedony, the area has yielded pink, yellow, and brown agate.

Cutting machines have been purchased from Germany, and the miners are planning to construct a polishing workshop in the future. So far, approximately 30 kg of rough violet chalcedony has been processed, yielding 8 kg of cabochons (ranging from 10 to 20 ct) and some polished slabs.

A 22.57 ct cabochon of grayish violet chalcedony displaying weak-to-moderate adularescence (figure 6) was examined by one of us (EPQ), and the following properties were recorded: diaphaneity—translucent; R.I.—1.538 (from the flat back); S.G.—2.59; Chelsea filter reaction—none; fluorescence—inert to long- and short-wave UV radiation; and no absorption lines were visible with the desk-model spectroscope. These properties are consistent with those reported for chalcedony by R. Webster (*Gems*, 5th ed., revised by P. Read, Butterworth-Heinemann, Oxford, England, 1994, pp. 232–233). Microscopic examination of the cabochon revealed a "fingerprint" and some agate-like color banding along with a very subtle botryoidal structure.

Makhmout Douman (makhmout@arzawa.com)
Arzawa Mineralogical Inc., New York

Elizabeth P. Quinn
GIA Gem Laboratory, Carlsbad

Clinohumite from the Pamir Mountains, Tajikistan. Clinohumite, $(Mg,Fe^{2+})_9(SiO_4)_4(F,OH)_2$, is a rather uncommon gem material that has a Mohs hardness of 6 and typically ranges from orangy yellow to brownish orange. Although faceted examples of clinohumite have been documented previously in *Gems & Gemology* (see Lab Notes, Winter 1986, p. 236 and Spring 1988, pp. 47–48; and Spring 1991 Gem News, p. 48), a recent increase in the availability of this material prompted this update. Samples and information were provided to these contributors by Vladyslav Yavorskyy of Yavorskyy Co. Ltd., Bangkok, who is marketing clinohumite from the Pamir Mountains of Tajikistan as "Sunflower stone." According to Mr. Yavorskyy, gem-quality clinohumite also is known from two localities in Russia: the southern Lake Baikal area and the Taymyr region of northern Siberia. The Pamirs constitute the main source, however, and over the past two decades Mr. Yavorskyy has stock-

Figure 6. This 22.57 ct cabochon of adularescent chalcedony from Iran is shown together with a piece of the rough material. The banding that is visible in portions of the rough is typically excluded from the polished stones, to achieve a homogeneous appearance. Courtesy of Makhmout Douman; photo by Maha Tannous.

Figure 7. Clinohumite is an uncommon gem that comes mainly from the Pamir Mountains of Tajikistan. The faceted examples shown here weigh 0.68 and 1.59 ct. Courtesy of Yavorskyy Co. Ltd.; photo by Maha Tannous.

piled a few hundred faceted stones from this mining area (see "'Sunflower stone' debuts in Asia," *Jewellery News Asia*, No. 242, October 2004, p. 30).

According to Mr. Yavorskyy, clean faceted stones from the Pamirs usually weigh less than 1 ct, and those in the 1–3 ct range are very rare. However, over the past few years some larger stones from this area have been cut, weighing up to 17.87 ct (U. Henn et al., "Gem-quality clinohumite from Tajikistan and the Taymyr region, northern Siberia," *Journal of Gemmology*, Vol. 27, No. 6, 2001, pp. 335–339). Most of the material contains noticeable eye-visible inclusions. The rough is mined by local people during the short summer season (June–August). Mineral dealer Farooq Hashmi (Intimate Gems, Jamaica, New York) reports that since the fall of the Taliban, some of the material has been smuggled into Afghanistan and eventually is traded in Peshawar, Pakistan. The rough is often sold as orange spinel (referred to as "lal" locally), since many of the traders are not familiar with clinohumite and it is commonly found in association with gem-quality spinel. The spinel and clinohumite occur in skarns at several localities in the southwestern Pamir Mountains (e.g., Kukh-i-Lal, Sumdzin, Changin), typically within altered gneiss adjacent to magnesian marbles (A. K. Litvinenko, "Nuristan–South Pamir province of Precambrian gems," *Geology of Ore Deposits*, Vol. 46, No. 4, 2004, pp. 263–268).

Mr. Yavorskyy loaned two faceted stones (0.68 and 1.59 ct) and one crystal of Tajikistan clinohumite to GIA for examination (figure 7). The following properties were recorded by one of us (EPQ) on the faceted stones: color—orange and orange-yellow, with moderate pleochroism in orange and yellow; diaphaneity—transparent; R.I.—1.632–1.665 and 1.632–1.666; birefringence—0.033 and 0.034; S.G.—3.23 and 3.21; Chelsea filter reaction—none; both stones were inert to long-wave UV radiation but displayed a characteristic moderate to strong chalky orange-yellow fluorescence to short-wave UV; and both displayed a general absorption to 430 nm with a desk-model spectroscope. Microscopic examination revealed two-phase inclusions, twin planes and transparent straight and angular growth lines in both stones. In addition, the 0.68 ct sample had a fracture that showed evidence of clarity enhancement, and the 1.59 ct stone contained "fingerprints" and mineral inclusions (transparent, near-colorless, low-relief, birefringent crystals) that could not be identified by Raman spectroscopy due to their position in the stone.

The properties of these two samples are comparable to those reported for clinohumite in mineralogical reference books (as well as those listed by Henn et al. [2001] and in the Lab Notes and Gem News entries listed above), although their S.G. values were slightly higher than those typically reported from the Pamirs (3.23 and 3.21 vs. 3.18).

BML

Elizabeth P. Quinn

Corundum-fuchsite-kyanite rock from India. A colorful new gem material was offered at the Tucson gem shows last February. Although this material—ruby/pink sapphire in a mottled green groundmass—sometimes resembles ruby in zoisite, the green component is mostly fuchsite, a green, chromium-rich variety of muscovite mica. A few samples were purchased separately by two GIA employees. Three of these samples were chosen for characterization (figure 8). The two cabochons (2.87 and 12.68 ct) were purchased from Rare Earth Mining Co., Trumbull, Connecticut, and the polished freeform (206.46 ct) was obtained from Jewel Tunnel Imports, Baldwin Park, California. All the samples were reportedly from India, and the larger piece was said specifically to be from Mysore.

The following gemological properties were determined: color—variegated and mottled bluish green to green and purplish pink to purplish red, sometimes with grayish blue and/or brownish white zones; diaphaneity—translucent to opaque; R.I. spot readings—1.76 from the pink/red zones, 1.57 or 1.58 from the various green zones, and 1.71 from the blue zones; Chelsea filter reaction—strong red reaction from the pink/red zones and pink to red reaction from the bluish green and blue-green zones, as well as the green groundmass. The pink/red portions fluoresced a mottled strong red to long-wave UV radiation and weak red to short-wave UV, whereas the bluish green, blue-green, and brownish white zones fluoresced a mottled weak-to-medium chalky blue to long-wave UV and a mottled very weak chalky blue to short-wave UV. For the most part, the green groundmass and grayish blue zones were inert to both long- and short-wave UV. With the desk-model spectroscope, we observed a typical ruby spectrum from the pink/red zones and lines in the red region of the spectrum from all the green areas. These properties confirm that the purplish red/pink zones were ruby/sapphire. They also indicate that the green zones, including the groundmass, are chromium rich. To confirm the identity of the green

Figure 8. The colorful patterns in these cabochons (2.87 and 12.68 ct) and polished freeform (206.46 ct) from India are created by assemblages of ruby/pink sapphire, green fuchsite, and grayish blue kyanite. Photo by Maha Tannous.

zones and better identify the grayish blue material, we turned to Raman analysis.

Raman analysis of the bluish green to green areas showed the presence of fuchsite mica, which is consistent with the characteristics given above. Considering the heterogeneous nature of this rock, additional minerals are most likely present in the bluish green to green areas—this is supported by differences in UV fluorescence of the different green zones. The grayish blue zones (which, when present, surrounded the corundum; see the large polished freeform in figure 8) were identified as kyanite; this also is supported by the limited gemological measurements that could be performed on these areas. The brownish white zones contained a mica, but the particular species could not be confirmed with Raman analysis.

Shortly after the Tucson show, Bill Heher of Rare Earth Mining Co., Trumbull, Connecticut, reported that there is a good supply of the rough material, and he has obtained approximately 75 kg so far. The material originally appeared on the market as obelisks and spheres. He also mentioned that some of the more highly fractured pieces are commonly stabilized with epoxy resin. We confirmed this by carefully testing the three samples with a thermal reaction tester (TRT). The polished freeform and the smaller cabochon sweated readily to the TRT; the latter stone also contained large, obviously filled cavities. The larger cabochon did not show evidence of a filler.

Although samples of this material that lack kyanite could be mistaken for the well-known ruby-in-zoisite from Tanzania, they are readily recognizable by the distinctive micaceous texture of the fuchsite. Similar corundum-fuchsite-kyanite assemblages have been documented from Zimbabwe and South Africa (C. C. Milisenda, "Gemmologie Aktuell: Ruby-fuchsite-kyanite rock from India," *Gemmologie: Zeitschrift der Deutschen Gemmologischen Gesellschaft*, Vol. 52, No. 4, 2003, pp. 124–125).

Elizabeth P. Quinn (equinn@gia.edu)

A new gem material from Madagascar: A mixture of cristobalite and opal. These contributors recently studied a round, milky white, 6.84 ct cabochon (figure 9) from Madagascar. The spot refractive index was 1.45, typical for opal, but the hydrostatic S.G. value was 2.18, which is higher than expected for an opal with that R.I. Based on extensive opal research done by one of these contributors (EF), an opal with this R.I. would be expected to have an S.G. value in the range of 1.98–2.10. Therefore, we examined the sample in more detail to check for the presence of inclusions, or another factor that would cause this anomalous behavior.

When viewed with a microscope, this sample presented two unusual characteristics: (1) a central apparent separation plane; and (2) sphere-, spicule-, and rod-like polarization features. The sphere-like features, which were about 0.5 mm in diameter, revealed a typical uniaxial optic figure between crossed polarizers, with a fibrous, polycrystalline rim of about 0.1 mm.

As we suspected the material to be opal, we used X-ray diffraction (XRD) and Raman scattering to investigate the sample further. Through the use of a special sample holder, XRD analysis was performed nondestructively on the near-flat base of the cabochon with a D-5000 Bruker powder diffractometer and a fixed reflection geometry. According to our reference (J. M. Elzea and S. B. Rice, "TEM and X-ray diffraction evidence for cristobalite and tridymite stacking sequences in opal," *Clays and Clay Minerals*, Vol. 44, No. 4, 1996, pp. 492–500), the pattern obtained was that of α-cristobalite (a polymorph of SiO_2). The full width at half maximum (FWHM) of the main peak was 0.08°, much lower than that for opal-C (a poorly crystallized cristobalite, with a FWHM of 0.2 to 0.9), and even lower than that of the reference α-cristobalite given by Elzea and Rice (0.15).

Figure 9. This 6.84 ct cabochon (26.5 × 26.5 × 6.8 mm) from Madagascar consists of highly crystalline cristobalite and opal. Photo by Alain Cossard.

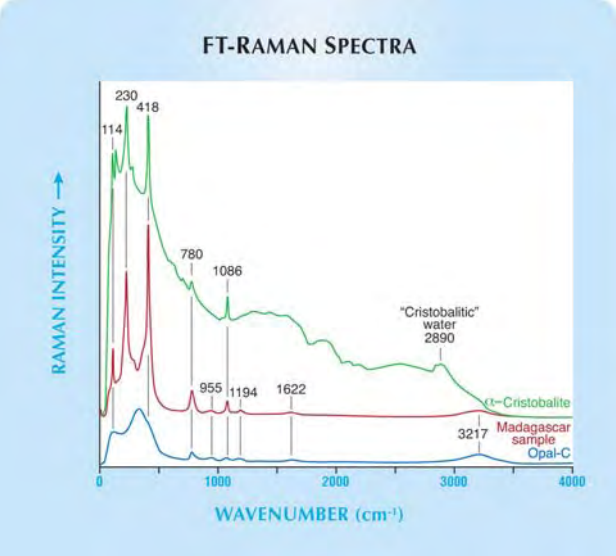

Figure 10. FT-Raman spectra of α-cristobalite, opal-C, and the Madagascar cabochon are shown here. The spectrum of the cabochon is dominated by features associated with cristobalite, but there are also some small features typical of opal.

Even taking into account possible instrumentation differences, the very small FWHM of this peak demonstrated the presence of highly crystalline cristobalite.

Fourier-transform Raman spectra were obtained with a Bruker RFS100 spectrometer. The spectrum of our sample (figure 10) was compared to reference spectra of opal-C from Mexico and α-cristobalite (taken from devitrified glass, a typical reference standard for cristobalite due to the large amount of material present). On the basis of this comparison, we concluded that our sample was a mixture of α-cristobalite and opal-C. The spectrum was dominated by cristobalite features, in particular peaks at 418 and 230 cm^{-1}, but there were small features typical of opal-C (or opal-CT, composed of disordered cristobalite with some tridymite-like stacking) at 1194 and 955 cm^{-1}, which are absent from the spectrum of cristobalite. In addition, the water signal around 3000 cm^{-1} was dominated by the water signal of opal, with a broad band centered at about 3220 cm^{-1}. The absence of "cristobalitic" water in the spectrum indicated that the cristobalite crystals in our sample contained little water compared to our reference devitrified glass specimen.

In XRD, the signal from a crystalline phase will always dominate the diffractogram; hence, it was not surprising that the opal signal was missing from our pattern, which was dominated by α-cristobalite. Also, the presence of cristobalite explains the relatively high S.G. value. As in many materials consisting of admixtures with silica, the R.I. is dominated by the silica matrix, whereas the S.G. reveals the presence of the included phase. Here the R.I. is typical for opal (1.45, versus 1.485 for cristobalite), but the S.G. of 2.18 is clearly affected by the presence of cristobalite (2.27–2.32); as noted, a typical S.G. value for opal with an R.I. of 1.45 is about 2.0. The cristobalite is apparently present as submicroscopic domains, as evidenced by the consistency of Raman spectra recorded on multiple points of the cabochon. The milky appearance of the material is consistent with the scattering of light from a mixture of submicroscopic domains, in this case of cristobalite and opal.

To the best of our knowledge, this is the first time that a mixture of highly crystalline cristobalite and opal has been documented as a gem material.

Since characterizing this cabochon, we have had a chance to briefly examine additional samples of this milky white gem from Madagascar (including a 10 ct emerald cut), which presented gemological properties and Raman spectra that were similar to those described for the 6.84 ct cabochon. However, the separation plane and polarization features noted in that cabochon were not seen in any of these additional samples.

Eloïse Gaillou (eloise.gaillou@cnrs-imn.fr)
and Blanca Mocquet
Centre de Recherches Gemmologiques Jean-Pierre Chenet (CRG)
Nantes, France

EF

Jeremejevite from Madagascar. In early 2004, a 7.88 ct near-colorless faceted oval (figure 11) was purchased in Madagascar from a local dealer as "achroite" (colorless tourmaline). The stone was uniaxial negative, but it had higher refractive indices and a lower birefringence than expected for tourmaline (1.642–1.650 and 0.008, respectively). It was inert to both long- and short-wave UV radiation. The S.G. was 3.28, which was too high for tourmaline. These properties, however, were a good match for jeremejevite. Since jeremejevite has not been documented

Figure 11. This 7.88 ct near-colorless jeremejevite represents the first report of this gem species from Madagascar. The numerous parallel channels are filled with brown, plate-like inclusions. Photomicrograph by E. Fritsch; magnified 2×.

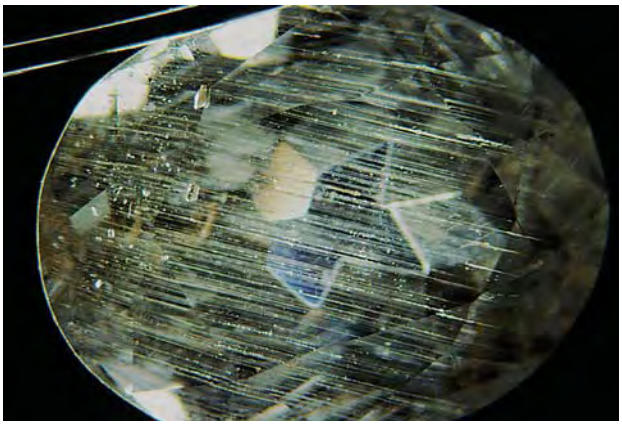

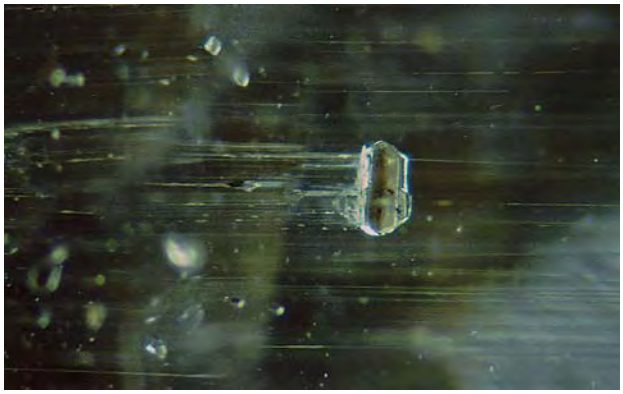

Figure 12. The jeremejevite contained this large cubo-octahedral inclusion that may be betafite or another pyrochlore-group mineral. Photomicrograph by E. Fritsch; magnified 11×.

Figure 13. The jeremejevite also contained pale yellow crystals that could be feldspar or danburite. Photomicrograph by E. Fritsch; magnified 9×.

previously from Madagascar, confirmation was sought using chemical analysis and Raman scattering.

A Jeol 5800 scanning electron microscope with a PGT energy-dispersive detector was used to obtain a qualitative chemical analysis. The only elements detected were oxygen, fluorine, and aluminum. Since the chemical composition of jeremejevite is $Al_6B_5O_{15}(F,OH)_3$, the analysis was consistent with that gem, and the absence of silicon ruled out tourmaline. A quantitative analysis was not possible since neither boron nor hydrogen can be detected with this instrument.

Raman spectra were obtained with two different instruments, a Bruker RFS100 Fourier-transform spectrometer and a T64000 Jobin-Yvon dispersive spectrometer, at a resolution of approximately 4 cm^{-1}. All spectra were consistent, with some intensity variation depending on crystallographic orientation. In general, the main features were sharp peaks at about 372, 328, and 178 cm^{-1}, with slightly broader bands at about 1065 and 960 cm^{-1}. This matched our reference spectrum for jeremejevite, obtained on a blue sample from Namibia.

These results confirmed that the stone was indeed jeremejevite, and we believe it to be the first reported from Madagascar. Prior to this discovery, jeremejevite was found principally in Namibia. The near-colorless appearance is unusual for this species, which is typically blue or yellow (see K. Scarratt et al., "Jeremejevite: A gemological update," Fall 2001 *Gems & Gemology*, pp. 206–211).

The stone contained numerous inclusions; the most noticeable were tube-like features (again, see figure 11). These elongated tubes showed significant necking and contained brown, plate-like inclusions that could be a Nb-Ta oxide, such as manganocolumbite. There were also a number of more equant inclusions with well-defined crystal forms. Among these were a gray crystal with an apparent cubo-octahedral morphology resembling betafite or another pyrochlore-group mineral (figure 12), and pale yellow crystals with the appearance of feldspar or danburite (figure 13). Unfortunately, none of these well-formed inclusions gave a useful signal when analyzed by laser Raman microspectroscopy.

According to Dr. Federico Pezzotta of the Museo Civico di Storia Naturale, Milan, Italy, since news of the jeremejevite discovery reached Madagascar in early 2004, several buyers have purchased all the available colorless "tourmalines" offered at the Antsirabe market. However, he is not aware of any additional samples of jeremejevite being found. Dr. Pezzotta reported that the dealer who sold the stone has purchased rough material with her husband from various locations in Madagascar for several years. It was impossible for her to recount when the rough jeremejevite was purchased, but she was confident that it came from local miners at Vohitrakanga, 65 km southwest of Antsirabe.

Blanca Mocquet (blanca.mocquet@free.fr)
and Yves Lulzac
CRG, Nantes, France

EF

Kyanite from Tanzania. Over the past year, small quantities of rough kyanite have been offered by local vendors in Arusha, Tanzania. The blue color and elongate crystal form have led some of the vendors to believe it was aquamarine. Dudley Blauwet of Dudley Blauwet Gems, Louisville, Colorado, saw about 10 kg of rough in March 2004, from which he selected 3 kg for faceting or to sell as mineral specimens. The crystals ranged up to 12.5 cm long and were coated by traces of mica, which is consistent with the common occurrence of kyanite in micaceous metamorphic rocks. Kyanite is a widespread mineral in high-grade gneisses of the Arusha area (S. Muhongo et al., "Pan-African pressure-temperature evolution of the Merelani area in the Mozambique Belt in northeast Tanzania," *Journal of African Earth Sciences*, Vol. 29, No. 2, 1999, pp. 353–365).

Mr. Blauwet reported that the kyanite rough is commonly color zoned: The pale greenish blue crystals contain elongate dark blue zones. The dark blue portions are generally more transparent than the pale-colored areas, so most of the cut stones are dark blue. The yield is typically rather

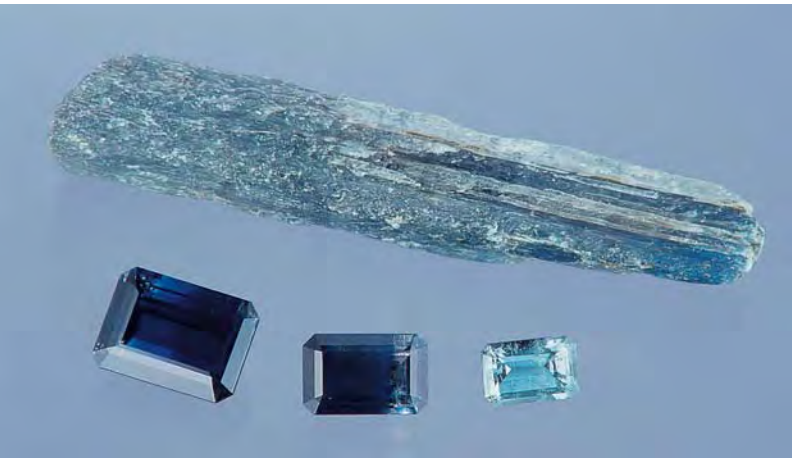

Figure 14. These emerald cuts (8.66, 5.04, and 2.28 ct) show the range of color (and color zoning) seen in kyanite from Tanzania. The crystal (approximately 6.7 cm long) shows the typical occurrence of facetable dark blue areas within the predominantly translucent pale greenish blue material. Courtesy of Dudley Blauwet Gems; photo by Maha Tannous.

small, however, due to cleavage problems. While it would be possible to facet long stones approaching 20 ct, more desirable length-to-width ratios are achievable only by cutting smaller gems.

Three emerald-cut stones (figure 14) and two kyanite crystals were loaned, and an additional crystal was donated to GIA, by Mr. Blauwet. The cut stones were characterized by one of us (EPQ), and the results are summarized in table 1. Microscopic examination of the two larger stones revealed fine needles, stringers of particles, and wispy clouds that were predominantly confined to the dark blue areas. The 5.04 ct kyanite also contained iridescent platelets that were predominantly confined to the dark blue portion. Using Raman analysis, we identified inclusions of near-colorless to light brown zircon and near-colorless muscovite in the two smaller stones, as well as near-colorless apatite in the largest sample. Etch tubes and cleavage cracks also were observed in all three of the kyanites. In addition, the smallest stone contained iridescent platelets (like those seen in the 5.04 ct stone), as well as elongate transparent near-colorless needles; however, we were not able to identify these inclusions by Raman analysis.

Elizabeth P. Quinn
BML

TABLE 1. Properties of three faceted kyanites from Tanzania.

Property	Sample		
	2.28 ct	5.04 ct	8.66 ct
Color	Light greenish blue	Bi-colored: very dark blue and near-colorless	Very dark blue (uneven)
Pleochroism	Moderate: greenish blue and near-colorless	Moderate: deep violet-blue and lighter blue	Moderate: deep violet-blue and lighter blue
Diaphaneity	Transparent	Transparent to semi-transparent	Transparent to semi-transparent
Refractive indices	1.712–1.728	1.711–1.727	1.711–1.727
Birefringence	0.016	0.016	0.016
Specific gravity	3.68	3.68	3.68
Chelsea filter reaction	Strong red	Weak red from the near-colorless zone, and no reaction from the very dark blue zones	Moderate to strong red from a near-colorless zone, and no reaction from the very dark blue portions
Transmission luminescence	Moderate red	None	Moderate red from a near-colorless zone, and none from the very dark blue portions
UV fluorescence			
Long-wave	Moderate red	Very weak red from the near-colorless zone, otherwise inert	Very weak red from a near-colorless zone, otherwise inert
Short-wave	Very weak chalky green	Very weak chalky green from the near-colorless zone, otherwise inert	Very weak chalky green from a near-colorless zone, otherwise inert
Absorption spectrum	680 nm line	670 nm cutoff	680 nm line and weak 450 nm line

Sapphires from Afghanistan and Pakistan. Gem dealer Farooq Hashmi of Intimate Gems, Jamaica, New York, shared some information on the recent production of gem-quality sapphires from Afghanistan and Pakistan, and he loaned or donated several samples to GIA for examination. Mr. Hashmi obtained these samples during a buying trip to Peshawar, Pakistan, in early 2004.

Blue sapphire from Maydan Shahr, Afghanistan. The Summer 2002 Gem News International section (p. 181) documented dark blue sapphires from a new deposit in Afghanistan, which was represented as "Medan Khar" in Vardak Province, west of Kabul. Since that time, this province has been the source of additional sapphires, reportedly from the Maydan Shahr area. It is not clear if this new production is from the same locality (with phonetic allowances for the different spellings) or a different deposit. The sapphires are enclosed by a hard white matrix, which makes their recovery quite labor intensive. Mr. Hashmi saw several kilograms of rough in Peshawar, and most had a hazy or velvety appearance, as well as a slightly grayish tinge, which differed from the Afghan sapphire we reported on in 2002.

An examination of the 2.10 ct oval mixed-cut sapphire in figure 15 by one of us (EPQ) showed the following properties: color—dark grayish greenish blue, with medium bluish green and dark violetish blue dichroism; diaphaneity—transparent; R.I.—1.761–1.770; birefringence—0.009; S.G.—4.03; fluorescence—inert to both long- and short-wave UV radiation; and strong absorption bands at 450, 460, and 470 nm visible with the desk-model spectroscope. This stone displayed a medium to strong blue scattering effect when viewed with a fiber-optic light. This effect was caused by the reflection of light off clouds of very fine particles throughout the stone, resulting in a somewhat hazy appearance. Microscopic examination revealed a "fingerprint," a twin plane, a transparent near-colorless birefringent crystal, stringers of pinpoints, and diffuse planar yellow and blue growth banding. No evidence of heat treatment was detected.

Pink sapphire from Batakundi, Pakistan. According to Mr. Hashmi, pink to purple (and rarely blue) corundum has been mined near the town of Batakundi in Pakistan's North West Frontier Province since 1999. Several diggings in the area have produced mostly low-quality material, but some facetable stones were recovered recently. Although gemstones exceeding 5 ct have been faceted, most weigh less than 2 ct.

Five Batakundi sapphires (0.74–1.98 ct; see, e.g., figure 16) were examined by one of us (EPQ) and the following properties were recorded: color—purplish pink, pink, and slightly orangy pink, with moderate dichroism in purplish pink to purple-pink and pinkish orange to pink-orange; diaphaneity—transparent to semitransparent; R.I.—n_e=1.759–1.760, n_o=1.767–1.768; birefringence—0.008; S.G.—4.00–4.03; fluorescence—moderate to strong red to long-wave and very weak red to short-wave UV radiation. The desk-model spectroscope showed general absorption to 430 nm, a weak 450 nm band, weak 470 and 480 nm lines, a 550–590 nm band, and lines in the red end of the spectrum.

Figure 15. This 2.10 ct sapphire is reportedly from Maydan Shahr, Afghanistan. Courtesy of Intimate Gems; photo by Maha Tannous.

All but the smallest stone displayed a moderate violet-blue scattering effect when viewed with a fiber-optic light. As with the Afghan sapphire reported above, this effect was caused by reflection of light off clouds of very fine particles throughout the stones, which gave them a hazy appearance. Microscopic examination revealed that all five samples contained "fingerprints," fractures, dark metallic inclusions, transparent near-colorless birefringent crystals (one of which was identified by Raman analysis as zircon), straight and/or angular growth banding (purplish pink to pink), and short needles resembling rutile. Also present were twin planes in four of the stones, needles (with the appearance of boehmite) and two-phase inclusions in three

Figure 16. Batakundi, northern Pakistan, is the source of these purplish pink to slightly orangy pink sapphires (0.96–1.98 ct, faceted). Courtesy of Intimate Gems; photo by Maha Tannous.

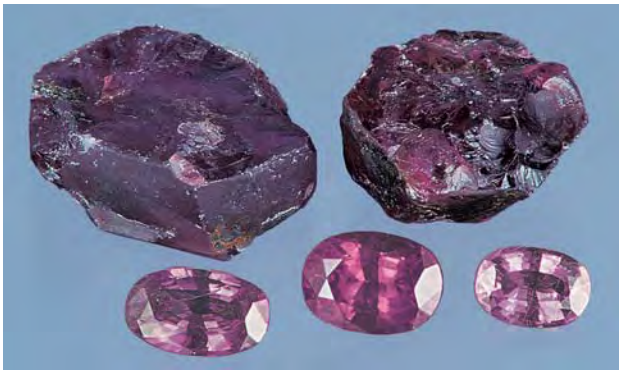

samples, and an angular blue color zone and large transparent crystals (one of which was identified by Raman analysis as apatite) in the smallest stone. No evidence of heat treatment was detected in any of the sapphires. However, one showed evidence of clarity enhancement (i.e., it "sweated" when tested with a thermal reaction tester).

Purple sapphire from northern Pakistan. Another deposit in northern Pakistan is the source of purple sapphires. Mr. Hashmi was not able to learn the specific locality. He reported seeing less than 1 kg of rough in the Peshawar market.

A 1.20 ct modified round brilliant sapphire (figure 17) from this area was studied by one of us (EPQ): color—dark pink-purple, with weak to moderate dichroism in pink-purple and orange-pink; diaphaneity—transparent; R.I.—1.761–1.769; birefringence 0.008; S.G.—4.01; fluorescence—weak red to long-wave and inert to short-wave UV radiation; transmission luminescence—weak red. The desk-model spectroscope showed absorption bands at 450, 460, and 470 nm, together with lines in the red part of the spectrum. Microscopic examination revealed "fingerprints," clusters of minute transparent near-colorless birefringent crystals, transparent light brown crystals (two of which were identified as monazite with Raman analysis), dark metallic crystals, and needles. No evidence of heat treatment was detected.

Elizabeth P. Quinn
BML

Sapphires from Baffin Island, Canada. In 2002, local prospectors Seemeega and Nowdla Aqpik discovered gem-quality sapphires in an outcrop southwest of the community of Kimmirut on the south coast of Baffin Island, Nunavut, northern Canada (figure 18). To date, six corundum occurrences have been discovered over a distance of 390 m.

Figure 17. Northern Pakistan is also the source of this 1.20 ct purple sapphire and crystal fragment. Courtesy of Intimate Gems; photo by Maha Tannous.

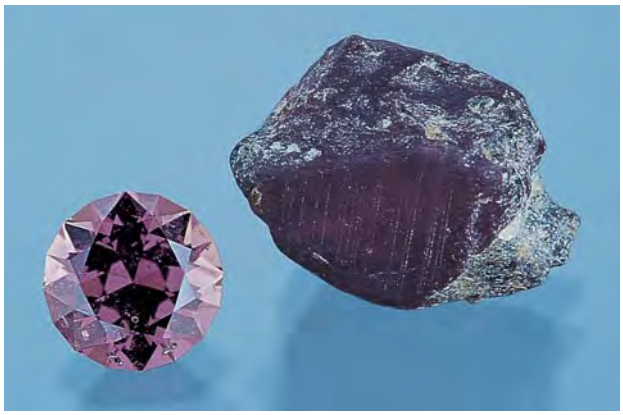

Figure 18. Deep blue sapphires were discovered in southern Baffin Island, Canada, in 2002. One of the original prospectors, Seemeega Aqpik, is shown with a matrix specimen containing a sapphire crystal that measures 7.7 cm long. Photo by William Rohtert.

The original occurrence, called "Beluga," contains deep blue sapphires with violet overtones (figure 19). Individual crystals up to 7.7 × 2.1 cm have been recovered (again, see figure 18), although most are in the range of 15 × 4 mm. Some of the sapphires are color-zoned (especially larger crystals), and may display concentric, irregular, or end-to-end variations in hue. The smaller crystals are generally free of inclusions, whereas the larger ones are often fractured and, in most cases, included with calcite and/or apatite. Needles of thomsonite, a zeolite mineral, coat grain boundaries and penetrate deeply into some of the crystals.

Most of the Beluga sapphire crystals exhibit spectacular zoning in cathodoluminescence which corresponds to the color zoning. Very faint compositional zoning was sometimes seen in backscattered-electron images obtained with a scanning electron microscope. Electron-microprobe analysis of 10 sapphire samples yielded maximum TiO_2 and FeO values of 0.13 and 0.30 wt.%, respectively.

In August 2004, fragments of yellow, colorless, and light blue sapphires were discovered at another occurrence located 50 m from the Beluga lens, over an area about 0.5 × 0.5 m. Called "Beluga South," this locality also contains weathered fragments of a corundum-bearing plagioclase-muscovite-calcite rock. Microprobe analyses of the yellow

and colorless sapphires (one sample of each) showed that the dominant chromophore in the yellow material was iron, with up to 0.04 wt.% FeO; all other potential chromophores were below the detection limit.

Two yellow sapphires from the Beluga South occurrence were loaned to GIA for examination (1.09 and 1.47 ct; figure 20). The following properties were recorded by one of us (EPQ): color—yellow to orangy yellow, with no pleochroism observed; diaphaneity—transparent; R.I.—1.758–1.766; birefringence—0.008; S.G.—3.99 and 4.01; Chelsea filter reaction—none; and fluorescence—moderate orange to long-wave and very weak orange to short-wave UV radiation. No absorption features were visible with a desk-model spectroscope. Microscopic examination revealed that both stones contained a few long white needles, and the oval sapphire also had a single "fingerprint." No evidence of heat treatment was seen.

The Baffin Island sapphires are hosted by calc-silicate lenses in a marble unit of the metasedimentary Lake Harbour Group, near a major terrane boundary within the Paleoproterozoic Trans-Hudson Orogen. Silica-poor (i.e., syenitic or ijolitic) magmas may have played a role in the initial formation of the calc-silicate lenses. The Beluga sapphires occur with plagioclase, clinopyroxene, phlogopite, muscovite, calcite, graphite, nepheline and scapolite. Apatite, rutile, titanite, and zircon are common in the host rock, and rare phases include chlorite, tourmaline (dravite), monazite, sanbornite, thorianite, and uraninite (identified by energy-dispersive spectroscopy). Petrographic studies suggest that this diverse mineral suite formed during retrograde metamorphism accompanied by infiltration of CO_2-bearing fluids. The area also hosts other gem varieties in complexly deformed, high-grade metamorphic rocks. These include diopside, pargasite, garnet, spinel, scapolite, tourmaline, apatite, zircon, moonstone, and lapis lazuli. The continental collision setting of southern Baffin is analogous to gem-producing areas within the India-Asia collision zone (i.e., from Afghanistan to Vietnam).

In late 2003, the mineral rights to the sapphire-bearing area of southern Baffin Island were acquired by True North Gems Inc. So far, True North has polished 137 sapphires from the Beluga lens, with a total weight of 19.33 carats. The largest stone is a 0.66 ct trilliant (figure 19). In addition, 67 yellow and colorless sapphires have been cut from the Beluga South occurrence, with a total weight of 10.62 carats. The largest yellow sapphire is a 1.47 ct oval (figure 20). All of the color varieties have been cut as calibrated round brilliants in sizes down to 1 mm, with most stones measuring 3 mm in diameter.

Anthony N. LeCheminant
(tony_lecheminant@rogers.com)
Petrogen Consultants
Manotick, Ontario, Canada

Lee A. Groat, Gregory M. Dipple, James K. Mortensen
University of British Columbia
Vancouver, British Columbia, Canada

Paul Gertzbein
Department of Indian Affairs
and Northern Development
Iqaluit, Nunavut, Canada

William Rohtert
True North Gems Inc.
Vancouver, British Columbia, Canada

Elizabeth P. Quinn

Figure 20. Baffin Island is also the source of these yellow sapphires. The cushion cut weighs 1.09 ct, and the oval is 1.47 ct. Photo by Roger Morton.

Figure 19. These sapphires are from the Beluga lens on Baffin Island. The round brilliants weigh 0.30 and 0.31 ct, and the trilliant is 0.66 ct. Photo by Brad Wilson.

Unusual star and "cat's-eye" sapphire. An unusual star sapphire was brought to the attention of these contributors by Denis Gravier of Le Minéral Brut, Poncin, France. The 1.10 ct, 6-mm-diameter round cabochon had an S.G. of 3.99, R.I.'s of 1.762–1.771, and was uniaxial negative. All of these properties are typical for sapphire. It was inert to both long- and short-wave UV radiation. With intense pinpoint illumination, a weak but well-centered six-rayed star was visible.

The most striking feature was a near-colorless band passing through the center of the stone (figure 21), which was reminiscent of a "cat's-eye" pattern. This zone also was composed of corundum, as established by qualitative chemical analysis with a Jeol 5800 scanning electron

microscope equipped with a Princeton Gamma-Tech energy-dispersive X-ray detector for chemical analysis. The areas adjacent to this band displayed both sharp color zoning and silk-like inclusions that were oriented parallel to the boundaries of the near-colorless area. Magnification revealed that the entire stone was traversed by several "fingerprints." Also present were some open fractures that contained small amounts of a semitransparent yellow to brown material that originated from outside of the stone.

The color zoning suggests that the sapphire formed via simultaneous growth on both sides of the central near-colorless plate. The most logical interpretation is that this plate acted as a seed for overgrowth. How such a perfect plate could be produced in nature is difficult to explain, but the stone showed no evidence of synthetic origin. Perhaps *Gems & Gemology* readers have already seen a similar gem or can suggest a mode of formation.

EF

Y. Lulzac
CRG, Nantes, France

Large cat's-eye topaz from Ukraine. Chatoyant topaz is extremely rare. Previously documented examples include 3.53 and 13.90 ct stones (see Summer 1990 Gem News, p. 164 [unspecified locality], and Fall 2003 Gem News International, pp. 236–237 [Myanmar]), as well as a much larger sample of 152 ct that originated from Brazil (see J. Hyrsl, "Some new unusual cat's-eyes and star stones," *Journal of Gemmology*, Vol. 27, No. 8, 2001, pp. 456–460).

Two cabochons of cat's-eye topaz were recently submitted to this contributor for examination by gem dealer and collector M. Steinbach of Köln, Germany. They were cut from the same piece of rough, which originated from the famous gem beryl deposits in the Volhynia region of central Ukraine (see, e.g., J. Sinkankas, *Emerald and Other Beryls*, Chilton Book Co., Radnor, PA, 1981, pp. 538–539). In addition to being the first chatoyant examples of topaz from this area known to this contributor, these cabochons were quite large: 270 ct (figure 22) and 154 ct. They were identified as topaz by traditional gemological methods, and their identity was confirmed by Raman spectroscopy.

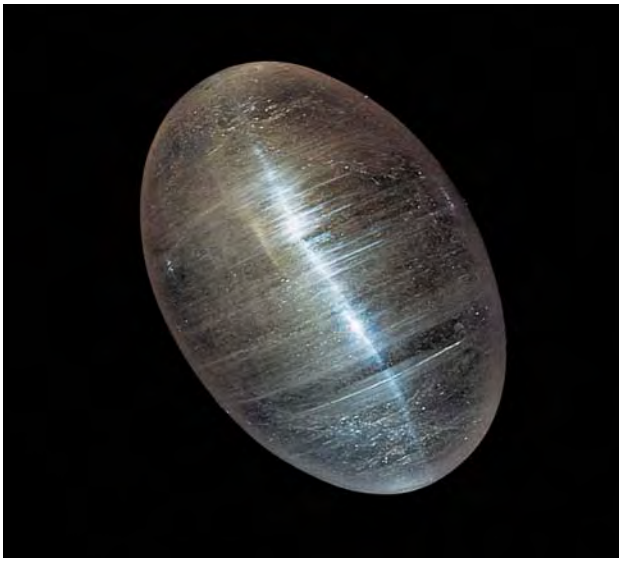

Figure 22. This 270 ct cat's-eye topaz is notable for its large size and Ukrainian origin. Photo by M. Glas.

Both samples were intrinsically colorless and revealed numerous partially healed fractures consisting of liquid and two-phase (liquid/gas) inclusions, which gave the stones a somewhat milky appearance. The chatoyancy was caused by numerous extremely thin parallel channels or tubes, which commonly showed a brownish or reddish brown staining. The staining of these fine tubes created the apparent pale brown bodycolor of the samples.

KS

Figure 21. This 6-mm-diameter sapphire shows both an unusual "eye"—actually a near-colorless band—and a weak six-rayed star. Photo by Denis Gravier.

A notable triplite from Pakistan. Triplite ($Mn_2^{2+}[PO_4]F$) is a rare mineral that forms in phosphate-rich granitic pegmatites, typically as irregular brown opaque masses. Transparent triplite is quite rare, and the material is not easy to facet due to its brittleness and cleavage. It also has rather low hardness for a gemstone, at 5–5$^1/_2$ on the Mohs scale.

These contributors were very surprised, therefore, when a transparent, reddish orange triplite weighing 7.16 ct was loaned to GIA for examination by Dudley Blauwet of Dudley Blauwet Gems. Mr. Blauwet stated that the rough was mined in the Shigar Valley in northern Pakistan, about 5–6 hours' walk from the village of Alchuri. He also indicated that transparent crystals of a similar phosphate mineral called väyrynenite ($Mn^{2+}Be[PO_4][OH,F]$) have been found in the same area. Attractive crystals of triplite were

reportedly mined in the Shigar Valley in 1995, on a matrix of albite and fluorite (A. Weerth and V. M. F. Hammer, "Mineralien vom 'Dach der Welt': Neue Überraschungen aus dem Pamir, dem Karakoram und dem Himalaya," *Lapis*, Vol. 25, No. 5, 2000, pp. 22–29). Most of this material was evidently sold as mineral specimens, and only a few small, dark brown triplites from Pakistan are known to have been cut (M. Kaufman, Kaufman Enterprises, San Diego, pers. comm., 2004).

The 7.16 ct triplite was faceted into an oval modified brilliant (figure 23). The following properties were obtained by one of us (EPQ): color—reddish orange, with weak pleochroism in reddish orange and yellowish orange; diaphaneity—transparent; R.I.—1.658–1.677; birefringence—0.019; S.G.—3.87; orangy red Chelsea filter reaction; and inert to both long- and short-wave UV radiation. General absorption to 450 nm, weak absorption bands at 470 and 490 nm, and a stronger band at 520–560 nm were observed with a desk-model spectroscope. Microscopic examination revealed "fingerprints," fractures, two-phase inclusions, and a phantom-like growth plane.

Powder X-ray diffraction analysis by WBS and AUF was performed using a piece of rough from which the 7.16 ct stone was cut, and it showed a close match to the triplite reference pattern. Electron-microprobe analysis of this fragment yielded the following composition (average of nine spots, in wt.%): 54.91 MnO, 31.92 P_2O_5, 6.87 F, 4.20 CaO, 3.91 FeO, 0.81 H_2O (calculated), 0.06 Al_2O_3, and 0.06 SiO_2. After subtracting 2.89 wt.% (calculated oxygen equivalent of fluorine, by weight), the total was 99.83 wt.%. The data represent what are close to the highest Mn and lowest Fe contents documented in the literature for triplite. By comparison, only one of the 11 analyses reported by C. Palache et al. (*The System of Mineralogy of James Dwight Dana and Edward Salisbury Dana*, Vol. 2, John Wiley and Sons, New York, 1951, pp. 849–852) has a greater Mn:Fe ratio, with 57.63 wt.% MnO and 1.68 wt.% FeO in a "salmon-pink" sample from White Pine County, Nevada.

Although the reddish orange color has not been reported previously for triplite, the R.I., birefringence, S.G., and chemical composition of the 7.16 ct stone are within the wide range of values given in the literature.

Figure 23. At 7.16 ct, this triplite from Pakistan is remarkable for its size, transparency, and attractive color. Courtesy of Dudley Blauwet Gems; photo by Maha Tannous.

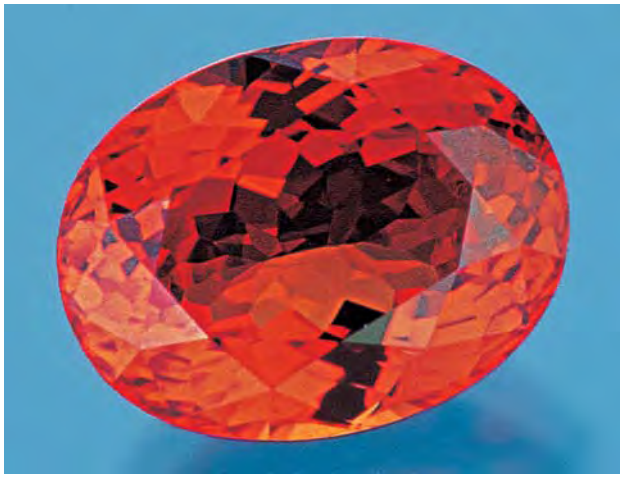

BML

Elizabeth P. Quinn

William "Skip" B. Simmons and Alexander U. Falster
University of New Orleans, Louisiana

Update on several gem localities in Zambia and Malawi. In September 2004, *Gems & Gemology* editor Brendan Laurs visited several gem deposits in Zambia and Malawi as part of a collaborative research project to gather first-hand information on the location, geology, and gem production of commercially important gem sources in southern Africa. The other collaborators were Dr. William B. "Skip" Simmons of the University of New Orleans, Louisiana; Dr. Hanco Zwaan of the National Museum of Natural History, Leiden, The Netherlands; and Bjorn Anckar of the European Union's Mining Sector Diversification Programme (MSDP) in Lusaka, Zambia. Mr. Anckar, a geologist and gemologist who has lived in Zambia for the past two and a half years, was our guide for much of the trip. The MSDP (www.msdp.org.zm/index.htm) is a five-year project supported by the European Development Fund to promote the sustainable development of the non-traditional mining sector in Zambia. Assisting the development of gem mining is an important component of this program. Recently, the World Bank began working closely with the MSDP on a separate Zambian aid program called Support for Economic Expansion and Diversification (visit www-wds.worldbank.org/default.jsp?site=wds and browse the Zambian documents). This program includes a gem component that "will support measures aiming to promote gemstones [sic] production and trade, and facilitate its inclusion into the formal economy, improve the sector's socio-economic contribution at the regional and national levels, and encourage private sector investments."

Our fieldwork in Zambia focused on three regions: Kafubu for emeralds, Mkushi for tourmaline and morganite, and Lundazi for "Canary" tourmaline and aquamarine. In addition, we visited the Chimwadzulu Hill ruby/sapphire deposit in Malawi.

Kafubu Emerald Region. With a reputation as the world's second most important source of emeralds by value (after Colombia), this broad area near the Kafubu River contains several large open-pit mines (e.g., figure 24) that are being actively mined by international companies using heavy equipment. The geology at all the mines is rather similar:

Figure 24. One of the largest emerald pits in Zambia is the Grizzly. As at other mines in the Kafubu area, the emeralds are extracted from phlogopite-biotite schist adjacent to tourmaline-quartz veins. Photo by Brendan Laurs.

Emeralds are hosted by phlogopite-biotite schist adjacent to quartz-tourmaline veins, although the mineralization is quite uneven and unpredictable. During the intrusion of the veins, hydrothermal fluids altered the talc-chlorite-amphibole host rocks to form a phlogopite-biotite zone within centimeters to meters of the vein contacts (see A. V. Seifert et al., "Emerald mineralization in the Kafubu area, Zambia," *Bulletin of Geosciences*, Vol. 79, No. 1, 2004, pp. 1–40).

We visited four pits: Grizzly, Chantete, Pirala, and Twampane. The first two were being mined using large haul trucks and excavators. The Pirala mine had recently reopened, with production expected to begin shortly after our visit. Excavations to expose the vein were being done with equipment brought in from the nearby Twampane mine, which had recently halted active mining. The largest mining concession in the area (consisting of several pits) continues to be operated by Kagem Mining Ltd., and another prominent operation, the Kamakanga mine, also was active. At all the big pits, the miners drill and use explosives to open the areas adjacent to the veins (figure 25), and emeralds are hand-picked from the mineralized schist by experienced "chiselers." One of the mining operators (Kagem) currently has a small washing plant, while a larger processing plant being constructed at the Grizzly mine is projected to process 50 tonnes/hour of ore.

Although production figures for Zambian emeralds are not generally available, the owner of the Chantete mine indicated that he produces 150–300 kg of beryl per month, but typically only 1% is gem quality. At best, 10% of the material can be polished into faceted stones and cabochons. Security remains a problem at all the mines, and we were told that some deposits lose more than 80% of their production to theft. Most of Zambia's emeralds are exported to India (for use in the domestic market) and Israel (for international distribution).

Figure 25. The Chantete emerald mine in Zambia has been worked by mechanized equipment since 2002 in an open pit up to 35 m deep. Occasionally, large emerald crystals are produced (see inset). Photos by Brendan Laurs.

Mkushi pegmatite region. In the mid- to late-1990s, the Jagoda mine was an important producer of pink-to-red tourmaline and some morganite. The near-vertical pegmatite dike trends north-northwest and has been explored to a depth of about 15 m in an elongate open pit. The pegmatite is geochemically quite highly evolved, being composed mainly of "cleavelandite" (albite), quartz, and albitized K-feldspar with local areas of lepidolite and tourmaline. One particularly large pocket produced some enormous tourmaline crystals that typically showed a thin layer of black to dark green covering a pink interior (figure 26). Mine owners Claire Chan and Ross Walker, of the Jagoda Gem Centre in Lusaka, have recently reactivated the deposit using heavy equipment. The open pit is being enlarged so the pegmatite can be mined at deeper levels, and surrounding areas will be explored through trenching.

The Kumanga mine is another source of gem tourmaline in the Mkushi area, and has been mined by Rajnish Sharma (Gemstone Marketing & Consultancy Ltd., Lusaka) since 1998. He has opened 15 pockets with tourmaline colors ranging from pink, bicolored pink-green, green, to dark blue. One portion of the pegmatite has been

Figure 26. Claire Chan shows one of the large tourmaline crystals mined from Zambia's Jagoda pegmatite in the late 1990s. The crystals from this pocket had distinctive pyramidal terminations and the pink interiors were overgrown by a thin black to dark green "skin" (as seen in the inset). Photos by Brendan Laurs.

mined in a deep trench to about 15 m, and future work will likely concentrate on adjacent areas closer to the surface.

Lundazi pegmatite area. Numerous pegmatites containing gem-quality aquamarine, tourmaline, and spessartine occur in eastern Zambia, in a large area west and southwest of Lundazi, and east of the Luangwa River. Since the early 1980s, this area has been a source of bright yellow Canary tourmaline (sometimes incorrectly reported as being from Malawi or Mozambique; see Gem News International, Summer 2001, pp. 151–152, and Spring 2004, p. 86). Since the mid-1990s, commercial quantities of this bright yellow tourmaline have been recovered from primary and secondary deposits in a localized area covered by two mining concessions: Kabelubelu and Tumbuka. Since late 2002, the deposit has been leased by Tommy Wu (Shire Trading Ltd., Hong Kong) and Rita Mittal (Southstream Enterprises Ltd., Lusaka). They have undertaken further exploration of the pegmatite and also used a washing plant to process eluvium and alluvium from several locations. At the time of our visit, exploratory mining for dark blue (or "double blue") aquamarine was occurring at a pegmatite on an adjacent mining concession (figure 27). The aquamarine occurs as fractured crystals that are frozen within the pegmatite, yielding faceted stones that are typically less than 0.5 ct but do not require any heat treatment. In contrast, most of the Canary tourmaline is heated to 500–550°C to bring out the bright yellow color from the typically brown to greenish yellow starting material. Future work will focus on mining Canary tourmaline from secondary deposits.

Chimwadzulu Hill ruby/sapphire deposit, Malawi. Since the reports on Chimwadzulu Hill that were published in the Spring 2000 Gem News (pp. 71–73) and Spring 2004 Gem News International (p. 71), mine owner David Hargreaves (Minex Ltd., Surrey, United Kingdom) has continued a systematic exploration program of auger holes, trenches, and pits to better define areas of ruby concentration in the eluvi-

Figure 27. In the Lundazi area of eastern Zambia, a pegmatite located near the Canary tourmaline deposit is explored for dark blue aquamarine. The pegmatite can be seen as the light-colored vertical dike in the wall behind the miners. Photo by Brendan Laurs.

Figure 28. Mine manager Hilton Cook examines a ruby that was recovered in late September 2004 at Chimwadzulu Hill, Malawi. Photo by W. B. Simmons. The inset shows a 0.80 ct "padparadscha" sapphire from this deposit; courtesy of Columbia Gem House, Vancouver, Washington.

um. About 2,000 test holes have been sunk at 5–10 m spacing, to a depth of 3–4 m. The most productive level of the eluvium typically ranges from 1.0 to 1.5 m below the surface. Future exploration will focus on completing the pitting/drilling program and exploring the underlying bedrock for *in situ* corundum, to help understand the mineralization and distribution of ruby and sapphire in the eluvium. In addition, a new washing plant equipped with jigs and a magnetic separator has been commissioned to help meet the demand for rubies and "padparadscha" sapphires from this deposit, which do not require treatment and are being marketed as Nyala ruby and sapphire. Mr. Hargreaves reported that the new washing plant will increase the processing capacity from 30 to 100 m^3 of eluvium per day, and should yield about 4,500 grams of facetable corundum annually. Historically, production from the deposit has consisted of approximately 30% ruby and 17% "padparadscha" sapphire (figure 28), with the remainder various fancy colors (mostly in the pink to purple range).

In this contributor's opinion, the gem areas described above show significant future potential. The Kafubu emerald area, in particular, is far from exhausted and could benefit from more systematic prospecting and the introduction of a modern washing plant. Zambia's pegmatite districts also show potential, although additional discoveries will depend on securing the necessary capital for further exploration and mining, as well as locating buried primary and eluvial deposits in the deeply weathered and poorly exposed near-surface horizon. The Chimwadzulu Hill deposit seems poised for a major expansion, in light of the advanced exploration program and modernized washing plant that was recently installed. Additional developments and further details on these deposits will be reported in future articles that are being prepared for submission to *Gems & Gemology*.

BML

INCLUSIONS IN GEMS

Barite "spears" in fluorite. At a recent street fair in Carlsbad, California, GIA director of gem identification Shane McClure discovered a tray of freeform polished pieces of bicolored purple and green fluorite. Although no locality was given by the vendor, their coloration resembled that of some fluorite from Hunan Province, China.

Upon closer inspection, he found a 261.47 ct specimen (48.2 × 38.6 × 10.9 mm) that appeared to contain white spear-shaped inclusions of some unknown mineral (figure

Figure 29. This 261.47 ct bicolored green and purple fluorite held an interesting suite of white spear-shaped inclusions. Photo by Maha Tannous.

Figure 30. Raman analysis was used to identify the spear-shaped inclusions in the bi-colored fluorite as barite. Photomicrograph by John I. Koivula; magnified 10×.

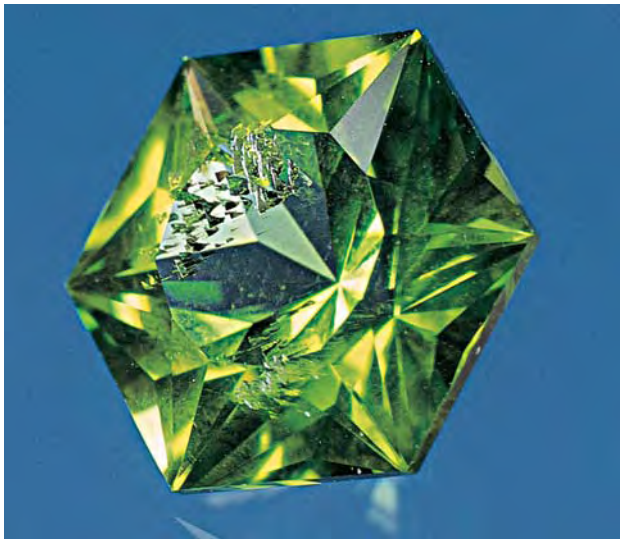

Figure 31. This 6.97 ct Arizona peridot contains unusual aligned surface-reaching inclusions reminiscent of etched dislocations. Courtesy of A. Wolkonsky; photo by Alain Cossard.

29). Since this was the only piece that contained these inclusions, and since solid inclusions of this shape have not been reported previously in fluorite, Mr. McClure purchased the stone for examination in the laboratory.

Microscopic examination showed that all the inclusions had a pointed, spear-like bladed habit; most were opaque white (figure 30). However, a few were transparent, and cross-polarized light showed them to be birefringent. One of the inclusions reached a polished surface, providing an ideal opportunity for Raman analysis, which served to identify the inclusion as barite.

Barite has been noted before as spherical inclusions in fluorite from Illinois (see J. I. Koivula and S. Elen, "Barite inclusions in fluorite," Winter 1998 *Gems & Gemology*, pp. 281–283), but never in this pointed habit. Interestingly, the spear-like shape of these barite inclusions looks quite similar to a primary fluid inclusion in a fluorite from Illinois reported by E. J. Gübelin and J. I. Koivula (*Photoatlas of Inclusions in Gemstones*, ABC Edition, Zurich, 1986, p. 83).

John I. Koivula (jkoivula@gia.edu)
and Maha Tannous

Arizona peridot with unusual inclusions. Alexandre Wolkonsky, a lapidary in Saint Cloud, near Paris, France, brought a remarkable peridot from San Carlos, Arizona (figure 31) to our attention. The 6.97 ct chevron-hexagon cut stone measured approximately 11.7 mm across and about 7.6 mm deep. The gem's identity was confirmed by R.I.'s of 1.650–1.688, a birefringence of 0.038, a biaxial positive optic character, and an S.G. of 3.35, all typical values for peridot.

The stone displayed several unusual white surface-reaching inclusions on its table. These had wedge- or dagger-like shapes plunging into the stone. They were all essentially parallel to one another, suggesting a relationship to crystallographic orientation (figure 32). Their intersection with the surface was also roughly parallel, although more irregular (figure 33), and never exceeded 0.05 mm wide. The overall shape and orientation of these inclusions suggested that they might be etched dislocations, as seen in spodumene, diamond, and many other gems.

What was unusual about these features was that they were filled with a white substance that Mr. Wolkonsky initially believed was glue added to reinforce the stone. However, close inspection revealed that it was a granular, somewhat glistening powder-like material, easily scratched away. Qualitative microanalysis of the inclusions obtained

Figure 32. The inclusions in the Arizona peridot were grouped essentially parallel to one another, possibly due to crystallographic orientation. Photomicrograph by E. Fritsch; magnified 2×.

Figure 33. With higher magnification, the slightly irregular shape of the inclusions' intersections with the table facet is visible. Note also the somewhat reflective appearance of the filling material in the inclusions. Photomicrograph by E. Fritsch, magnified 9×.

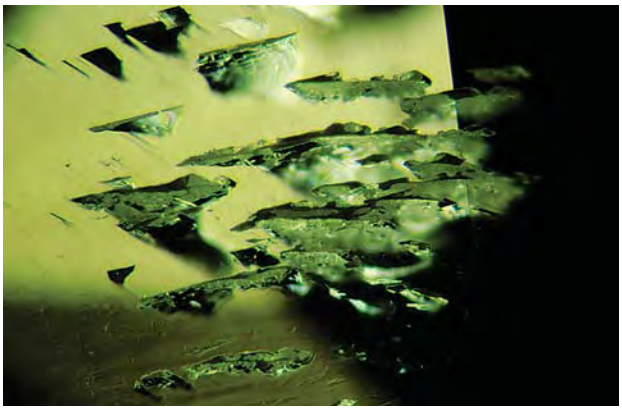

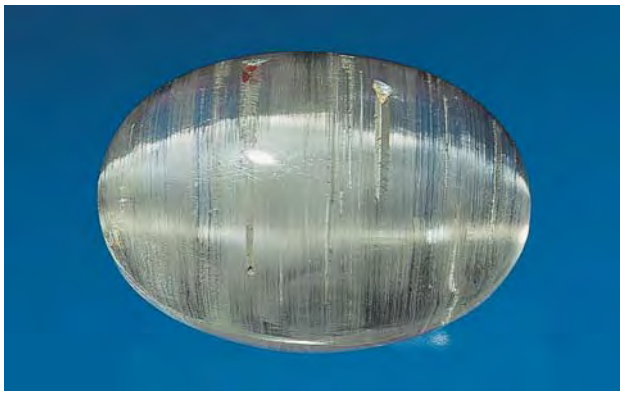

Figure 34. This unusual 11.94 ct cabochon of rock crystal quartz shows two strong chatoyant bands under a single light source. Courtesy of Elaine Rohrbach; photo by Maha Tannous.

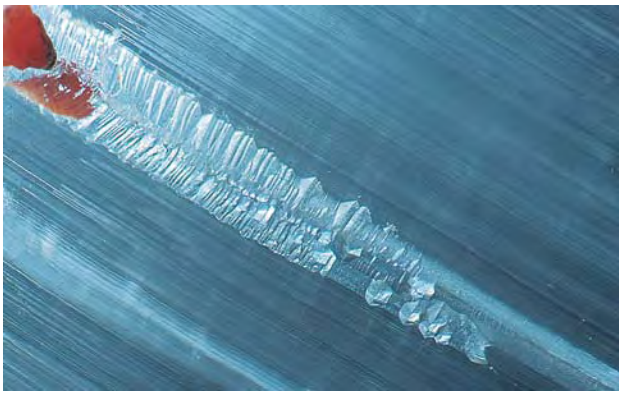

Figure 35. The complex angular shape of the etch tubes in the cat's-eye quartz causes light to be reflected simultaneously in two directions, forming two chatoyant bands instead of one. Photomicrograph by John I. Koivula; magnified 10×.

using a Jeol 5800 scanning electron microscope equipped with a PGT energy-dispersive X-ray detector revealed magnesium, silicon, oxygen, and traces of iron, with Mg>Si but a variable Mg/Si ratio (the analyzed volume did not include the peridot matrix). No useful signal was obtained by Raman analysis, probably because of the very reflective nature of the material. We surmise that the included material might be a hydrated alteration product of peridot, such as some variety of fine-grained serpentine.

EF

Y. Lulzac
CRG, Nantes, France

Double-eye chatoyant quartz. Cat's-eye gems characteristically show a chatoyant band of reflected light oriented perpendicular to the phenomenon-causing inclusions, which are commonly thin hollow tubes resulting from growth blockage (growth tubes) and/or post-growth dissolution features (etch tubes). In either case, the cat's-eye appears as a single band of reflected light when illuminated from above with a single beam of light. If a chatoyant gem is examined under two light sources simultaneously, then two chatoyant bands will be visible. Virtually all chatoyant gems display their cat's-eye phenomenon in such a manner.

However, a most unusual 11.94 ct cabochon of cat's-eye rock crystal quartz was recently acquired by Elaine Rohrbach of Gem Fare in Pittstown, New Jersey, while on a buying trip to Brazil. What made this gem intriguing was that it displayed two near-parallel chatoyant bands of virtually equal strength when illuminated with only a *single* light source (figure 34).

Since a few of the chatoyancy-causing inclusions were relatively large, it was possible to determine by microscopic examination that at least the larger tubes resulted from etching, and that some contained an epigenetic iron-stained residue (figure 35). The size of the largest inclusions also made it possible to see what caused two chatoyant bands to appear from a single light source. The etch tubes, which were all oriented in the same direction, were sharply angular down their length and also very mirror-like in their reflectance. This angularity caused incident light to be reflected simultaneously in two directions, which resulted in two chatoyant bands instead of just one.

John I. Koivula and Maha Tannous

Graphite inclusions in quartz from Brazil. "Graphite" has been mentioned many times as an inclusion in quartz, but until now these specimens have proved to contain only amorphous hydrocarbons, sometimes referred to as "anthraxolite" or "asphaltite" (see Spring 2004 Gem News International, pp. 79–81). The most famous examples of hydrocarbon-included quartz are the splendid groups of doubly terminated "Herkimer" rock crystals from Middleville, Herkimer County, New York, which originate in silicified dolomites. Similar geoenvironments have

Figure 36. Quartz crystals with cylindrical graphite inclusions, such as this 5.2-cm-wide intergrown crystal, have recently come on the market, reportedly from Bahia, Brazil. Photo by J. Hyrsl.

produced such quartz crystals all over the world, with plentiful deposits recently found in Sichuan Province, China (B. Ottens, Ed., *China—extraLapis* No. 26/27, Christian Weise Verlag, Munich, Germany, 2004,198 pp.). In such specimens, the black anthraxolite has an irregular form, although very rarely it is present as phantoms in some of the crystals from China.

Recently, this contributor encountered quartz crystals containing some unusually lustrous graphite inclusions (figure 36). They reportedly came from the state of Bahia, Brazil, although the exact locality is still unknown. The crystals were doubly terminated and typically up to about 3 cm long, although exceptional examples reached nearly 10 cm. The graphite inclusions formed cylinders up to 3 cm long and 3 mm wide (rarely, they were botryoidal). Almost all the graphite cylinders viewed by this contributor were broken at both ends; only very rarely did they show a hemisphere-shaped termination on one end. When the cylinders were viewed down their long axis, a radiating fibrous structure was quite visible in some cases. The identification of the inclusions as graphite was established by X-ray powder diffraction analysis. Some of the expected X-ray lines were missing, and this may be due to the formation of the graphite from the metamorphosis of the amorphous hydrocarbons. It is common for quartz crystals containing hydrocarbons to form during the lithification of sediments (i.e., diagenesis); subsequent higher grade metamorphism could cause these inclusions to recrystallize into graphite by driving off the volatiles (hydrogen and oxygen) from the hydrocarbons.

The graphite cylinders were in most cases completely enclosed by the quartz and therefore quite pristine. Only in specimens where the cylinders reached the surface was the graphite replaced by yellow-brown iron oxides or (rarely) absent, leaving a hollow cavity. Because many of the host quartz crystals are quite transparent, they can be faceted into very interesting cut stones (figure 37).

Jaroslav Hyrsl (hyrsl@kuryr.cz)
Kolin, Czech Republic

Figure 37. This 117.10 ct faceted quartz contains inclusions of well-formed graphite cylinders. Photo by J. Hyrsl.

Quartz with molybdenite. A recent discovery of transparent rock crystal in Chile has provided those interested in inclusions with some very unusual specimens. The well-formed crystals are singly or doubly terminated, with the doubly terminated specimens being less prevalent, as would be expected. Crystals weighing over 10 kg have been recovered from this locality, which is reported as the Confianza mine, Tilama, Valparaíso. Four gem-quality crystals were provided to these contributors by well-known mineral collectors and dealers Russell E. Behnke of Meriden, Connecticut, and William W. Pinch of Pittsford, New York. As shown in figure 38, the largest of the four weighed 378.73 ct and measured 42.8 × 40.9 × 37.6 mm.

The highlight of this discovery was that the quartz crystals contained phantoms decorated or dusted with thin platy crystals or crystal clusters of molybdenite (MoS_2), which was identified by EDXRF and X-ray diffraction analysis. Some of these inclusions were very well-formed and showed distinct surface growth features as well as the expected lead-gray metallic luster of molybdenite (figure 39).

John I. Koivula and Maha Tannous

Rutile "moth" in quartz. Rutile is a relatively common inclusion in quartz. However, fine examples showing well-developed six-rayed stars, four-rayed crosses, or beautiful sagenitic patterns are rare (see, e.g., Summer 2001 Gem News International, p. 146). Recently we had the opportunity to examine an interesting 13.97 ct rutilated quartz

Figure 38. These Chilean quartz crystals contain phantoms formed by molybdenite inclusions. The largest crystal weighs 378.73 ct, while the longest one measures 65.8 mm. Courtesy of Russell E. Behnke and William W. Pinch; photo by Maha Tannous.

Figure 39. The molybdenite inclusions in the Chilean quartz display a characteristic lead-gray color and platy hexagonal form. Photomicrograph by John I. Koivula; magnified 10×.

from the Golconda mine, Minas Gerais, Brazil, which was provided by Luciana Barbosa of the Gemological Center in Belo Horizonte. Prominently displayed under the table facet was a most unusual rutile inclusion pattern.

The inclusion formation consisted of numerous densely packed parallel light yellowish brown needles of rutile that were swept back at an angle from a central opaque silvery black inclusion of hematite. The plane of this inclusion combination was oriented just slightly off-parallel to the plane of the table facet. As shown in figure 40, this orientation allowed the inclusion pattern to reflect light without interference from any reflection off the table facet. The precise epitaxial growth of rutile needles from the hematite, together with their dense, parallel formation and simultaneous reflectance, created the appearance of moth wings, while the contrasting black hematite formed the insect's "body" (figure 41). Through the years we have examined many fine examples of rutilated quartz. This is the first such hematite-rutile "moth" pattern we have encountered, so in our estimation this stone is not just unusual, it is unique.

John I. Koivula and Maha Tannous

Figure 40. Oriented rutile needles extending from the edges of a hematite plate form an unusual moth-shaped inclusion in this 13.97 ct rock crystal from Brazil. Courtesy of Luciana Barbosa; photo by Maha Tannous.

Figure 41. The orientation of the rutile inclusions, together with their dense, parallel formation and simultaneous reflectance create the appearance of moth wings, while the contrasting black hematite forms the "body." Photomicrograph by John I. Koivula; magnified 10×.

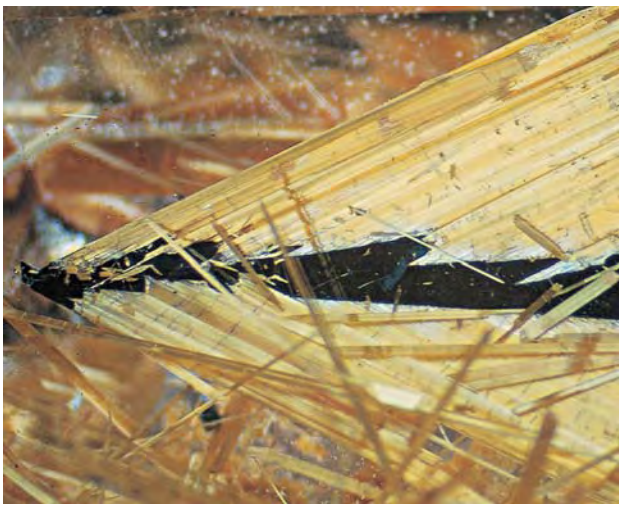

SYNTHETICS AND SIMULANTS

Synthetic Verneuil corundum with unusual color zoning. During a trip to Sri Lanka in mid-2004, one of our clients purchased, among other faceted corundums, a red 1.05 ct modified round brilliant with unusual color zoning. Refractive indices of 1.760–1.770 and a hydrostatic S.G. of 4.00 confirmed that it was corundum.

Viewed face-up, the sample appeared uniformly purplish red (figure 42, left). From the side, however, it appeared very light blue in the crown portion, while the culet area was purplish red (figure 42, right). Such color zoning has been observed in various colors of sapphire from Songea (Tanzania) and Sri Lanka, especially in blue and orange stones. A strong red fluorescence to long-wave UV radiation was observed in the culet area, and Raman spectroscopy confirmed that both parts were corundum.

With magnification, it became obvious that this was a Verneuil (flame fusion) synthetic sapphire, as numerous gas bubbles were visible in the very light blue portion (figure 43). When immersed in methylene iodide, the bound-

Figure 42. This 1.05 ct synthetic corundum appears uniformly purplish red when viewed face-up (left), while the color zoning is clearly visible from the side (right). Composite photo by H. A. Hänni, © SSEF.

ary between the purplish red and very light blue zones appeared curved (figure 44). However, no curved striae were observed in the purplish red portion. A qualitative chemical analysis of the table facet by EDXRF showed only Al; no Ga was detected, as expected for a flame-fusion synthetic corundum.

These observations indicated that the sample was cut from a color-zoned boule of Verneuil synthetic corundum, with the purplish red part representing the small center of the otherwise very light blue boule. This also explained the large fissures observed perpendicular to the growth direction (again, see figure 44). Verneuil boules usually have some tension along their growth axis along which they are split before being cut. Obviously this was not done in this case, and therefore the tension cracks developed.

Lore Kiefert (gemlab@ssef.ch)
SSEF Swiss Gemmological Institute, Basel
HAH
KS

Figure 44. With immersion, the curved growth boundary in this synthetic corundum (4.7 mm from table to culet) is clearly visible. The gray area at the top of the image is a tension crack. Such fractures are characteristically oriented perpendicular to the growth axis of the boule. Photomicrograph by H. A. Hänni, © SSEF.

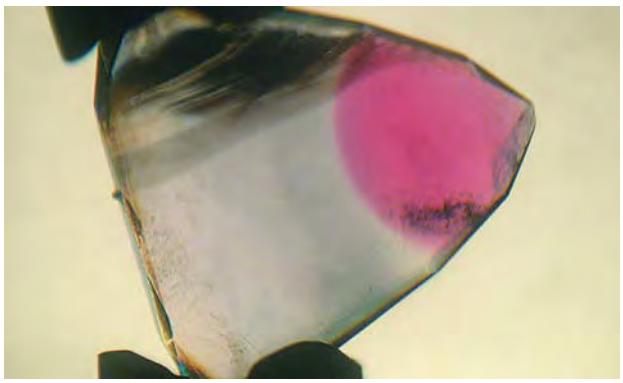

Figure 43. Gas bubbles appear to be radiating from the center of the color-zoned synthetic corundum (5.0–5.2 mm in diameter). Photomicrograph by H. A. Hänni, © SSEF.

Imitation clam "pearl." Throughout history, shell material has often been fashioned to resemble true pearls and non-nacreous "pearls," sometimes for the purpose of deceiving the consumer. The West Coast laboratory, for example, recently inspected several specimens of conch shell that were carefully and convincingly fashioned to mimic conch "pearls." Even more recently, this contributor examined an item that at first appeared like a natural pearl-like calcareous concretion (figure 45). It was donated to GIA by Bill Larson of Pala International, Fallbrook, California, who had obtained it at a jewelry store in La Paz, Baja California, Mexico. The store had about a dozen of these samples, which were represented to Mr. Larson as "genuine clam pearls" that had been polished. However,

Figure 45. This imitation clam "pearl" (17.5 × 10.8 × 10.2 mm) proved to be polished shell material from an unknown mollusk. Photo by Maha Tannous.

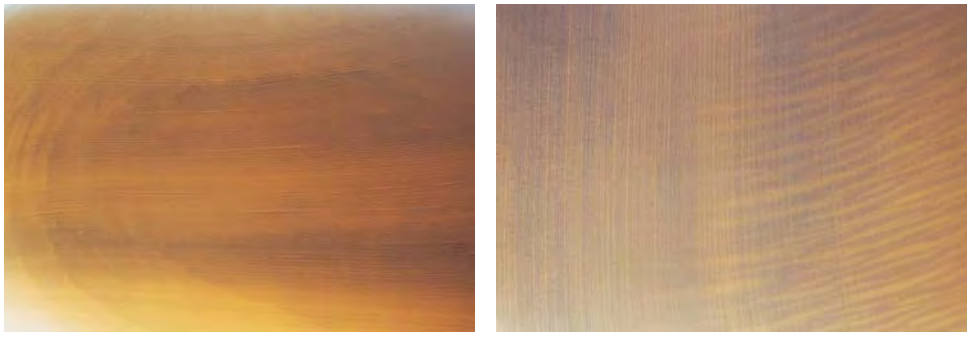

Figure 46. With transmitted light, the imitation "pearl" shown in figure 45 displayed banding (left) and "flame" structures (right). Note also the fine lamellar structure of the banding that is nearly perpendicular to the flame-like structure. Photomicrographs by Maha Tannous (left, magnified 10×) and John I. Koivula (right, magnified 15×)

he suspected that they were imitations, and purchased one sample for closer examination.

The 15.31 ct semitranslucent ovoid specimen was pure white, with a very uniform appearance and shiny, porcelaneous luster. With low magnification, its true nature was evident: The absence of nacre confirmed that the item was not a pearl, and transmitted fiber-optic illumination revealed a prominent parallel banded structure, immediately identifying the sample as shell material rather than any type of pearl-like concretion (figure 46, left). Most interesting was the coarse to fine flame-like structure oriented perpendicular to the banding (figure 46, right).

The refractometer showed a cutoff at approximately 1.65 with a birefringence blink; the lower value was not distinguishable. The S.G. (determined hydrostatically) was roughly 2.76. Long-wave UV fluorescence was weak to moderate chalky yellowish white with very weak light brown streaks corresponding to the structural banding; short-wave UV fluorescence was similar, but even weaker. No distinguishing spectrum was seen with the desk-model spectroscope.

"Flame" structure is commonly found in porcelaneous non-nacreous "pearls" from some mollusks such as the conch, giant clam (*Tridacna gigas*), and Pacific Ocean thorny oyster (*Spondylus calcifer carpenter*; see Winter 1987 Lab Notes, p. 235); the latter is found in the Gulf of California. The flame structure in this imitation clam "pearl" may have fooled an unwary buyer into believing that it was a pearl-like concretion, rather than shaped and polished shell material. However, as this example shows, flame structure also may be seen in the shell of these and similar mollusks. Although it would have been interesting to identify the specific type of mollusk from which this shell material originated, this was not possible because we did not have access to the shells needed for comparison.

Cheryl Y. Wentzell (cwentzell@gia.edu)
GIA Gem Laboratory, Carlsbad

ANNOUNCEMENTS

Visit *Gems & Gemology* in Tucson. Meet the editors and take advantage of special offers on subscriptions and back issues at the *G&G* booth in the Galleria section (middle floor) of the Tucson Convention Center during the AGTA show, February 2–7, 2005.

GIA Education's traveling Extension classes will offer hands-on training in Tucson with "Gem Identification" (January 31–February 4) and "Advanced Gemology" (February 5). To enroll, call 800-421-7250, ext. 4001. Outside the U.S. and Canada, call 760-603-4001.

The GIA Alumni Association will host a Dance Party in Tucson on February 5, featuring a silent auction, an industry awards presentation, and a live auction. To reserve tickets, call 760-603-4204 or e-mail events@gia.edu.

Gem treatment seminar in Tucson. An update on the treatment of corundum and other gem materials will be presented by Ted Themelis during the Tucson gem shows on February 3, 2005 at the Marriot University Park Hotel. Among the subjects covered will be laser-induced breakdown spectroscopy (LIBS) and new treatment methods in Sri Lanka and India. Prior reservation is required; contact veronica@themelis.com or visit www.themelis.com/Tucson2005.

2005 Gem-A field trips. The Gemmological Association of Great Britain is planning two field trips for 2005, a visit to Idar-Oberstein, Germany, March 13–19, and a tour of Minas Gerais State, Brazil, August 15–29. Both field trips will visit local cutting centers and gem mines. E-mail doug@gem-a.info or visit www.gem-a.info/membership/fieldTrips.htm.

Exhibits

Cartier Collection in Houston. "Cartier Design Viewed by Ettore Sottsass," an exhibition of over 200 objects from the Cartier Collection, will be on display at the Museum of Fine Arts, Houston, through March 27, 2005. Among the pieces displayed are diadems, brooches, and rings, as well as jeweled accessories such as cigarette cases, clocks, and watches. E-mail visitorservices@mfah.org or visit www.mfah.org.

Native American Jewelry at AMNH. "From Totems to Turquoise: Native North America Jewelry Arts of the

Northwest and Southwest," an exhibition of more than 500 pieces of contemporary and historic Native American jewelry, is being held at the American Museum of Natural History in New York City until July 10, 2005. Visit www.amnh.org/exhibitions/totems/ or call 212-769-5100.

Conferences

WJA in New York. The Women's Jewelry Association "Women In the Know" business conference will be held on Friday, March 4, at the Fashion Institute of Technology in New York City. Topics will include leadership development, Internet business strategy, and customer service management. Visit www.womensjewelry.org or call 310-937-8997.

PDAC 2005. The Prospectors and Developers Association of Canada convention will take place March 6–9 in Toronto. Diamonds will be featured in a session called "Diamonds—Around the World in 120 Minutes," and also will be included in other sessions. Visit www.pdac.ca/pdac/conv.

BaselWorld 2005. The BaselWorld show will be held March 31–April 7 in Basel, Switzerland. GIA will host GemFest Basel on April 2, 4–6 pm, at the Basel Convention Center, Hall Montreal. The program will be followed by a reception. During the show, *Gems & Gemology* editor-in-chief Alice Keller will be available at the GIA Booth in Hall 2, Stand W23. For more information on BaselWorld, visit www.baselshow.com, call 800-922-7359, or e-mail usvisitor@baselworld.com.

Russian gemology. A session on gemology will be held during *VII International Conference: New Ideas in Earth Science* at the Moscow State Geological Prospecting University April 5–6, 2005. E-mail science@msgpa.ru.

GemmoBasel 2005. The first open gemological conference in Switzerland will be presented by the SSEF Swiss Gemmological Institute at the University of Basel, April 29–May 2, 2005. Among the events scheduled is a field trip to a Swiss manufacturer of synthetic corundum and cubic zirconia. Visit http://www.gemmobasel2005.org or contact gemlab@ssef.ch.

ICNDST-10 in Japan. The 10th International Conference of New Diamond Science and Technology will be held at the National Institute of Advanced Industrial Science and Technology Conference Hall in Tsukuba, Japan, May 11–14, 2005. Among the topics covered will be HPHT synthesis and processing and the growth of CVD synthetic diamond. Visit www2.convention.co.jp/ICNDST-10 or email icndst-10@convention.co.jp.

Diamonds at GAC-MAC. The 2005 joint meeting of the Geological Association of Canada and the Mineralogical Association of Canada will be held May 15–18, 2005, in Halifax, Nova Scotia. "From Cratons to Carats: A symposium to honour the career of Herwart Helmstaedt" will feature presentations on geotectonic controls on diamond exploration. E-mail hfx2005@gov.ns.ca or visit www.halifax2005.ca.

Bead Expo in Miami. The 2005 International Bead Expo will be held in Miami, Florida, May 18–22. Over 60 workshops and educational lectures on bead jewelry design and manufacture are scheduled. E-mail info@beadexpo.com or visit www.beadexpo.com.

Goldschmidt Conference. The 15th Annual Goldschmidt Conference will take place May 20–25, 2005, in Moscow, Idaho. The meeting will include a session on the geochemistry of gem deposits, and also will include numerous presentations on advanced analytical techniques. E-mail gold2005@uidaho.edu or visit www.uidaho.edu/gold2005.

ERRATA

1. The Winter 2003 Gem News International entry, "Some interesting pearls from the North American West Coast" (pp. 332–333), may have given the impression that the green abalone (*Haliotis fulgens*) and the pink abalone (*H. corrugata*) can be legally fished in the United States. In fact, both commercial and sport fishing of these particular species have been banned in the U.S. since 1996 (limited sport fishing for red abalone is allowed under strict regulations). The near-round abalone pearl described in this entry was recovered from a green abalone in waters off the coast of Mexico; the abalone pearl with the unusual growth structure was from a red abalone and purchased from an old collection.

2. Since the publication of the Summer 2004 Gem News International entry, "'Shell pearls' with *Tridacna* clam shell beads" (p. 178), it has come to our attention that *Tridacna* giant clams are protected under the Convention on International Trade in Endangered Species of Wild Fauna and Flora (CITES), Appendix II (www.cites.org/eng/append/appendices.shtml). Materials listed in CITES Appendix II may not be exported without a license, and listed marine materials recovered from international waters may not be imported into the United States without a permit from the U.S. Fish and Wildlife Service. Those contemplating international trade in any cultured or imitation pearls using *Tridacna* nuclei should take care to comply with permitting regulations; however, as noted in the entry, the use of *Tridacna* shell as pearl nuclei is a practice best avoided (see also Summer 2002 Gem News International, p. 179).

Book REVIEWS

2004

Bernd Munsteiner: Reflexionen in Stein [Reflections in Stone]

*Edited by Wilhelm Lindemann, 224 pp., illus., publ. by Arnoldsche, Stuttgart, Germany, 2004 (in German and English). US$75.00**

This extraordinary new book on Bernd Munsteiner sets the famous lapidarist's work firmly within the realm of art—showing it to us not as we are accustomed to seeing it, as the stonecutter's craft taken to the edge of possibility, but as something more. In the complex argument that opens the book, Lindemann explains how the development of faceting during the Renaissance took cutters away from the ancient view of precious stones as earthbound sources of divine light: In other words, even as gems grew more sparkly, their beauty lost its connection to the underlying material. But it is in such dynamic spaces that art flourishes. Much as Cubism bridges two- and three-dimensional representation, the reconciliation of the tensions between crystal and light through cutting is, in Lindemann's view, the driving force behind Munsteiner's creativity. A series of essays from American collectors Si and Ann Frazier and Michael M. Scott, German jeweler Deborah Aquado, and art historian Christianne Weber-Stober extend this thesis and offer personal glimpses of both the man and his work.

The heart of the book, though, is its more than 200 breathtaking photographs, most of them taken by Jürgen Cullmann and Harold and Erica Van Pelt. Pieces are grouped thematically and "hung" on the white space of the pages as if on a gallery wall, interspersed with close-ups of the rutile inclusions in the "Metamorphosis" crystal and of gem minerals in various stages of cutting. Loose gems and jewelry from the earlier agate series are featured, as well as the more familiar "fantasy cut" tourmalines, aquamarines, and quartzes. Also seen are the sculptural works, outdoor installations, and several pieces of glasswork done for ceramics manufacturer Royal Copenhagen. A special section is devoted to "Dom Pedro," the 10,000 ct aquamarine Munsteiner cut in 1993.

For both the serious collector and the jeweler/gemologist, this book offers a comprehensive guide to one of the most important lapidary artists in the world. I particularly enjoyed seeing Munsteiner's complete body of work treated as a retrospective. As a museumgoer, I found that this approach helped me understand the whole as well as revel in the parts. And as someone who had understood these works primarily as exercises in "gee-whiz" lapidary technique, their intellectualism was as much of a surprise as their sensuality.

Beyond its obvious value as a reference, *Reflexionen in Stein* successfully accomplishes its goals: It carves out a space for Bernd Munsteiner's work within the broader context of Western art history—and then celebrates what happens there, even as the work itself invites us to do.

LISA SCHOENING
Gemological Institute of America
Los Angeles

Illustrated Guide to Jewelry Appraising, 3rd Edition

*By Anna Miller, 200 pp., illus., publ. by GemStone Press, Woodstock, VT, 2004. US$39.99**

With this edition, the late Anna Miller updated and expanded her respected *Illustrated Guide to Jewelry Appraising*. Every evaluator, whether newly minted or a seasoned professional, will find it a valuable resource.

The book covers a wide range of important topics, beginning with the appraiser's role and responsibilities in the first chapter. The second deals with understanding the different valuation methods, researching price points, and making the proper identification. Readers will find the third chapter especially rich in jewelry "forensic" identification. The process of estimating values for every conceivable form of wearable jewelry is covered next, while chapter 5 reviews the appraisal as a legal document. The book closes with tips on identifying and valuing unfamiliar pieces.

The *Illustrated Guide* discusses just about every major aspect of a carefully crafted and accurate appraisal for antique, period, and modern jewelry. It is organized logically and is refreshingly easy to read. Miller found ample room for detail, but did not overdo it. This edition includes an updated listing of market information and price guides, an additional jewelry period ("Consumerism," 1990–2002), and a new chapter called "Valuing the Unfamiliar," which covers reproduction, Asian antique, and Berber jewelry.

Although the quality and value of the text is as expected from someone with decades of experience, it is unfortunate that both the paper quality and

*This book is available for purchase through the GIA Bookstore, 5345 Armada Drive, Carlsbad, CA 92008. Telephone: (800) 421-7250, ext. 4200; outside the U.S. (760) 603-4200. Fax: (760) 603-4266.

the photographs are not up to the same standard. After reading the first-rate text, it is disappointing to be let down by dark, murky, and sometimes out-of-focus photographs.

In this reviewer's opinion, this book is a great reference guide, but it would have been outstanding if the production issues had been resolved. Nevertheless, Anna Miller has provided another useful tool that would certainly add value to any appraiser's library.

M. ADAM NAMEROW
Chippewa Lake, Ohio

Magic World: Inclusions in Quartz

By Jaroslav Hyrsl and Gerhard Niedermayr, 240 pp., illus., publ. by Bode Verlag, Haltern, Germany, 2003 [German and English]. € *49.00*

This attractive book offers a fascinating look into a truly magical world: the approximately 130 minerals that have been documented as visible inclusions in crystalline quartz. The objectives of this book are not only to describe the minerals known to occur in quartz, but also to help gemologists identify them and encourage more collectors to study them. To meet these objectives, the authors have provided some 290 photos and photomicrographs.

The book begins with a general discussion of quartz, its modes of formation, and the kinds of inclusions that these differing modes produce. The paragenesis of fluid and solid inclusions is described, as well as what the presence of these inclusions tells us about the growth environment. Highlights of this section are photos of specimens and original labels from the W. E. Hidden collection, which is now housed in the Natural History Museum of Vienna.

The next eight chapters cover the inclusions themselves, organized according to their chemical classification (oxides, carbonates, silicates, etc.); the last chapter is devoted to inclusions in synthetic quartz. Short descriptions of the inclusions are given, along with locality and other information that collectors might find valuable. Some of these, such as diamond as an inclusion in quartz, are stated to have been reported but not actually verified.

Notables such as Rock Currier, Si and Ann Frazier, and John Koivula contributed to this book. The specimens, superbly photographed by the authors and others (including Werner Lieber, Olaf Medenbach, and Jeff Scovil) capture outstanding examples of the varied and often breathtakingly beautiful inclusion scenes in quartz from a number of prominent collectors and institutions. These include: a 1 cm cinnabar crystal in doubly terminated quartz from Guizhou, China (p. 55); a 1.2 cm spray of pääkkönenite needles from the Cryo-genie mine in California (p. 67); a large rock crystal quartz with actinolite needles from Switzerland (p. 164); a scepter-growth quartz, also from Switzerland (p. 168); and a Japan-law quartz twin with andradite from Peru (p. 196).

Only a few minor criticisms can be made. In some places, the English text has misspelled words or confusing syntax, such as "about 1 cm big, nicely formed cinnabar." Does this mean the cinnabar is 1 cm in size or that 1 cm is considered big for a well-formed cinnabar inclusion? (I favor the latter.) Sometimes the locality information given for the photos and the names of the minerals listed in the index are not translated into English. In addition, the text assumes an audience versed in basic mineralogy, which might force the novice reader to consult other texts for technical definitions and further data on the minerals themselves.

Still, this is the best new book on mineral collecting I've seen in a long time, and it is certainly the finest yet on inclusions in quartz. I hope the authors' aim, that many collectors will be attracted to quartz inclusions, will become a reality, just as long as there are still some left for me.

MICHAEL EVANS
Gemological Institute of America
Carlsbad, California

Minerals: Their Constitution and Origin

By Hans-Rudolf Wenk and Andrei Bulakh, 668 pp., illus., publ. by Cambridge University Press, Cambridge, United Kingdom, 2004. US$130.00 (hardcover); US$70.00 (softbound).

This is an introductory college-level mineralogy textbook. As such, it may not seem a natural for the library of a gemologist; yet a basic knowledge of modern mineralogical principles and methods can be a tremendous advantage in understanding the latest advances in gemology. Such knowledge can also lead to a broader appreciation of the properties of gemstones and of the occurrence of gem materials in the context of natural processes. The gemologist stands to gain greatly from expanding his or her mineralogical background. This book may not be the perfect mineralogical primer for a gemologist, but it has much to offer.

Minerals: Their Constitution and Origin covers a very broad range of topics, and does so clearly and succinctly. It doesn't delve into any topic in great depth, but it provides a good understanding of those it addresses. The diagrams and photographs are well chosen and a great help, although it should be noted that many of the topics assume a basic background in physics, chemistry, and/or mathematics.

Those topics that would probably be of greatest interest to the gemologist include crystal morphology, crystal growth, optical properties, color, spectroscopic techniques, mineral identification, and mineral formation. Besides having a chapter devoted to mineral genesis, the book also covers specific types of mineral deposits in the context of the various mineral groups.

The last part of the book deals with applied mineralogy and includes a chapter on gems, both natural and synthetic. While the coverage of gemstones is very cursory, it is interesting to see how they are viewed in a mineralogical context.

In my opinion, one of the best books ever written on minerals was John Sinkankas' *Mineralogy for Amateurs* (called simply *Mineralogy* in later editions). No other book I have seen does a better job of explaining basic mineralogical concepts so that virtually anyone can understand them. Unfortunately, with the rapid advances in modern scientific mineralogy, this and other classic books for the layperson have become quite dated. *Minerals: Their Constitution and Origin* provides an excellent contemporary introduction to mineralogy. It may not be as enjoyable a read as some of the nontechnical mineral texts available, but if you make the effort, you will come away with a lot of good, up-to-date mineralogical insight.

ANTHONY R. KAMPF
Natural History Museum of Los Angeles County
Los Angeles, California

Rocks Pebbles and Stones: Confessions of a Private Jeweler

By Fred Feldmesser, 100 pp., publ. by Farrington Press, Boston, 2004. US$30.00 (E-mail: parker@feldmesser.com)

It's not often that total strangers welcome you to share in the most personal milestones of their lives. Jewelers are not only allowed, but also *trusted*, to help guide and be a part of the special moments in life: engagements, weddings, anniversaries, and so forth. Jewelers sell diamonds and gems, love and romance, and for this receive payment. In a style resembling a personal journal, private jeweler Fred Feldmesser shows that there are definitely more than monetary rewards to be gained. For all the books available on every aspect of the gem and jewelry industry, it is rare to come upon one such as this. Mr. Feldmesser opens up to the reader and relates how his love of jewelry has led him on a journey to interact with people and gems, as well as the life lessons he has learned.

Rocks Pebbles and Stones: Confessions of a Private Jeweler is composed of 20 vignettes spread over 100 pages in a magnificently bound volume. Each essay shares a key moment in Mr. Feldmesser's distinguished 30-plus-year career, or an insight he has gained. He begins with his father's guidance in introducing him to the world of diamonds, gemstones, and New York City's 47th Street. He then proceeds with his visits to exotic corners of the world, the inner sanctums of prestigious jewelers, and the homes of prominent clients, as well as his charitable endeavors with Boston Children's Hospital. (A portion of the book's proceeds will go to children's hospitals in Boston and New York.) The reader will learn why Mr. Feldmesser has such an impassioned view of the role of a jeweler in people's lives.

One of the most charming essays, "Two Small Stones," begins in Mr. Feldmesser's home, where a client has stopped by with her two young boys to consult about some jewelry. As they leave, Mr. Feldmesser gives the children some Brazilian geodes as gifts. A few weeks later, he receives a package in the mail from the two boys with a letter saying they loved their geodes and decided to send him two favorite pebbles from their rock collection in thanks. Shortly thereafter, at the end of a lecture at Sotheby's, Mr. Feldmesser displayed an Art Deco bracelet, a Colombian emerald—and the two small stones he received from the boys. The point illustrated was that all gemstones, by their very nature, are rocks, pebbles, or stones: Sometimes a personal attachment is a more meaningful determinant of a stone's value than the market might otherwise suggest.

JOSHUA SHEBY
Gemological Institute of America
New York

2004 Manuscript Reviewers

Gems & Gemology requires that all articles undergo a peer review process in which each manuscript is evaluated by at least three experts in the field. This process is vital to the accuracy and readability of the published article, but it is also time consuming for the reviewer. Because members of our Editorial Review Board cannot have expertise in every area, we sometimes call on others in our community to share their intellect and insight. In addition to the members of our Editorial Review Board, we extend a heartfelt thanks to the following individuals who reviewed manuscripts for *G&G* in 2004:

Mr. George Bosshart
Dr. Jim Butler
Mr. Paul Cory
Dr. Janet Douglas
Mr. Si Frazier
Mrs. Ann Frazier
Ms. Cecilia Gardner, Esq.
Dr. Gaston Giuliani
Mr. Mike Gray
Mr. Mark Gronlund
Mr. Eli Haas
Dr. George Harlow
Mr. Hertz Hasenfeld
Ms. Bev Hori
Dr. Jaroslav Hyrsl
Dr. Chankon Kim
Dr. Peter Leavens
Dr. Robert Mason
Mr. Mark Maxwell
Mr. Sofus Michelsen
Mr. Roland Naftule
Mr. Franck Notari
Dr. Ilene Reinitz
Mr. Russell Shor
Mr. Yasukazu Suwa
Mr. Jack Townsend
Dr. Wuyi Wang
Dr. Chris Welbourn

Gemological **ABSTRACTS**

2004

COLORED STONES AND ORGANIC MATERIALS

Alexandrite effect. A. V. Vasiliev. *Gemological Bulletin*, No. 8, 2003, pp. 28–38 [in Russian with short English abstract].

A specially designed computer-controlled spectrometer was used to obtain absorption spectra to study color-change phenomena in minerals. The following samples were studied: chrysoberyl, emerald, corundum, several garnets, fluorite, apatite, stillwellite, and lovchorrite [rinkite]. Using various light sources (i.e., tungsten, mercury, direct sunlight, scattered daylight, D65 fluorescent lamp, and "equal energy source E"), characteristics of hue, tone, and saturation were evaluated and integrated into an analysis of the influence of spectral light distribution on color perception. Particular attention was paid to crystal orientation in the anisotropic minerals.

Rubies from Myanmar, Cambodia, and Tanzania, as well as blue sapphires from the Ural Mountains (Russia), showed particularly significant color differences between daylight and the other sources. Spessartine-grossular garnets from Tanzania showed a distinct color change, comparable to alexandrite from the Urals. Much less color change was seen in samples of spessartine-grossular from Sri Lanka and pyrope from Yakutia. Fluorite from an emerald mine in the Urals showed a noticeable change. A "reverse" alexandrite effect (i.e., blue rather than red in tungsten illumination) was observed in grossular from Noril'sk (Siberia). Technical explanations for all of these observations are given. In the case of apatite, stillwellite, and lovchorrite, which contain rare-earth elements, color change was seen only when they were compared in daylight and with a mercury lamp.

BMS

This section is designed to provide as complete a record as practical of the recent literature on gems and gemology. Articles are selected for abstracting solely at the discretion of the section editor and his reviewers, and space limitations may require that we include only those articles that we feel will be of greatest interest to our readership.

Requests for reprints of articles abstracted must be addressed to the author or publisher of the original material.

The reviewer of each article is identified by his or her initials at the end of each abstract. Guest reviewers are identified by their full names. Opinions expressed in an abstract belong to the abstracter and in no way reflect the position of Gems & Gemology or GIA.

Features of chemical composition and optical properties of peridot. A. A. Zolotaryov, A. K. Buiko, A. A. Buiko, and N. O. Ovchinnikov, *Gemological Bulletin*, No. 10, 2003, pp. 14–20 [in Russian with short English abstract].

The properties of 28 faceted gem-quality peridots from China, Egypt, Pakistan, Russia, Tanzania, and the U.S. were determined. Electron-microprobe analyses showed that all the samples were predominantly forsterite (Mg_2SiO_4) with 5–15 mol.% fayalite (Fe_2SiO_4). Peridots from Pakistan and Tanzania had lower Fe contents, whereas those from Russia and the U.S. had higher Fe contents. Variations in Fe affected the colors and R.I. values. Trace elements (e.g., Ni, Mn, and Ca) had a negligible effect on these properties.

The main hues varied between yellowish green and orange-yellow. The yellow component was correlated to Fe. A good correlation was found between Fe content and the highest refractive index (n_γ), which ranged between 1.680 and 1.698. Peridots from Pakistan (lower Fe contents) were optically positive, whereas those from Russia and the U.S. (higher Fe contents) were optically negative. The birefringence was at least 0.017; this is a distinguishing characteristic and enables peridot to be separated from sinhalite ($MgAlBO_4$, birefringence 0.008), which otherwise has optical properties very similar to peridot. *BMS*

High-pressure, metasomatic rocks along the Motagua fault zone, Guatemala. G. E. Harlow, V. B. Sisson, H. G. Avé Lallemant, S. S. Sorensen, and R. Seitz, *Ofioliti*, Vol. 28, No. 2, 2003, pp. 115–120.

The Motagua fault zone in central Guatemala forms the present boundary between the North American and Caribbean plates, and is the world's second most important source of jadeite (after Myanmar). It consists of two major subparallel faults, the San Augustín and the Cabañas, where high-pressure/low-temperature rocks occur. Jadeite is hosted by sheared serpentinite bodies, primarily on both the northern and southern sides of the Cabañas fault. However, there are distinct mineralogical differences in the jadeite belts on either side of the fault. Late-stage alteration, grain-boundary alteration, and albitization are present in jadeites from the northern side of the fault, whereas these features have not been documented in jadeites from the more recently discovered southern bodies. Further, jadeites from some areas of the southern belt are more translucent and darker colored (in addition, some are blue) than their northern counterparts.

The authors propose that the Guatemalan jadeites crystallized from seawater-like fluids derived from a subducting plate that entered into a serpentinizing peridotite body. The jadeite formed at temperatures of 100–400°C and pressures of 5–11 kbar. Because jadeites (and associated high-pressure/low-temperature rocks) in the two belts show different mineral assemblages with distinctive properties, the Motagua fault zone may record two collisional events. Alternatively, these two belts may represent different structural levels of one subduction complex. *KSM*

Problem in Chinese fresh-water pearl industry and countermeasure. J. Zhao and R. Yang, *Journal of Gems and Gemmology*, Vol. 5, No. 4, 2003, pp. 42–45 [in Chinese with English abstract].

China is both the world's largest producer and largest exporter of freshwater cultured pearls. However, compared to the late 1990s, much of the industry is facing problems of decreasing quality and falling prices, which threaten to hinder further development. Reasons for these problems include the following: (1) There are no controls on production, (2) technological advances to improve cultivation and the quality of production have not been implemented, and (3) water quality in some of the most important growing areas is afflicted by pollution (i.e., excessive amounts of nutrients, toxic materials, and suspended matter).

Possible solutions to these challenges are offered: (1) Scientific management and state regulation of production should be implemented; (2) the industry should be reorganized with the consolidation of small operations into larger, more efficient companies and cooperatives; (3) research aimed at improving all aspects of the industry should be encouraged and more specialists trained; (4) laws to reduce pollution and improve the growth environment for the pearl-producing mollusks should be enacted and enforced; and (5) brand names for Chinese cultured pearls on the international markets should be developed to help add value. *TL*

TPR, EPR and UV-Vis studies of Ni(II) speciation in chrysoprase. Z. Sojka, S. Witkowski, W. Zabiński, K. Dyrek, and E. Bidzińska, *Neues Jahrbuch für Mineralogie, Monatshefte*, No. 1, 2004, pp. 11–25.

TPR (temperature programmed reduction), EPR (electron paramagnetic resonance), and ultraviolet-visible spectroscopic methods were used to study the local environment (i.e., lattice sites) in which nickel ions (the green chromophore) occur in chrysoprase from three localities: Szklary, Lower Silesia, Poland ("apple" green, 1.71 wt.% Ni); Marlborough Creek, Australia ("emerald" green, 0.98 wt.% Ni); and an unknown African locality (dark green, 4.38 wt.% Ni). The authors demonstrated that nickel is present in two different forms: It is predominantly dispersed into 2:1 phyllosilicates (similar to Ni-talc), and less commonly it is found as extra-framework species adsorbed onto the surface of the chalcedony. *RAH*

DIAMONDS

Electron microscopy analysis of debris produced during diamond polishing. F. M. van Bouwelen, J. E. Field, and L. M. Brown, *Philosophical Magazine*, Vol. 83, No. 7, 2003, pp. 839–855.

Diamond's hardness is anisotropic, and therefore it shows different polishing rates according to crystallographic direction. Historically, diamond polishing was explained

in terms of microcleavage along octahedral planes, as tiny irregularities on a diamond's surface contact the scaife. However, various investigations conducted in the 1990s of the details of polished diamond surfaces found no evidence for this hypothesis. Other studies have attempted to examine the debris from polishing, but they were marred by the difficulties in obtaining pristine samples.

The present authors collected polishing debris on a small copper screen coated with a SiO film, hung slightly above the scaife and about 2 cm behind the diamond being polished. The debris ejected from various diamond faces and from different polishing directions was examined both visually and chemically.

High-resolution electron microscopy showed abundant amorphous carbon in the debris taken from all polishing directions. Patches of graphite also were found in the debris. In the sequence of samples from softer to harder direction, the ratio of graphite to amorphous carbon decreased. However, attempts to polish the octahedral planes themselves produced debris with relatively large sheets of graphite and angular fragments of diamond (but no cleavage fragments).

Electron-energy-loss spectroscopy enabled the authors to characterize the debris chemically and to calculate a bulk density of 1.9 g/cm^3 for the debris from the softer directions, 2.2 g/cm^3 for debris from a harder direction along the cubic plane, and 2.3 g/cm^3 (the density of graphite) for debris from the octahedral plane. High-energy-loss spectra indicated the presence of a form of amorphous carbon. The spectra revealed no nitrogen, but oxygen was present at 2–4 atom%, with more oxygen in the debris from softer directions. Assuming only carbon and oxygen in the debris, the authors calculated an sp^2-to-sp^3 ratio (the ratio of graphite bonds to diamond bonds) that indicates graphite constitutes 80–100% of the debris for all samples except those from the octahedral plane.

Rather than microcleavage, the authors concluded that the pressure of polishing transforms the surficial layer of diamond to graphite, which is then readily removed. Studies by other researchers of the anisotropic distribution of compressive stress during diamond polishing along different directions also support this conclusion. Last, the authors use this conclusion to explain why a layer of black powder is created when preparing a new scaife. *Ilene Reinitz*

FISH—State-of-the-art technology in final diamond recovery. L. du Plessis and M. Sewawa, *Journal of the South African Institute of Mining and Metallurgy*, Vol. 103, No. 9, 2003, pp. 557–562.

This process-engineering article reviews diamond recovery technology recently employed at Debswana's Jwaneng mine in Botswana. FISH, or Fully Integrated Sort House, has improved three key areas of final diamond recovery: sorting efficiency, availability of production information (turn-around time), and security. FISH, in combination with CARP (or Completely Automated Recovery Plant), was jointly installed at the Jwaneng recovery plant (called "Aquarium") in late 2000.

Through the integration of several commercially proven technologies, the FISH process streamlines feed preparation and the sorting, cleaning, and packing of recovered diamonds. Sorting efficiency improvements were realized by introducing X-ray and laser (Raman spectroscopy) equipment. In turn, decommissioning the maintenance-intensive grease belts improved turn-around times. The new equipment allows "hands-off" operation and maintenance (i.e., human hands do not touch diamonds or diamond concentrate), thus improving product security.

The article also discusses lessons learned from the implementation of these new technologies, such as personnel issues, data collection, and operational feedback. For example, an increase in the number of technical staff was required to cope with the new equipment demands, yet overall operational costs dropped due to efficiencies gained in other areas. Interestingly, Debswana concluded that the successful integration of various technologies proved to be more innovative than the individual technologies themselves. *KAM*

On grading the asymmetry of a round brilliant-cut diamond. S. B. Sivovolenko, Yu. B. Shelementyev, and G. Holloway, *Gemological Bulletin*, No. 9, 2003, pp. 18–25 [in Russian with short English abstract].

Symmetry in round brilliant cut diamonds is evaluated differently in Russia, Belgium, and the U.S. This article summarizes and compares characteristics of the symmetry-evaluation methods used in these countries, with particular emphasis on the cause, effect, and importance of asymmetry. Asymmetry is explained as the degree of mutual deviation from the ideal of the table and pavilion axes. Based on a computer-generated 3D model, a new method for grading asymmetry in round brilliant diamonds is proposed. The article is critical of some aspects of the HRD and GIA methods, particularly where certain deviations from the "ideal" are designated as "important" or "unimportant." The authors maintain that it is more correct to separate the deviations into two categories: (1) those that influence optical properties, and (2) those that simply reflect the skill of a cutter—that is, they are easily visible but not very significant. *BMS*

Options for selling rough. J. Chapman, *Rough Diamond Review*, No. 2, 2003, pp. 16–18.

In an industry where rough diamond producers have unique production profiles and monthly outputs, the successful sale of rough requires careful consideration. No longer is De Beers virtually the sole buying organization, as in decades past. Today, several avenues are available to primary producers. Sellers of (legitimate) rough may use diamond bourses or exchanges, find contract buyers, enter into investor-dealer arrangements, use tendering agents or

brokers, or establish a sales office. Some caveats for these options are given, such as the care required in assembling parcels that will appeal to purchasers, as well as the necessity of well-defined contractual obligations regarding contract sales and investors. The article recommends that experts be consulted in many cases, such as for valuation purposes, product presentation, advice on local demand and governmental regulations, and marketing. Although optimizing sales of rough is complex, current high demand places producers in a position of strength, which can be exploited with an appreciation of the advantages and shortcomings of various selling practices. *DMK*

The preservation of alluvial diamond deposits in abandoned meanders of the middle-Orange River. P. G. Gresse, *Journal of the South African Institute of Mining and Metallurgy*, Vol. 103, No. 9, 2003, pp. 535–538.

The Orange River has transported diamonds eroded from kimberlites and intermediate secondary sources in South Africa's interior and deposited them within gravel terraces along much of its length. These terraces are typically preserved at distinct elevations above the current river level, but were not recognized during most of the 20th century as they were capped by younger sediments. Within the past four years, some of these terraces have been successfully mined, particularly along the "mid-Orange River" section between Douglas and Prieska in South Africa's Northern Cape Province.

Each terrace has a characteristic diamond content and age. For example, the most consistent diamondiferous paleodeposit is located 60–90 m above the current river level and was formed in the mid-Miocene (~8 million years ago). Each time the river cut more deeply into the valley as a result of sea-level or other changes, it would partially rework the previous cycle's gravel deposits, including its diamonds. The diamond content of any one gravel terrace is dependent on the amount of diamonds introduced from upstream by the paleoriver, the number of reworked diamonds from the previous cycle's gravels, and the amount of dilution material present. Data on the internal structure and morphology of these deposits are obtained through drilling and high-resolution aeromagnetic surveys, the latter being particularly effective in delineating those terraces that contain a large amount of iron (originally sourced from banded iron formations in the area). A high iron content correlates with a higher diamond content; apparently, the added density of the iron-bearing gravels enhanced the trapping mechanism for diamonds. *KAM*

Revival of the Skeleton Coast. R. Baxter-Brown, *Rough Diamond Review*, No. 3, 2003, pp. 27–30.

The Skeleton Coast, a narrow, 800-km-long stretch of desert bordering the Atlantic Ocean in northern Namibia, encompasses rugged terrain lacking in infrastructure; it is an inhospitable environment for diamond exploration. Rusting pieces of machinery and prospecting pits from exploration between 1943 and 1971 are reminders of failed ventures. Urged to open the Skeleton Coast for exploration once again, the government of Namibia granted the first diamond prospecting licenses for the region in recent times in 1999. Exploration activities were delayed until 2001 due to environmental concerns. Since then, some successful ventures have been launched in the area, and ore-reserve evaluation programs have identified several potentially profitable areas.

The origin of the Skeleton Coast diamonds is problematic. Various possibilities have been proposed, but the most favored is that the diamonds originated in kimberlites in Angola and were brought to the Skeleton Coast by south-flowing Angolan rivers starting in late Tertiary time. *MT*

Selection of plant for diamond ore concentration. T. Mason, *Rough Diamond Review*, No. 2, 2003, pp. 33–38.

One of the most important steps in diamond mining is the concentration of diamonds, along with other heavy minerals, from the kimberlite or alluvial ore prior to routing the concentrate to an X-ray sorter or grease-table separator. The goal is to minimize the volume of material that must be processed during the final recovery stage. The techniques of primary concentration are based on density, and their principle of operation is called "densimetric separation." Dense-medium separators such as HM (heavy-medium) cyclones, jigs, and pans are described, and their efficacy is discussed. Although cyclones are very efficient, a more economic concentration of diamondiferous ore can be attained by using them in conjunction with simpler devices such as jigs, pans, and shakers. The author recommends that diamond mining projects use densimetric ore profiles to develop effective and efficient plant designs. *DMK*

INSTRUMENTS AND TECHNIQUES

Aplicações de microscopia eletrônica de varredura (MEV) e sistema de energia dispersiva (EDS) no estudo de gemas: Exemplos Brasileiros [The application of scanning electron microscopy (SEM) and energy-dispersive spectroscopy (EDS) to gem research: Brazilian examples]. L. da C. Duarte, P. L. Juchem, G. M. Pulz, T. M. M. Brum, N. Chodur, A. Liccardo, A. C. Fischer, and R. B. Acauan, *Pesquisas em Geociências*, Vol. 30, No. 2, 2003, pp. 3–15 [in Portuguese with English abstract].

The inclusions in several Brazilian gems were studied using SEM and EDS techniques. Emeralds from Campos Verdes, Goiás State, were found to contain inclusions of talc, dolomite, chromite, pyrite, magnetite, and sylvite (KCl; in fluid inclusions). The emeralds are color zoned,

with outer green regions that are richer in Cr^{3+} than the inner near-colorless zones. Amethysts from Rio Grande do Sul State contain needle-like inclusions of goethite, rather than cacoxenite and rutile as suggested previously. Agate and quartz geodes from the same state contain pyrolusite and hollandite. The "silk" effect in corundum from Barra Velhe (Santa Caterina State) is due to inclusions of diaspore, while asterism in this corundum is attributed to needle-like channels. Rounded zircons are common inclusions in corundum from various localities in Minas Gerais State, and some have sillimanite and/or kyanite inclusions that suggest a metamorphic origin. *RAH*

The detection of colour-enhanced and synthetic gem diamonds by optical spectroscopy. A. T. Collins, *Diamond and Related Materials*, Vol. 12, No. 10–11, 2003, pp. 1976–1983.

More than five decades of fundamental research on the optical properties of defects in diamond provide the basis for today's gem-testing laboratories to assess gem-quality diamonds. In the majority of cases, spectroscopic analysis enables the determination of the origin of color—natural or treated—as well as the differentiation of synthetic from natural. This paper is a compendium of benchmark optical properties that define these separations.

It begins with an overview of the specific defects—nitrogen, boron, and plastic deformation—responsible for the various natural and treated colors seen in diamond. It then reviews the primary optical characteristics resulting from radiation damage and subsequent annealing, as well as HPHT processing. Concluding paragraphs detail the distinguishing defect properties of both near-colorless and colored HPHT-grown synthetic diamonds. *SW*

In situ mobile subaquatic archaeometry evaluated by nondestructive Raman microscopy of gemstones lying under impure waters. D. C. Smith, *Spectrochimica Acta Part A*, Vol. 59, No. 10, 2003, pp. 2353–2369.

Laboratory simulation experiments were conducted to determine the feasibility of identifying cultural heritage objects at an underwater archaeological site with a mobile Raman microspectroscopy (MRM) system. Three gem materials (zircon, amazonite, and sodalite) were placed under different kinds of pure and impure waters (the latter representing waters containing dissolved or suspended organic or inorganic material that might typically be found at an underwater site). The optical objective of the Raman microscope was immersed in the water to eliminate the normal aerial pathway of the laser beam between the objective and the item being analyzed.

Raman spectral band intensities were found to be stronger than, similar to, or weaker than spectra for the same gem minerals recorded in air. Nevertheless, diagnostic bands could be recognized in the spectra recorded for samples in the pure and impure waters, although some of the inherent problems presented by Raman analysis (e.g., fluorescence) remained. A number of technological, scientific, and archaeological considerations for *in situ* MRM analysis of objects underwater are discussed, and it is concluded that subaquatic archaeometry by MRM could be a viable technique at certain sites. On-site experiments to authenticate this new approach have not yet been conducted. *JES*

Rank correlation of laser-induced breakdown spectroscopic data for the identification of alloys used in jewelry manufacture. A. Jurado-López and M. D. Luque de Castro, *Spectrochimica Acta Part B*, Vol. 58, No. 7, 2003, pp. 1291–1299.

Laser-induced breakdown spectrometry (LIBS) is a minimally destructive, rapid, reliable, and relatively inexpensive spectroscopic technique. This article describes the application of LIBS to the multi-element analysis of 32 alloys that are widely used in jewelry manufacture; 25 were chosen as library standards, and the remaining seven were used as samples. The alloys were divided into two groups: one for gold alloys used in jewelry manufacturing and the other for low-melting welding points. Each alloy was subjected to five laser shots to obtain a representative spectrum. The Spearman rank correlation coefficients of the spectra were compared to the library standards by mean of ranks from 1 to 1024 (the latter representing the most intense pixel in a given spectrum). The maximum rank was obtained when the composition of the alloy was similar to that of the standard.

Cu and Zn were detected in all the alloys, whereas Ag was found in most of them. Ni was found only in white gold; Ir was common (~12–30 wt.%) in most of the alloys used for welding points. Although Cd is currently not permitted in jewelry because of its toxicity, this element was detected in one of the welding point alloys.

In addition to its usefulness in the jewelry trade, LIBS has great potential for a wide range of industrial applications, especially in the mining and chemical processing industries. *KSM*

Spectra of gem materials. G. Pearson, *Australian Gemmologist*, Vol. 21, No. 12, 2003, pp. 478–485.

Discrepancies are commonly observed in the spectra of gem materials seen with a hand spectroscope and those obtained with a UV-Vis spectrophotometer. This raises questions about the visibility, in hand-held spectroscopes, of absorption features that have been long-recognized as characteristic of many gems, such as sapphire and peridot. By defining and illustrating the "relative luminous efficiency" curve, which represents the sensitivity of human vision across the visible wavelength range, the author concludes that some of the instrumentally derived absorption spectra presented in many gemology texts cannot be seen with a hand-held spectroscope. *RAH*

The using of luminescence in gemology. B. S. Gorobets, O. V. Kononov, A. A. Rogojine, and T. D. Kvitko, *Gemological Bulletin*, No. 10, 2003, pp. 34–56 [in Russian with short English abstract].

This comprehensive review of the applications of luminescence methods in gemology contains five tables, 52 figures with spectra of minerals (including their synthetic analogues and simulants), and 11 color photos. General topics include a discussion of luminescence types (e.g., cathodo- and thermoluminescence) and the nature of luminosity—with special attention paid to the effects of Fe, Cu, and radiation defects. The techniques and instruments used for obtaining luminescence spectra also are described. Recommendations are given for the visual observation of thermal and UV luminescence in diamonds and emeralds, and methods are provided by which their synthetic counterparts can be distinguished.

Future work by the authors will be directed toward creating an extensive database for natural and treated gems, compiling specific instructions for using luminescence to distinguish natural from synthetic gems, and establishing a research center in Russia dedicated to developing methods and instrumentation for luminescent determinations of gems and related materials. *BMS*

JEWELRY RETAILING

The role of branding in the diamond industry. A. Murray, *Rough Diamond Review*, No. 3, 2003, pp. 34, 37–38.

With its "Diamonds are Forever" campaign, De Beers has provided sustained global guidance since the 1940s. Although diamonds had been highly revered for generations, they did not become a mass consumer product until De Beers promoted them. As new producers and corporate players have entered the diamond market in recent years, the consumer's choice has increasingly been influenced by branding. The initial brands, usually based on particular cuts of polished diamonds (e.g., the Quadrillion and Ideal cut), have increased consumer confidence and given diamonds an added prestige that makes them popular and sought after. Another brand dimension is provided by country of origin (e.g., Australia or Canada) or specific mines in those countries (e.g., Argyle or Ekati, respectively). These can summon strong, sometimes patriotic feelings from customers. Positioning also plays an important role in diamond branding, as having a corporate identity can help a company in various commercial ways as well as distinguish it from other players.

Branding and positioning require commitment, as their benefits pay off over the long run; results take at least a year or two to become evident. The long-term view is consistent with the soul of the diamond industry, which has always been about building and maintaining relationships, as well as establishing values. *MT*

SYNTHETICS AND SIMULANTS

Effect of HPHT annealing on the photoluminescence of synthetic diamonds grown in the Fe–Ni–C system. A. Yelisseyev, S. Lawson, I. Sildos, A. Osvet, V. Nadolinny, B. Feigelson, J. M. Baker, M. Newton, and O. Yuryeva, *Diamond and Related Materials*, Vol. 12, No. 12, 2003, pp. 2147–2168.

Absorption and photoluminescence (PL) spectra were employed to characterize the effects of HPHT annealing on synthetic diamond crystals containing high concentrations of nitrogen and nickel impurities. Twenty synthetic diamond crystals were grown from an Fe-Ni-C system at 1,600 K and 5.5 GPa in a split-sphere type apparatus. Some of the crystals were subsequently annealed for 4 hours at either 1,950 K or 2,200 K. Additional samples used for comparison included crystals grown in a Ni-free (Fe-C) system as well as several Yakutian diamonds with relatively high Ni concentrations for natural stones.

Numerous narrow lines were observed in the PL spectra of the synthetic diamonds containing nickel and nitrogen impurities. More than 20 vibronic systems were identified, some for the first time, and their responses before and after annealing were recorded. Based on analysis of these data, the authors proffer the following main groups for characterizing these systems:

I. Systems existing in as-grown synthetic diamonds that decrease in intensity with annealing at 1,950 K
II. Systems that appear after annealing at 1,950 K and then decrease in intensity or disappear with annealing at 2,200 K
III. Systems that appear after annealing at 1,950 K and do not decrease in intensity with annealing at 2,200 K

Group I systems are identified by individual impurity ions such as negatively charged substitutional nickel. Group II systems relate to a nickel ion in a di-vacancy position and intermediate nickel-nitrogen complexes containing single nitrogen atoms. Group III systems correlate with more complicated nickel-nitrogen complexes comprising at least two nitrogen atoms surrounding the nickel. *SW*

Optical properties of synthetic diamond single crystals. A. V. Mudryi, T. P. Larionova, I. A. Shakin, G. A. Gusakov, G. A. Dubrov, and V. V. Tikhonov, *Semiconductors*, Vol. 38, No. 5, 2004, pp. 520–523.

Synthetic diamond crystals (4–7 mm in diameter) with potential for use in precision scientific instruments were grown by the thermal gradient method (Ni-Fe-C system; 1,750–1,800 K; 5.4–5.5 GPa) and subsequently subjected to HPHT treatment (2,000–2,200 K and 6.0–6.5 GPa for 3–24 hours). The untreated crystals were yellow-green and exhibited a prominent S3 band at 496.7 nm in their cryogenic PL spectra. The HPHT-treated synthetic diamonds had a pale green color and displayed the S3 band in addition

to three S2 bands at 523.3, 489.1, and 477.8 nm (i.e., A, B, and C defects, respectively, of S2). Although the S2 bands were found occasionally in untreated samples, their intensities increased by factors of 5–10, and the overall luminescence of the synthetic diamonds increased by factors of 3–5, after HPHT treatment. The increase in luminescence is attributed to a redistribution of Ni and N impurities within the synthetic diamonds during treatment and a corresponding change in bodycolor. Luminescence excitation spectra further indicated that S2 (A) and S2 (B) are independent features related to different defects. IR absorption spectra of the same samples show that HPHT treatment resulted in aggregation of >90% of the C defects (single substitutional N) into A defects and the near-complete annealing of Me-X centers (Me = metal solvent; X may be carbon and/or nitrogen). PL and IR data confirmed that HPHT treatment resulted in significant reconfiguration of the defects in the synthetic diamond lattice.

Christopher M. Breeding

Properties and diagnostics of natural and synthetic malachite. T. V. Chernenko and E. P. Melnikov, *Gemological Bulletin*, No. 8 (pp. 11–27) and No. 9 (pp. 31–35), 2003 [in Russian with short English abstracts].

This in-depth, well-illustrated two-part article on malachite reviews the history of its use in jewelry and as a decorative stone, the geology of its major deposits, and methods by which it is synthesized. Based on a study of 150 natural and ~20 synthetic malachites, the authors identified textural, structural, chemical, and other differences between the natural and synthetic samples. For example, their densities are distinctive (3.87–3.92 g/cm^3 for natural and 3.61–3.70 g/cm^3 for synthetic). Chemically, natural malachites contain P (due to admixed pseudomalachite), Be, Co, and V that distinguish them from synthetic malachites, which contain Pb, Sn, and Ga (not found in natural samples). Numerous other trace elements may be present in both natural and synthetic malachites, and in some cases these can be correlated to differences in color and texture. Individual crystallites in natural malachites are larger than similar crystallites in the synthetic varieties.

Chemical and temperature parameters are determined for the formation of the two most attractive varieties of natural malachite, with the Russian names "plissovy" (radiating fibers) and "biryuzovy" (light green "turquoise-like"). "Plissovy" forms in gossans over Cu-Fe deposits from solutions with low concentrations of Cu and CO_2 at temperatures of 60–70°C. "Biryuzovy" usually forms in Cu-bearing clays associated with limestones in karst terranes from concentrated solutions at temperatures of 20–50°C. *BMS*

Study on large-sized ruby grown by temperature gradient technique. C. Song, S. Zhou, J. Si, H. Li, G. Zhou, Y. Hang, and J. Xu, *Journal of Synthetic Crystals*, Vol. 32, No. 5, 2003, pp. 423–426 [in Chinese with English abstract].

Large crystals of synthetic ruby (not of gem quality) were grown by the temperature gradient technique from seed plates using Al_2O_3 powders mixed with 0.5–3% Cr_2O_3. Crystallization started at 2,050°C; cooling rates were 0.5–2.5°C/hour. The largest crystal measured 75 mm in diameter, 45 mm long, and weighed 1,076 g. This crystal was dark red in the center and even darker red (almost black) at its edges and bottom. Wave-like growth bands were observed in the top portion, while clouds of minute inclusions were concentrated near the seed plate. The concentration of the inclusions decreased from edge to center and from bottom to top, resulting in a "trumpet"-shaped distribution along the growth direction similar to that found in synthetic Ti-doped sapphire crystals grown by the same technique.

Electron-microprobe analysis showed that the inclusions were mainly uncrystallized Al_2O_3 powder. Gas bubbles or voids also were observed. Microprobe and spectroscopic (visible range) data showed that the Cr^{3+} concentration increased in two directions (i.e., from center to edge and from bottom to top), corresponding to the growth progression. The authors propose that the quality of synthetic ruby crystals produced by this method could be improved by optimizing the cooling rate, purifying the raw materials, and controlling the temperature during growth. *TL*

A Verneuil synthetic ruby showing diverse veil-like 'fingerprints.' J. M. Duroc-Danner, *Journal of Gemmology*, Vol. 28, No. 8, 2003, pp. 483–488.

Today the treatment of gem corundum is of such concern that it tends to overshadow the topic of natural vs. synthetic. This article brings that topic back into the forefront, as its focus is on a 2.06 ct, oval-shaped, flame-fusion synthetic ruby that was discovered in a parcel of natural rubies being checked for country of origin.

This synthetic ruby was treated (i.e., quench-crackled with flux "fingerprints" later induced) to more closely resemble a natural ruby. The fingerprints were similar to those seen frequently in Mong Hsu rubies and could easily fool anyone viewing the stone with a 10× loupe. Only careful observation at higher magnification revealed the telltale signs of the stone's synthetic origin: curved striae and clouds of tiny gas bubbles, both hidden beneath numerous wispy, veil-like, flux-induced fingerprints that varied in their appearance throughout the stone. Also helping to mask the evidence of synthesis were many surface-reaching fractures and straight, heavy polish lines. *WMM*

The LAST Page

Diamond Animation on Our Fall Cover

Even if you've never heard of a "lenticular" image, chances are you've seen one. The term refers to a type of two-dimensional printed image, typically seen in novelty and promotional items, that creates the illusion of motion when tilted or viewed from different perspectives. The odd name comes from the grooved plastic lenses, or *lenticules*, that you feel when you run a fingernail across the surface.

Lenticular images are often confused with holograms, which also show apparent depth and motion, but the two are actually quite different. Unlike holograms, which are produced by the reflection of laser light onto a very thin metallic or transparent sheet, lenticular printing is done using a traditional lithographic printing press. And while holograms are usually monochromatic (but with a rainbow-like cast), lenticulars are much clearer and brighter, with full photographic color.

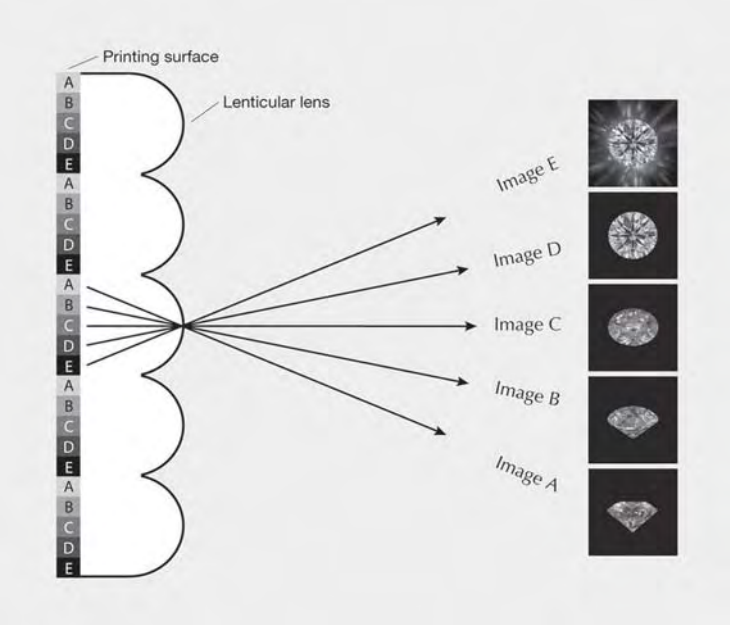

Lenticular imaging is by no means a new technology. The principle was first developed nearly a century ago by Gabriel Lippman (1845–1921), the French physicist better known for developing the first color photograph plate. After World War II, when improvements in plastics technology made them commercially viable, lenticulars became popular in advertising displays and collectibles such as baseball cards and political campaign buttons. Most of these were simple "flips" between two images. Today's far more sophisticated products can show a variety of visual effects, including video-like animation, three-dimensional depth, and seamless morphing from one image to another.

FOR THE FALL 2004 *G&G* COVER, we used a lenticular image to replicate a basic yet meaningful routine familiar to every jeweler and gemologist: tilting a diamond to observe it from different angles. The Fall cover's five-frame sequence demonstrates how a diamond's appearance changes based on the viewing direction, a key concept from the lead article, "A Foundation for Grading the Overall Cut Quality of Round Brilliant Cut Diamonds" (pp. 202–228).

So how was this unique *G&G* cover created? First, photographers Harold and Erica Van Pelt shot a 4.01 ct round brilliant cut diamond from a variety of different angles. From these, five source photos (illustrated on pp. 197–198 of the Fall issue) were chosen and color corrected, and the color separations were sent to the printer, Standard Register, for lenticular processing. The photos were digitally divided into narrow, linear strips and interlaced—imagine a deck of cards being shuffled—to produce a sequential combination of the five frames. This interlaced image was printed and then mounted behind a plastic lens screen containing horizontal rows of lenticules. Each lens was matched precisely with the narrow strip of image behind it, focusing on and magnifying it. In the finished lenticular, the eye sees only one set of strips (i.e., one image) at a time depending on the viewing angle. Any shift in the horizontal viewing angle, either by tilting the cover or changing the viewing position, brings a different set of strips into focus and changes the appearance of the overall image.

We'd like to think of our Fall 2004 lenticular cover as not just an eye-catching visual, but as a medium that actively engaged and involved everyone who picked up a copy. We hope it reinforced the landmark article on diamond cut—and maybe pushed our boundaries a little in the process.

Stuart Overlin
Associate Editor